

Neutron-rich matter in the heavens: Taking stock and looking ahead.

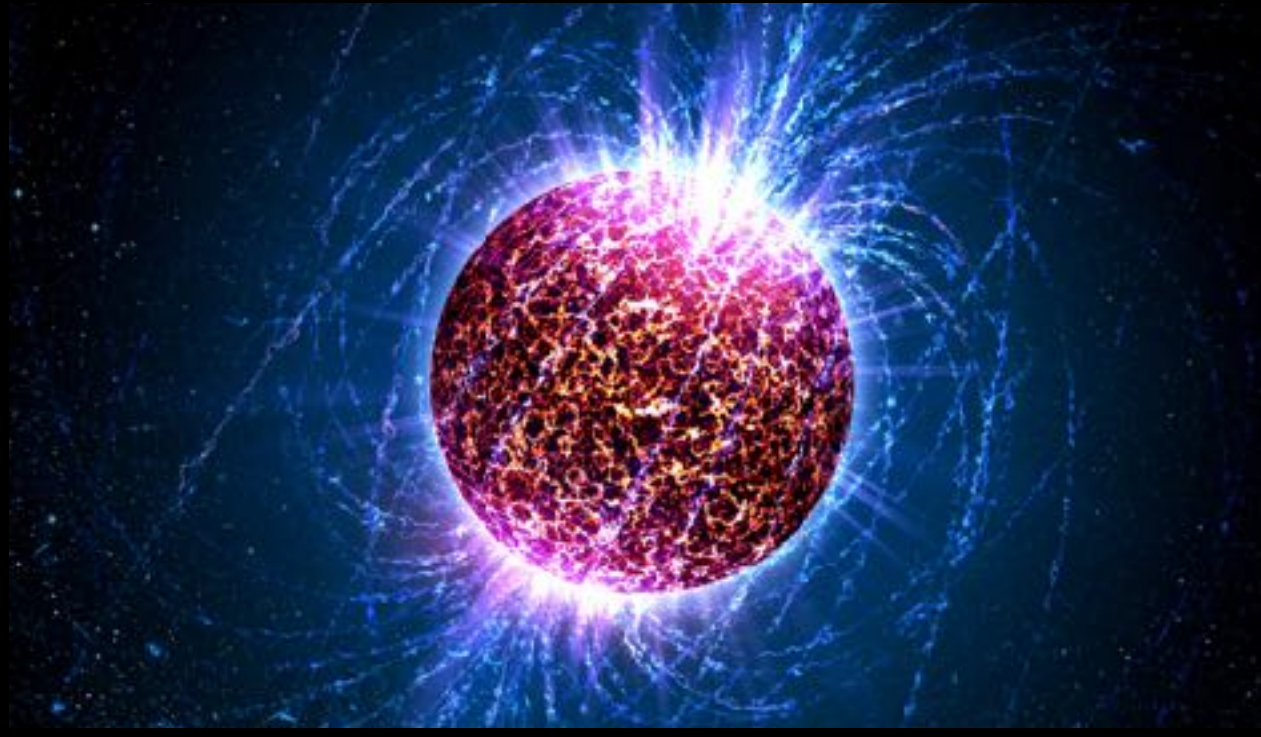
Sanjay Reddy, University of Washington, Seattle

- Dense matter & the phases of QCD
- Neutron star structure
- Cooling of accreting neutron stars
- Neutron stars in the 3G GW detector era.
- Dark matter and neutron stars

Big Questions



What powers the most extreme phenomena in the universe?



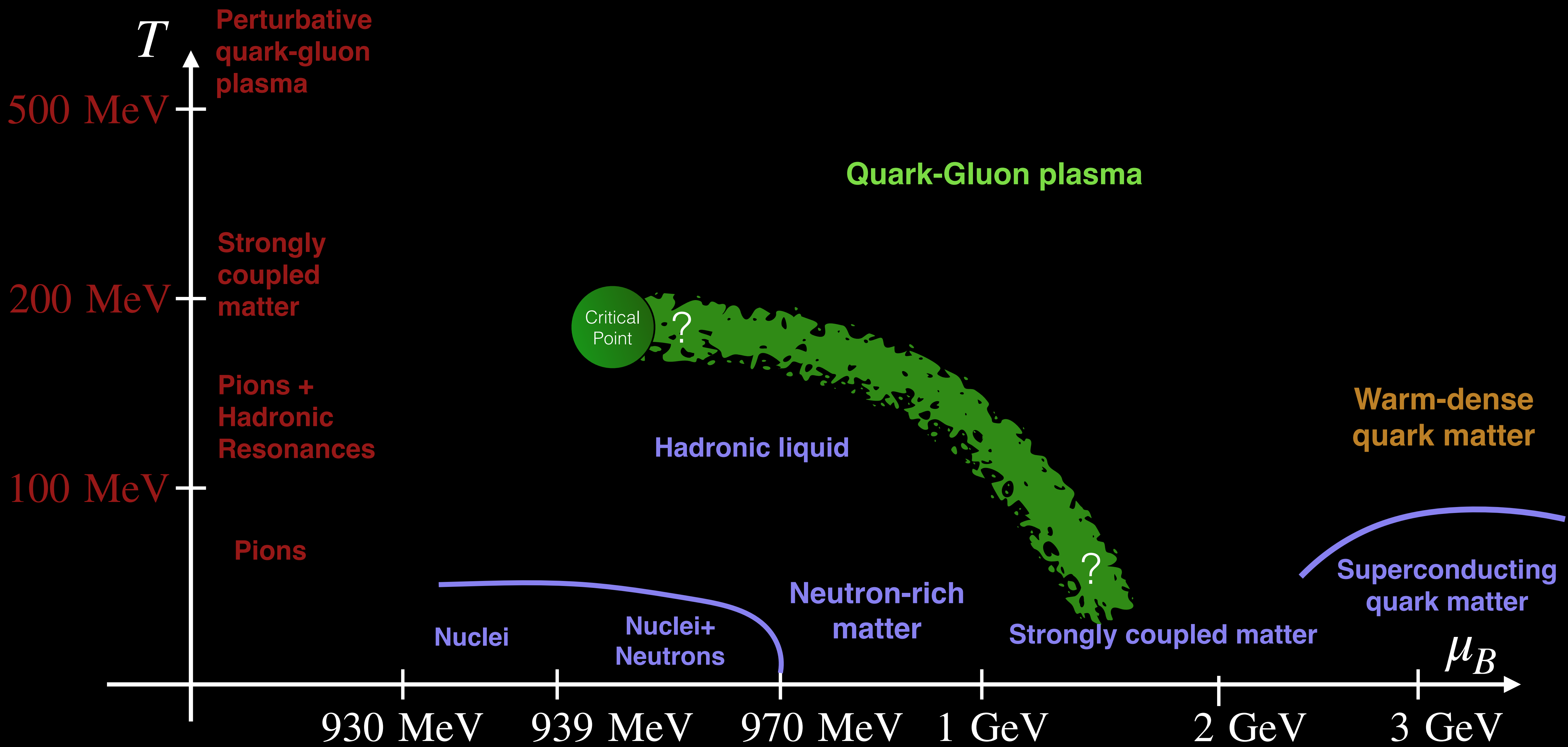
What are the states of matter encountered inside neutron stars?

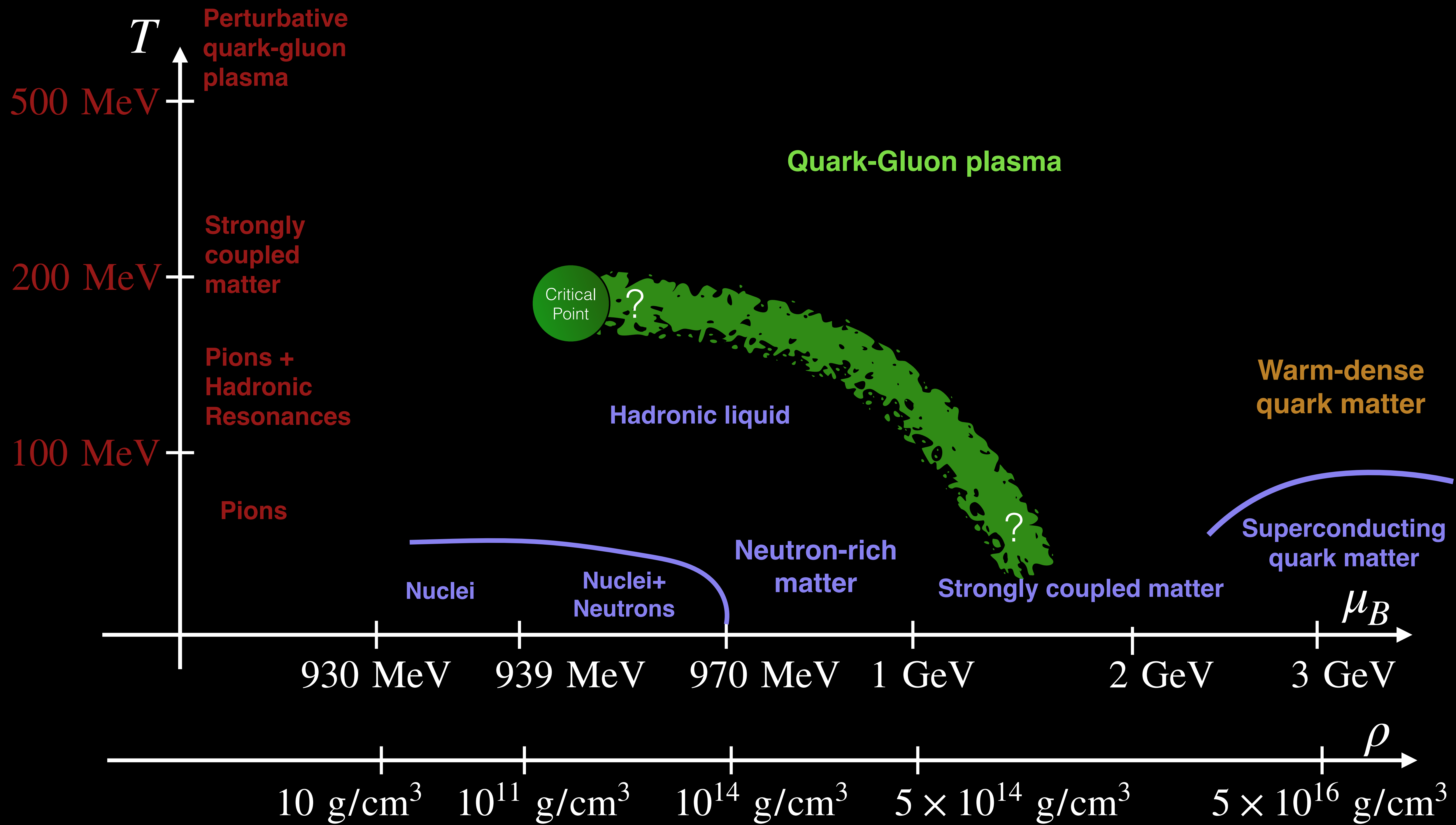


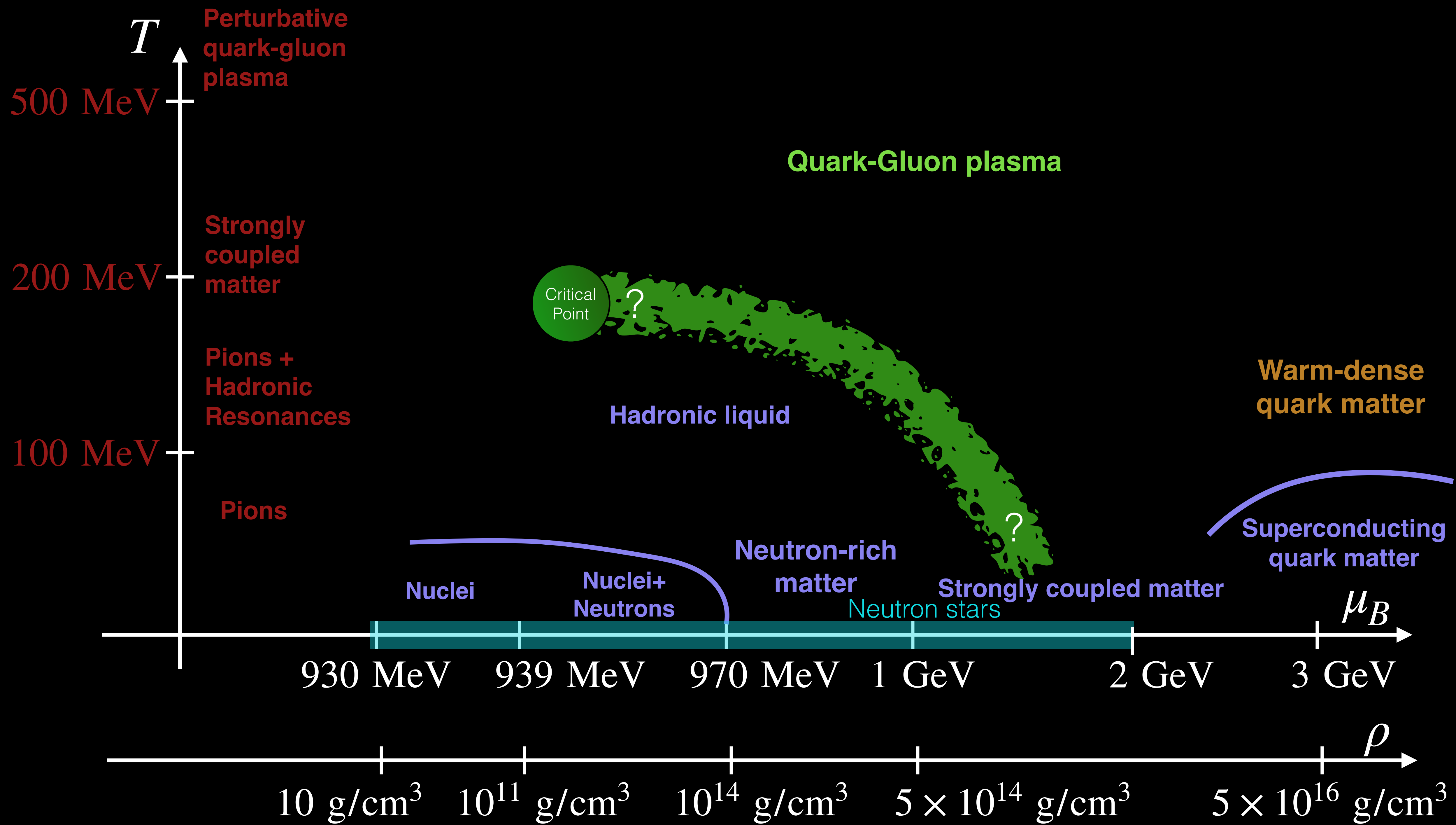
Where and how are the heavy elements such as gold, platinum and uranium made?

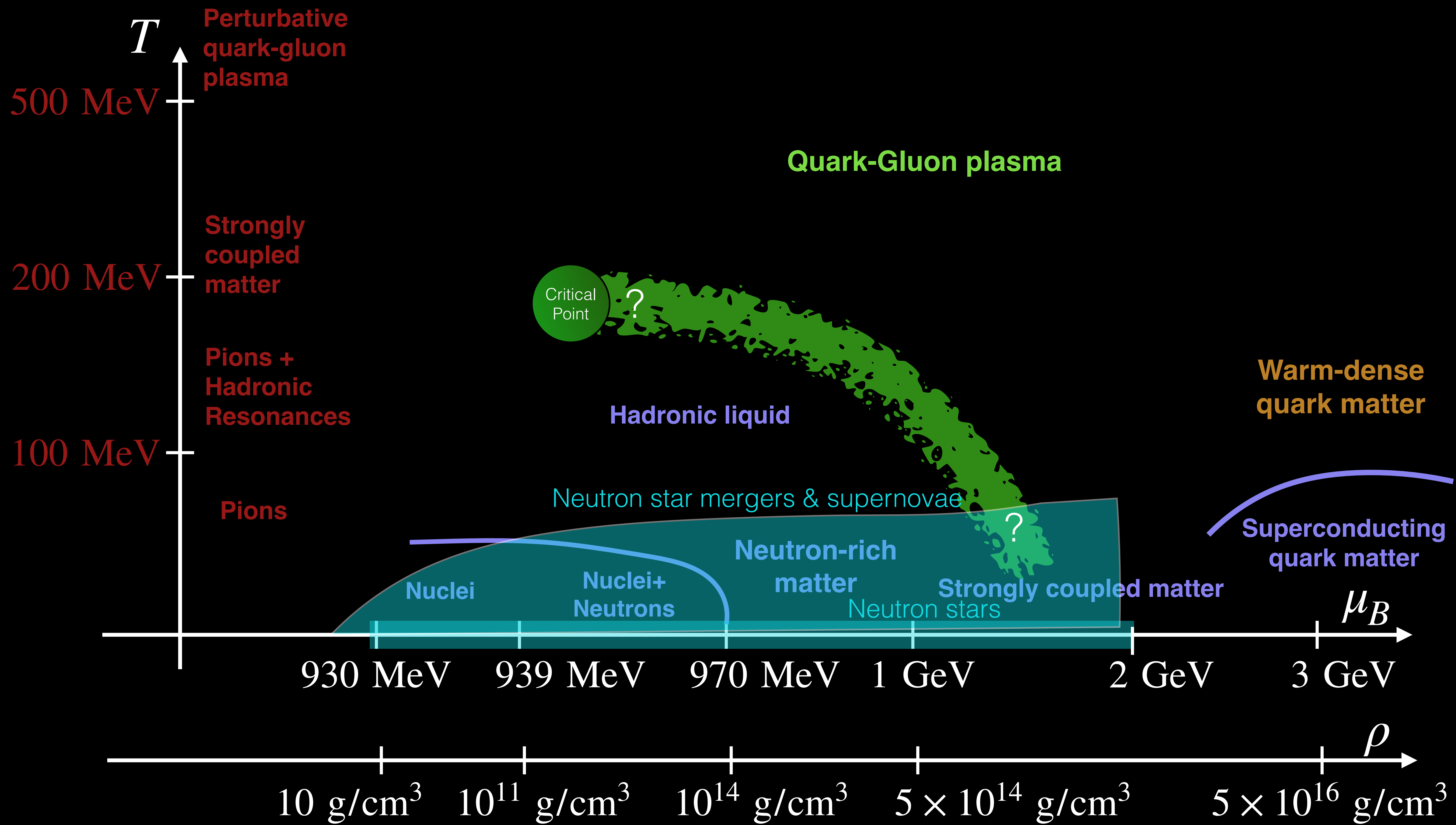


What is dark matter? Can we use neutron stars to map the universe?

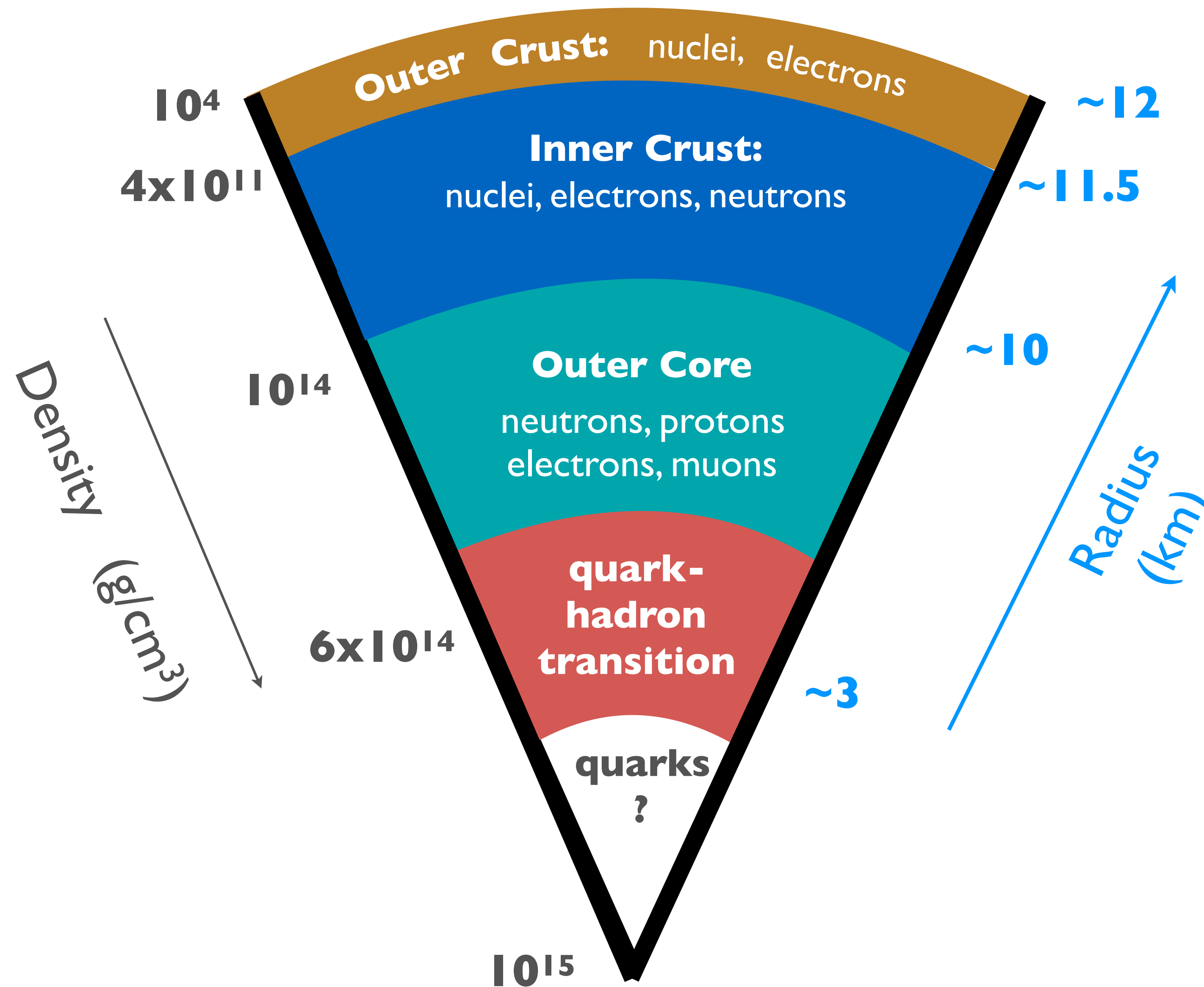




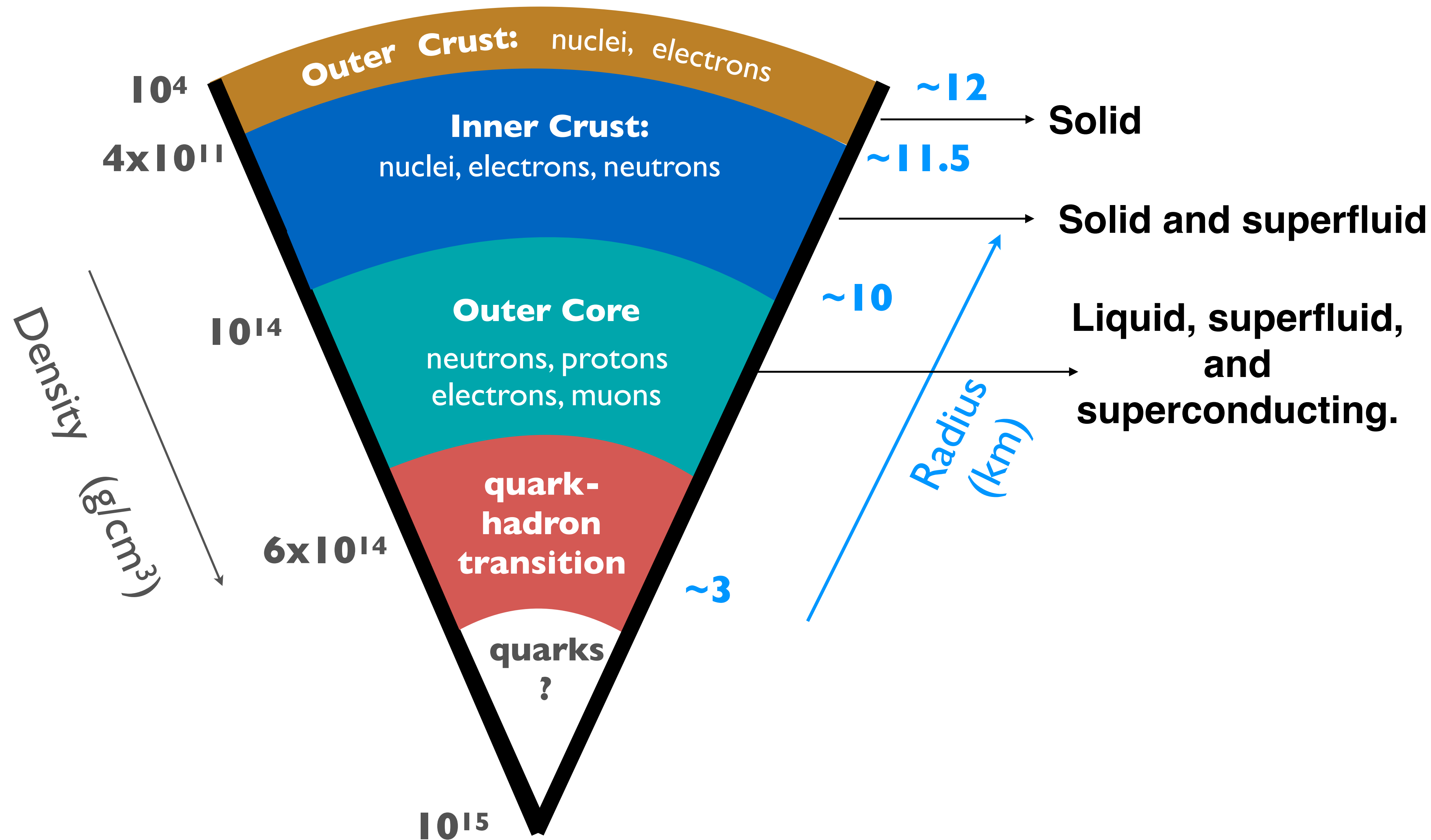




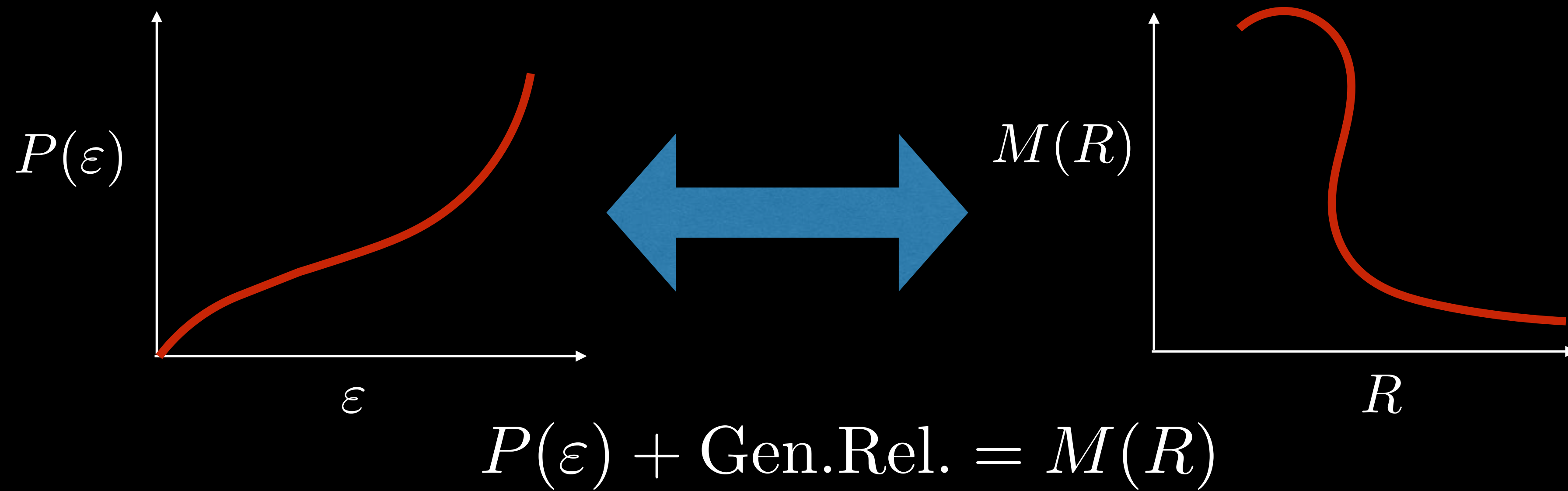
Composition of Dense Matter in Neutron Stars



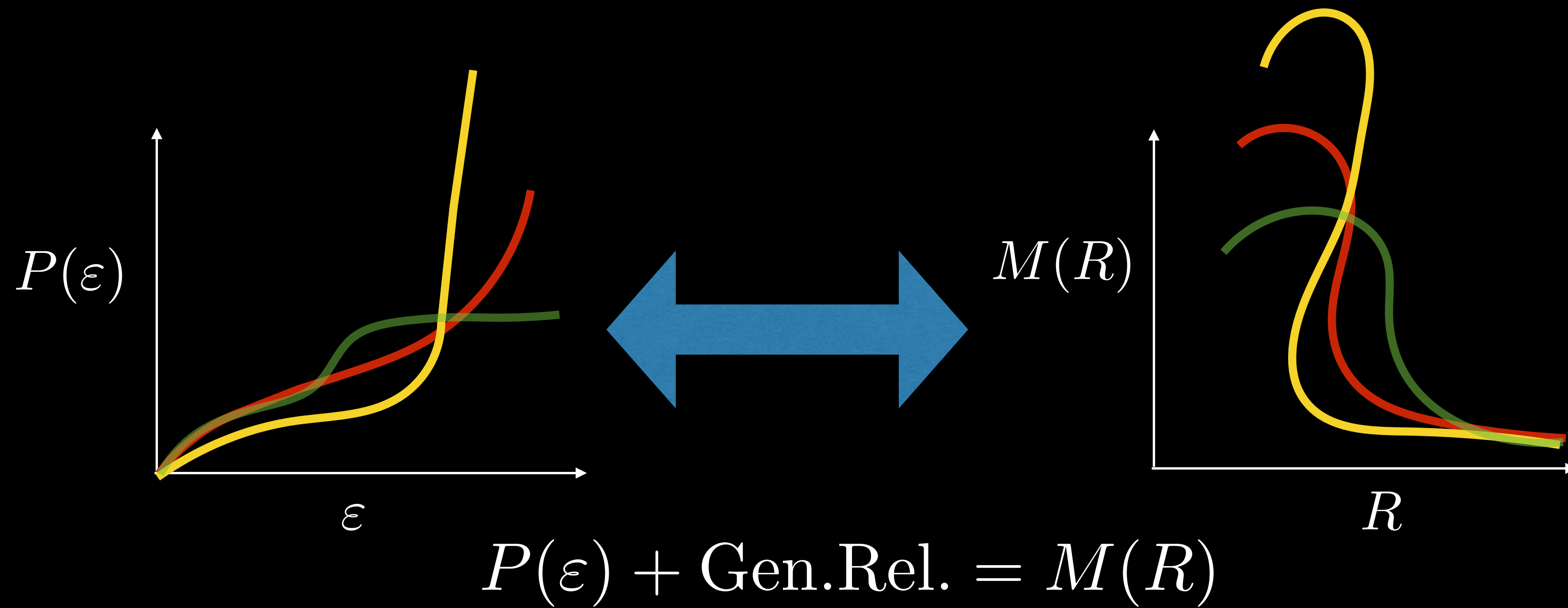
Composition of Dense Matter in Neutron Stars



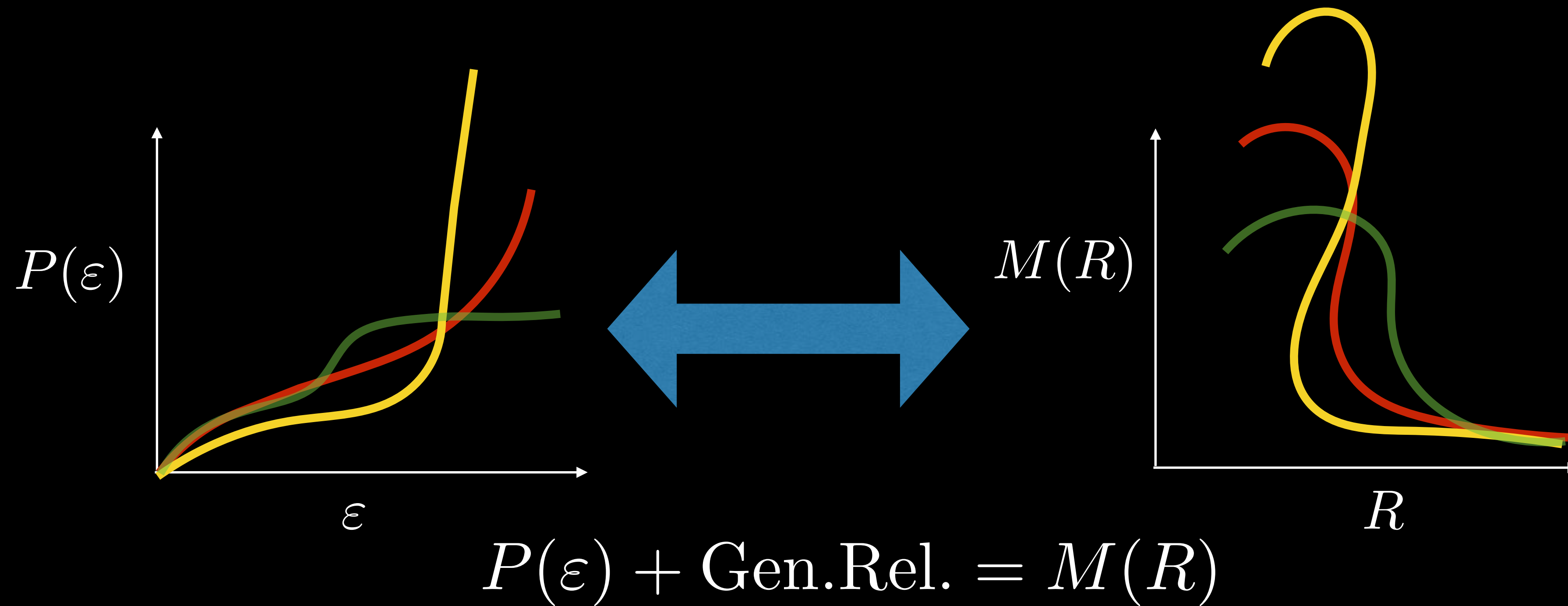
Equation of State and Neutron Star Structure



Equation of State and Neutron Star Structure

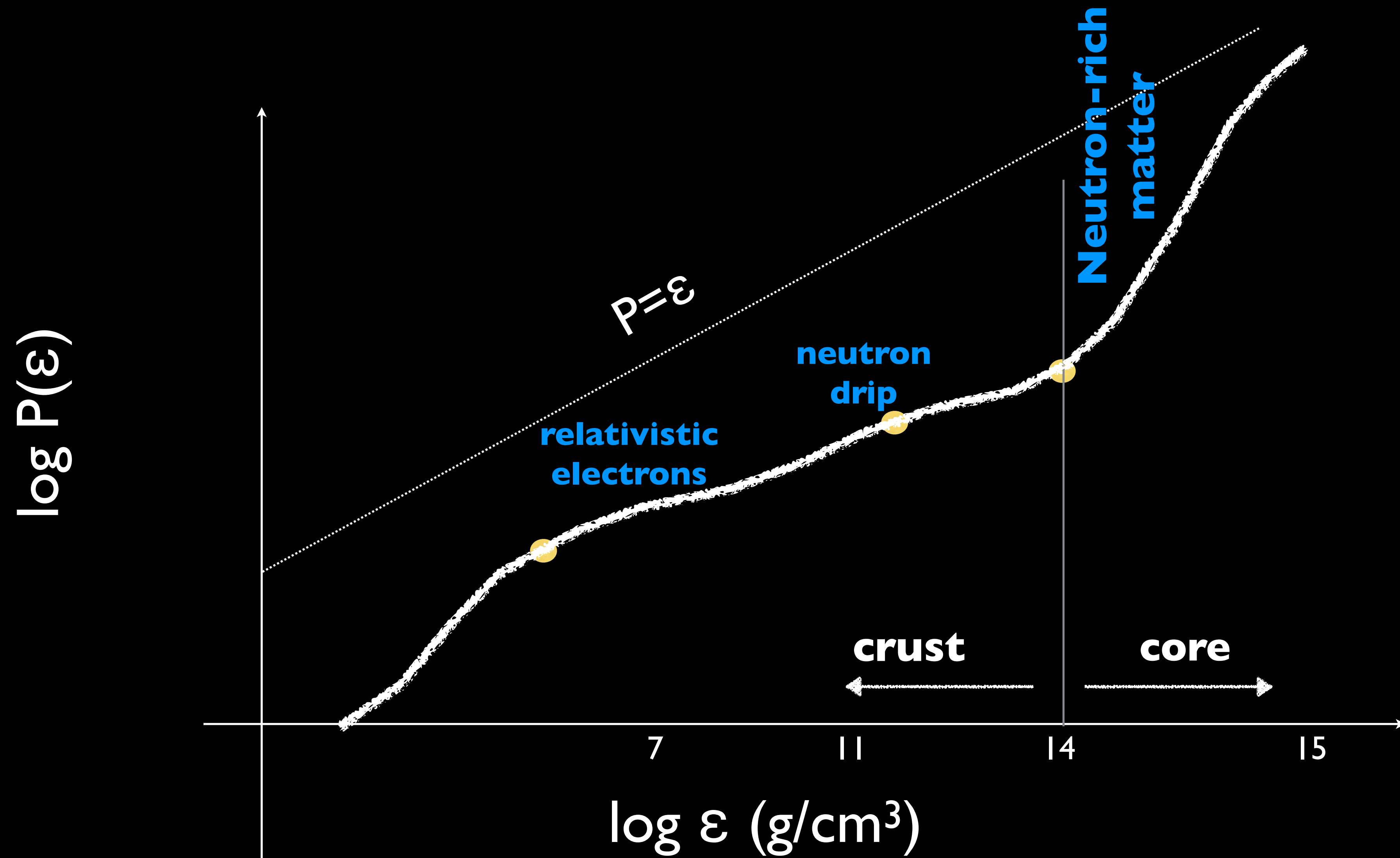


Equation of State and Neutron Star Structure

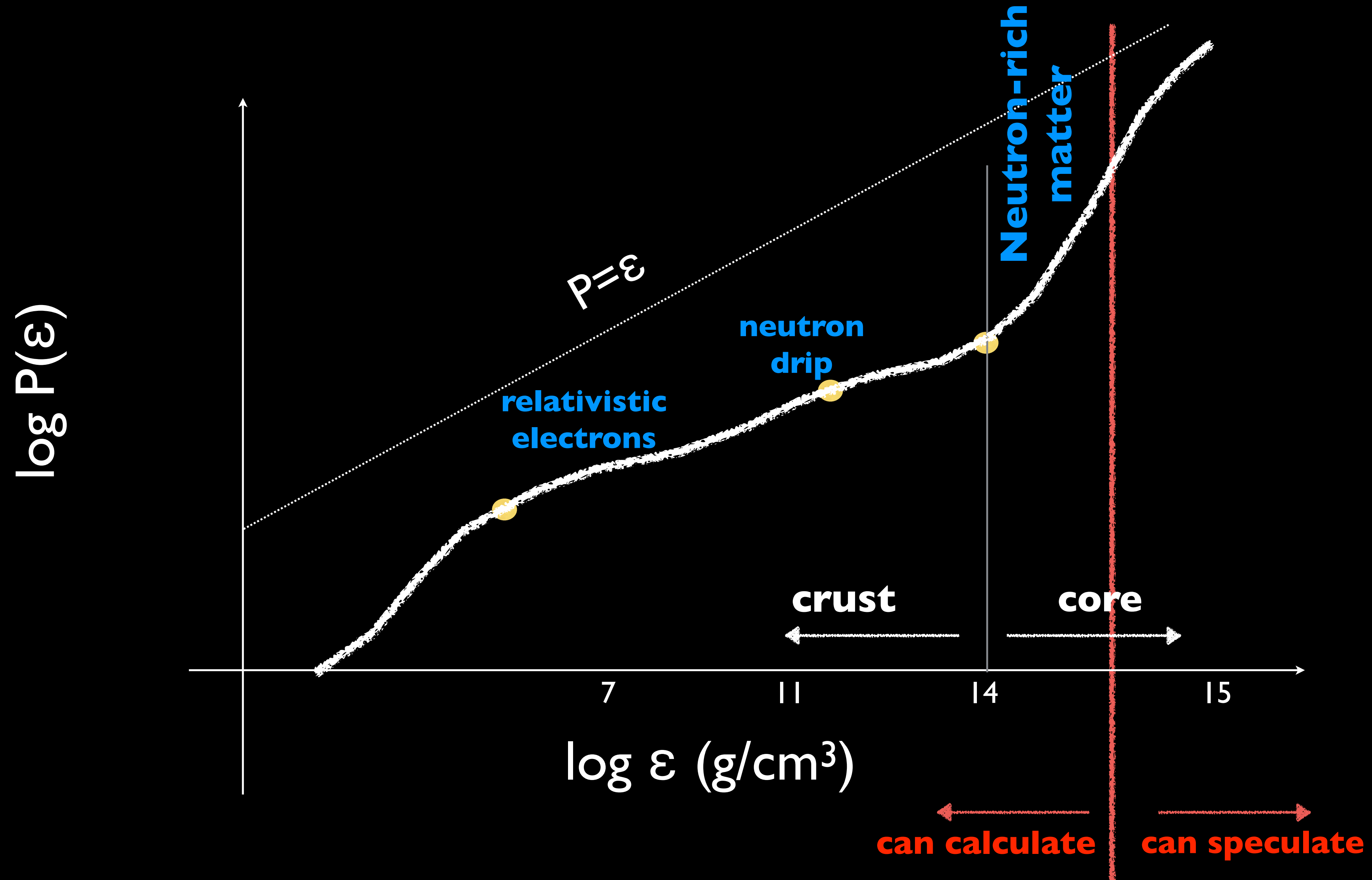


A small radius and large maximum mass imply a rapid transition from low to high pressure with density.

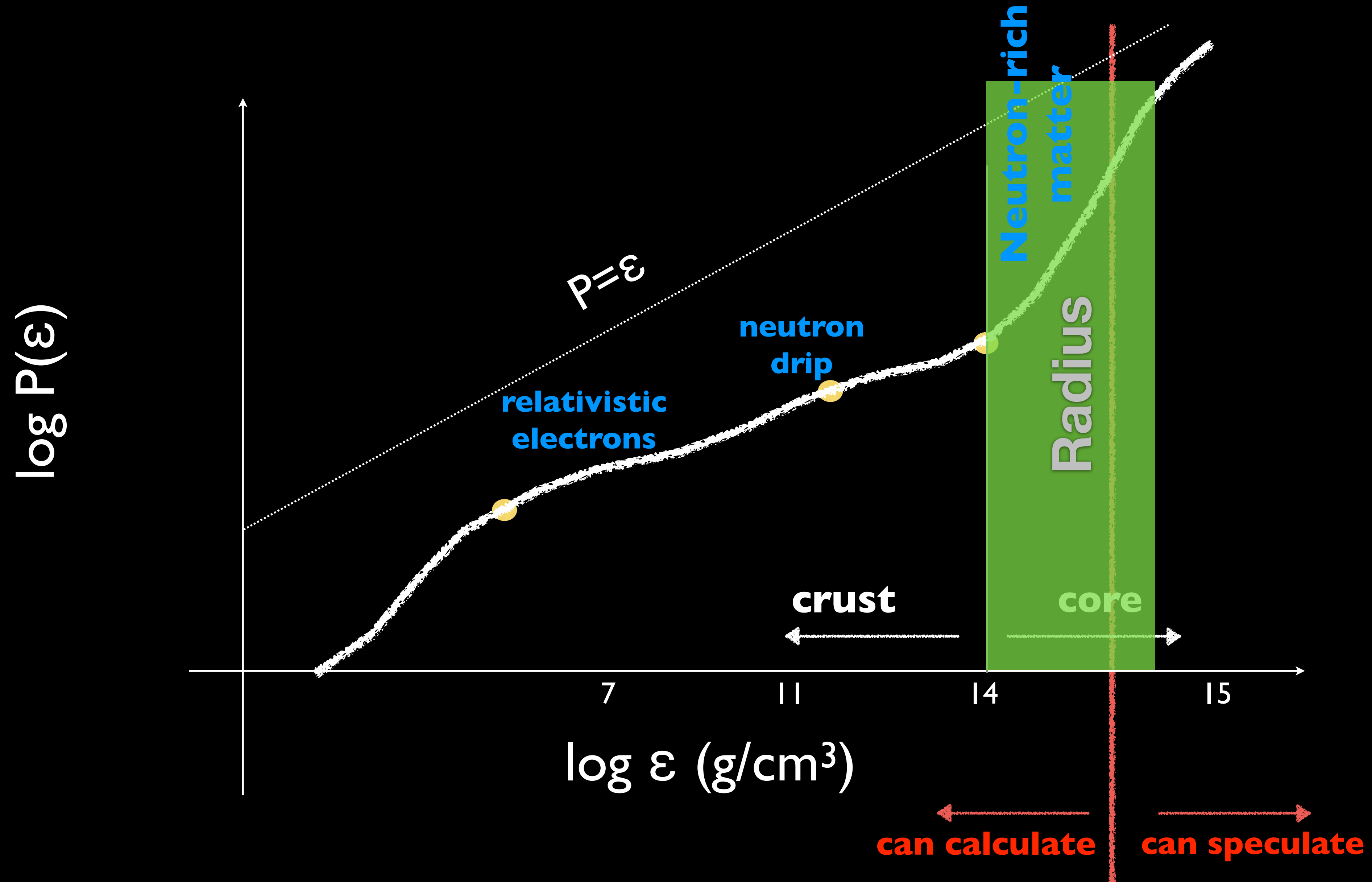
Pressure v/s Energy Density (EoS)



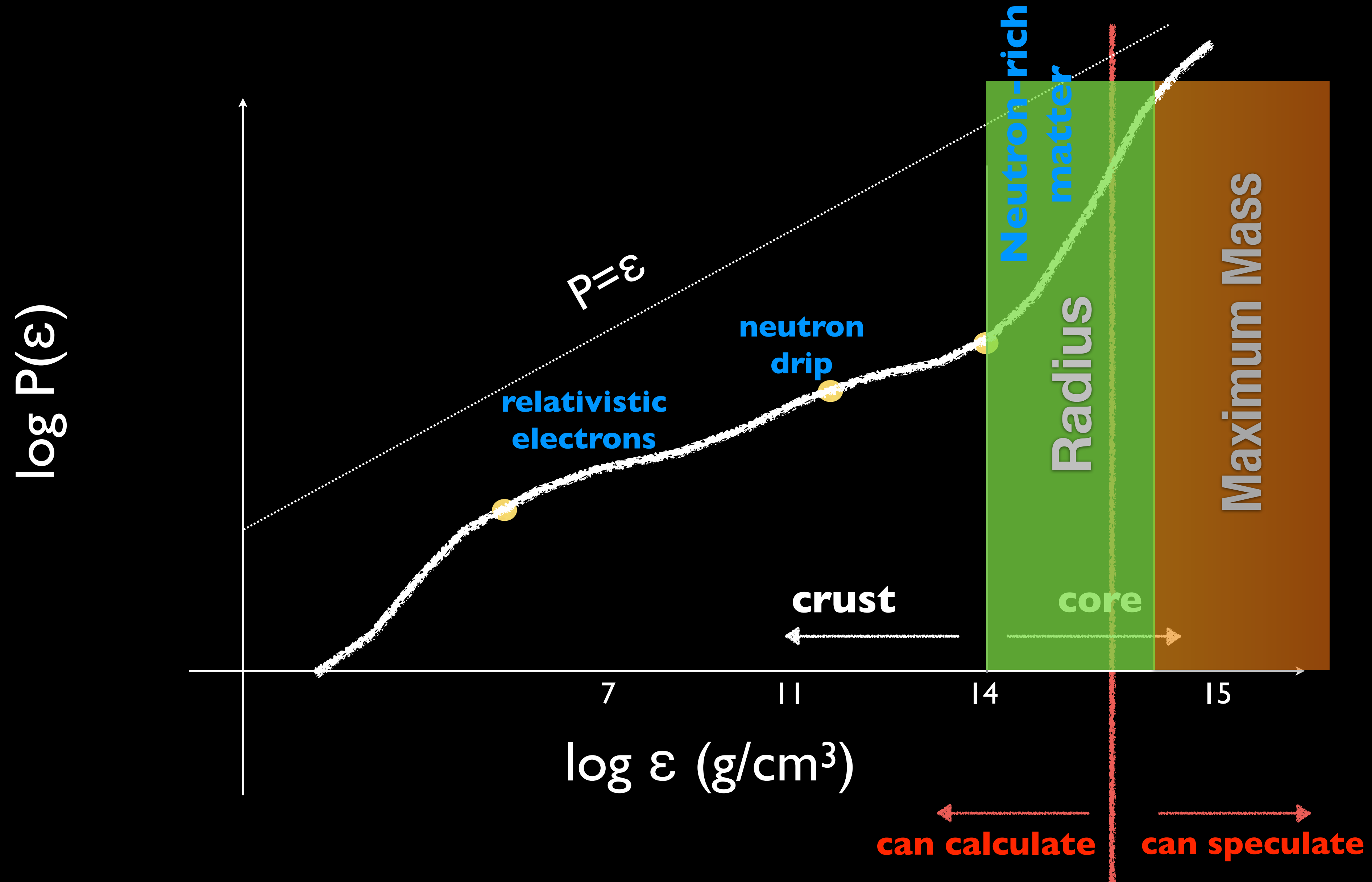
Pressure v/s Energy Density (EoS)



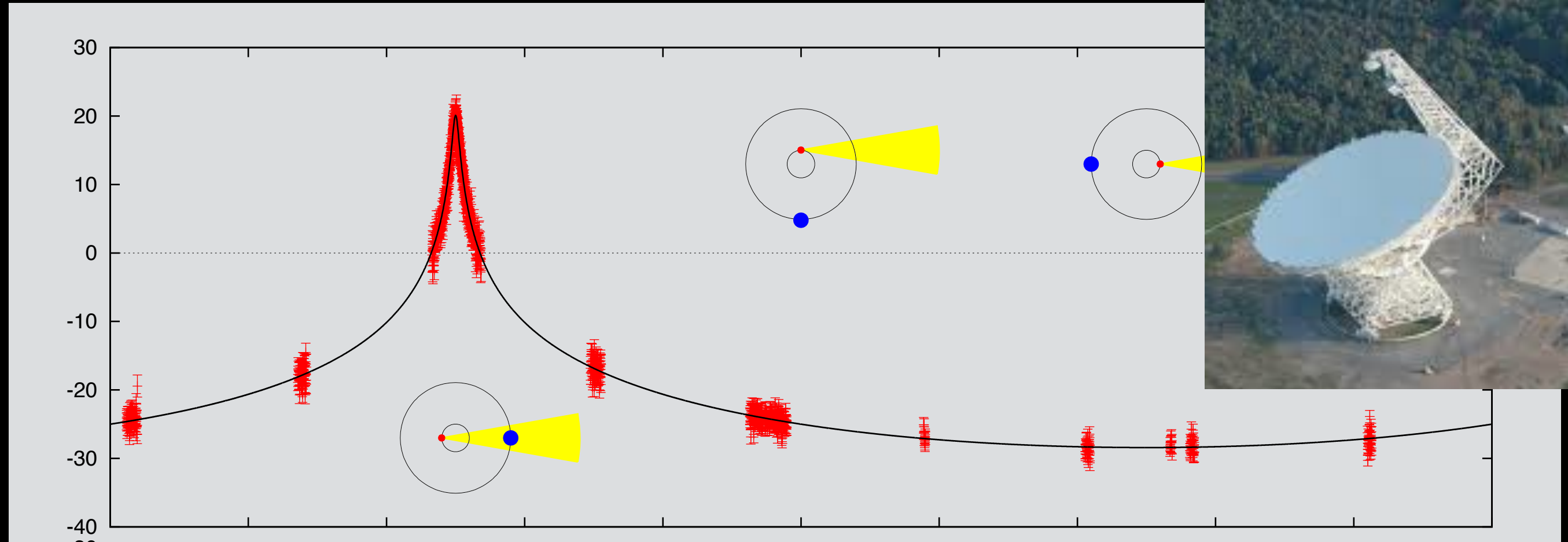
Pressure v/s Energy Density (EoS)



Pressure v/s Energy Density (EoS)



Neutron Star Structure: Observations



2 M_{\odot} neutron stars exist.

PSR J1614-2230: $M=1.93(2)$

Demorest et al. (2010)

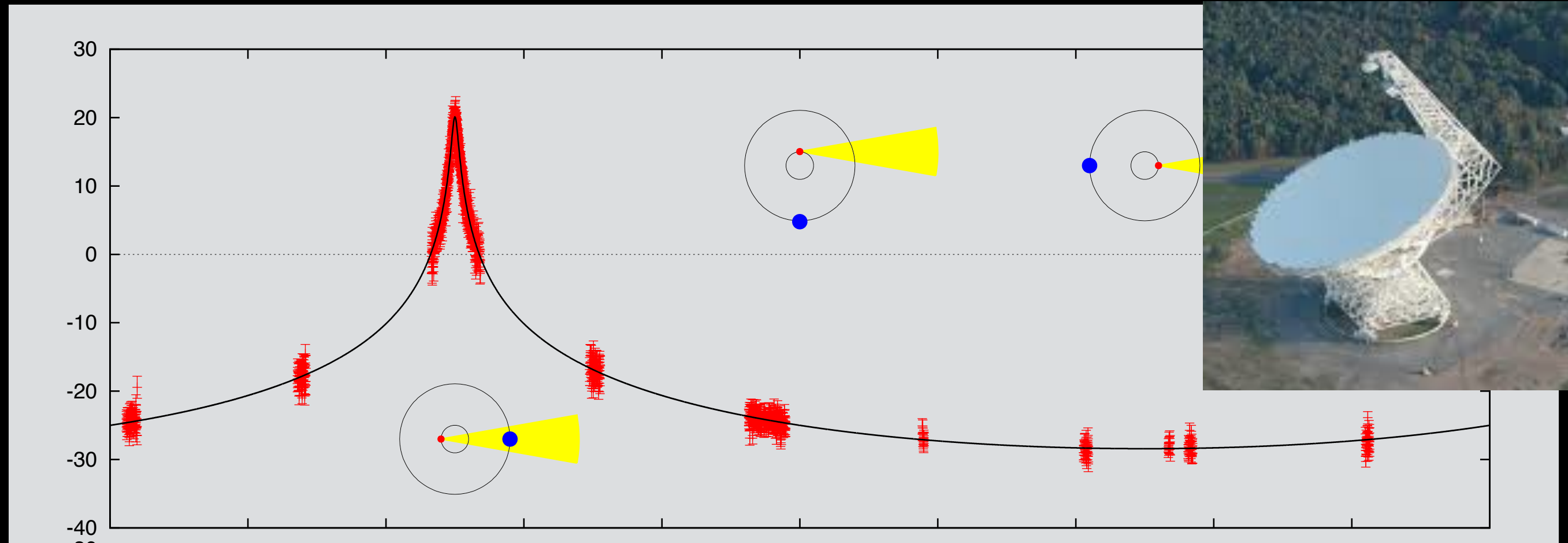
PSR J0348+0432: $M=2.01(4) M_{\odot}$

Anthoniadis et al. (2013)

MSP J0740+6620: $M=2.17(10) M_{\odot}$

Cromartie et al. (2019)

Neutron Star Structure: Observations



2 M_{\odot} neutron stars exist.

PSR J1614-2230: $M=1.93(2)$

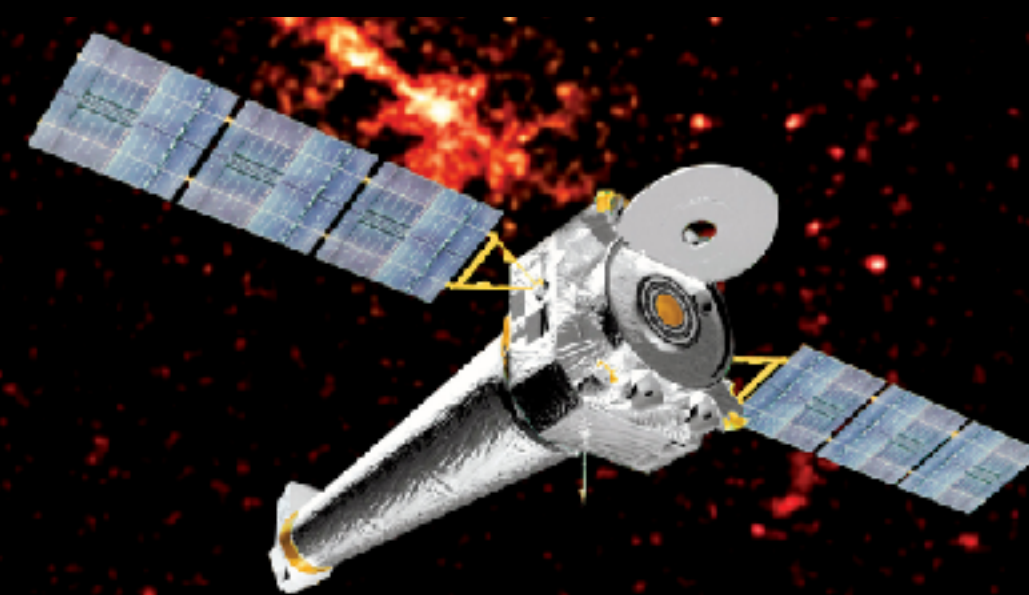
Demorest et al. (2010)

PSR J0348+0432: $M=2.01(4) M_{\odot}$

Anthoniadis et al. (2013)

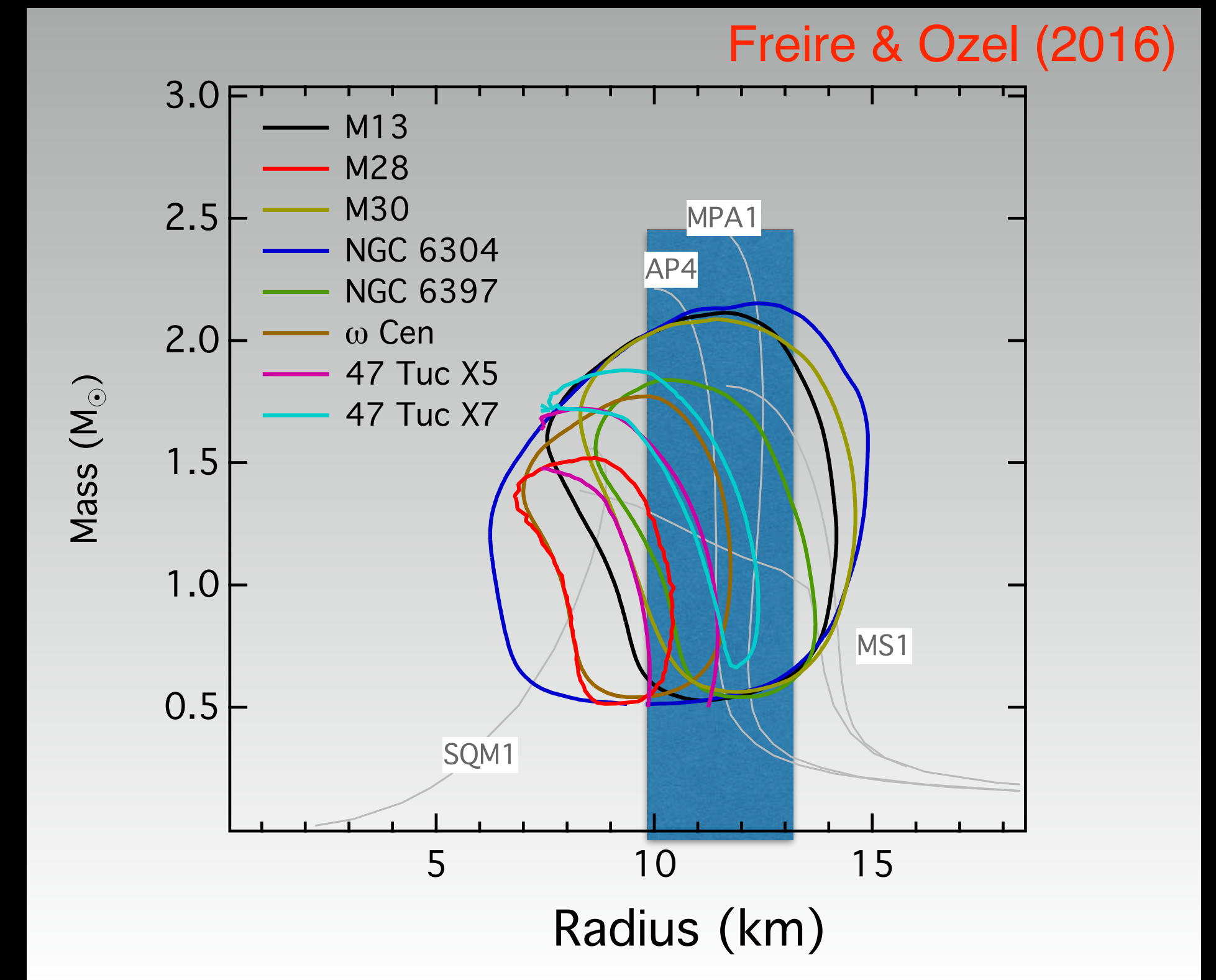
MSP J0740+6620: $M=2.17(10) M_{\odot}$

Cromartie et al. (2019)



NS radii are difficult to measure:

Poorly understood systematic errors, preclude the determination of NS radius using x-ray observations of surface thermal emission.



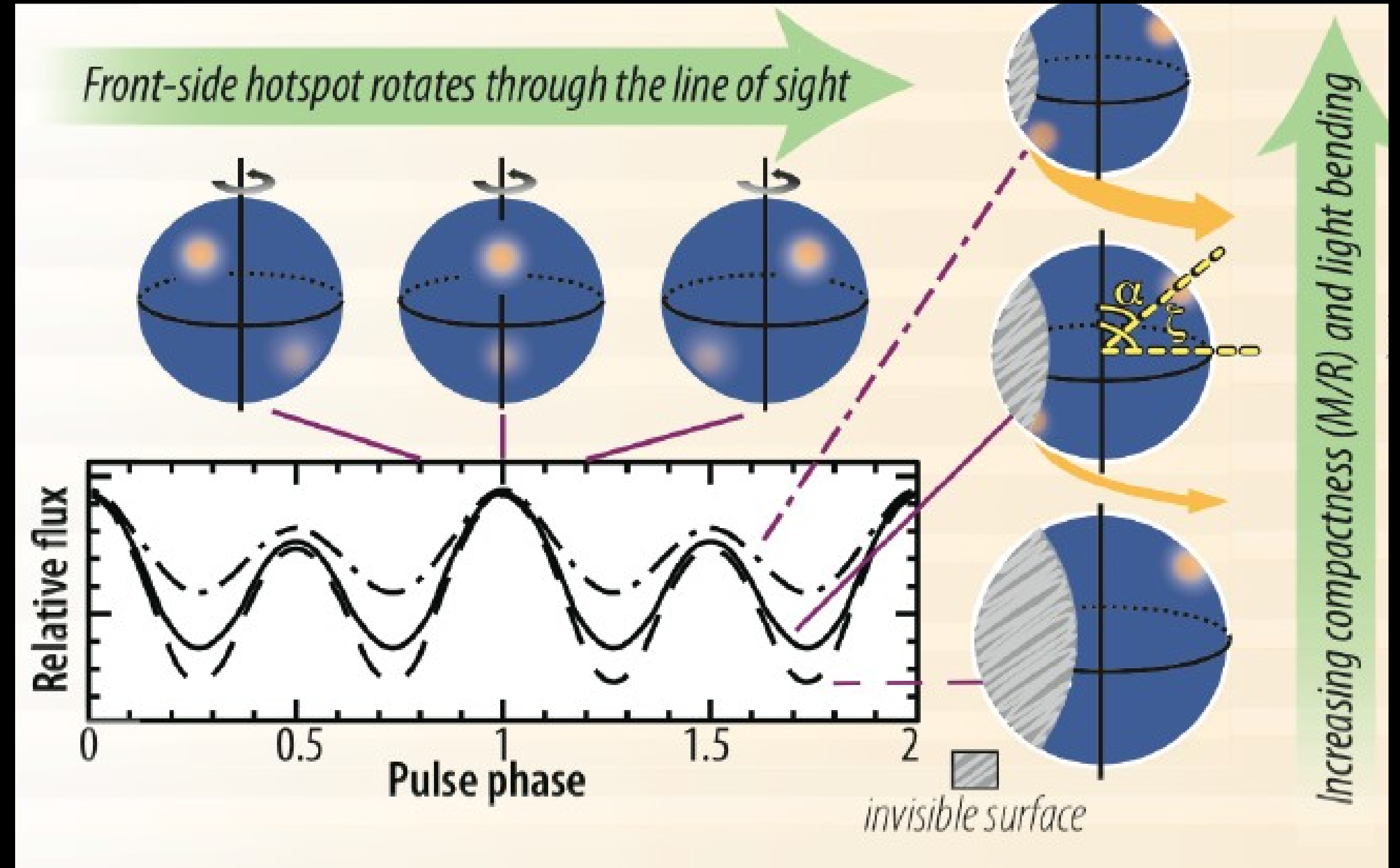
NICER: Radii from Hot Spots

Emission from rotating neutron stars with hot spots is sensitive to the space-time geometry.

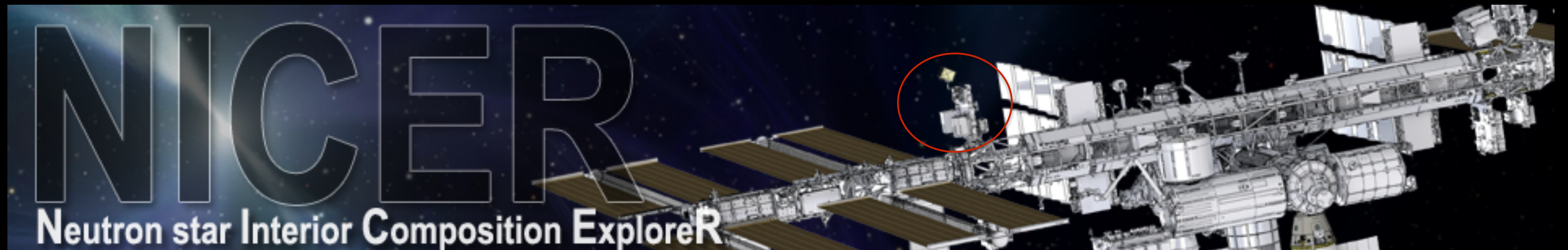
X-ray pulse profiles contain information about the source compactness.

NASA's NICER mission has acquired data from a couple of neutron stars. Models that fit data favor radii in the range of 12-14 km.

[Riley et al. \(2019\)](#), [Miller et al. \(2019\)](#)



NICER Science Overview Arzoumanian, et. al. (2014)



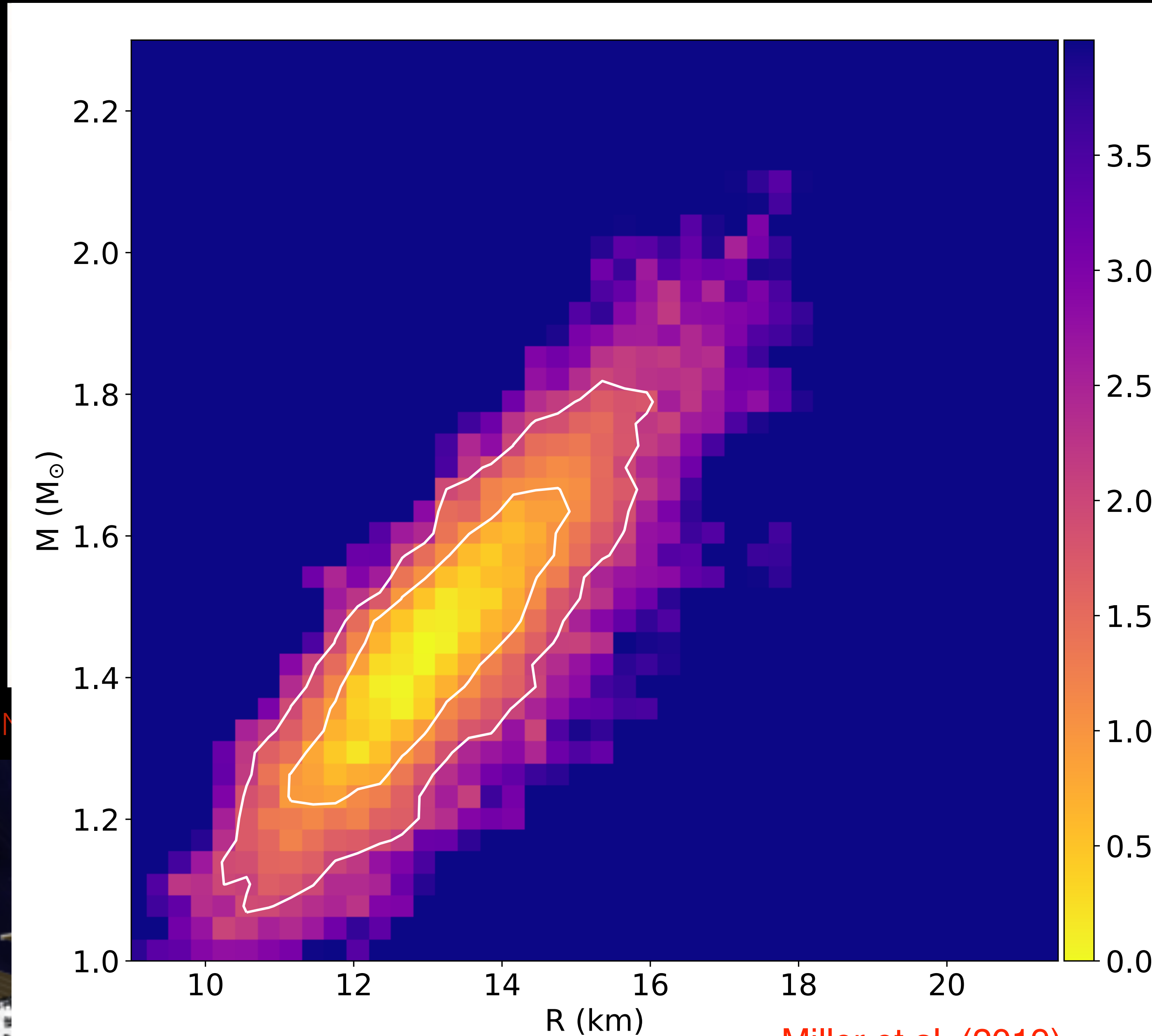
NICER: Radii from Hot Spots

Emission from rotating neutron stars with hot spots is sensitive to the space-time geometry.

X-ray pulse profiles contain information about the source compactness.

NASA's NICER mission has acquired data from a couple of neutron stars. Models that fit data favor radii in the range of 12-14 km.

[Riley et al. \(2019\)](#), [Miller et al. \(2019\)](#)



GW170817: Gravitational Waves from Neutron Stars

PRL 119, 161101 (2017)

Selected for a **Viewpoint** in *Physics*
PHYSICAL REVIEW LETTERS

week ending
20 OCTOBER 2017



GW170817: Observation of Gravitational Waves from a Binary Neutron Star Inspiral

B. P. Abbott *et al.**

(LIGO Scientific Collaboration and Virgo Collaboration)

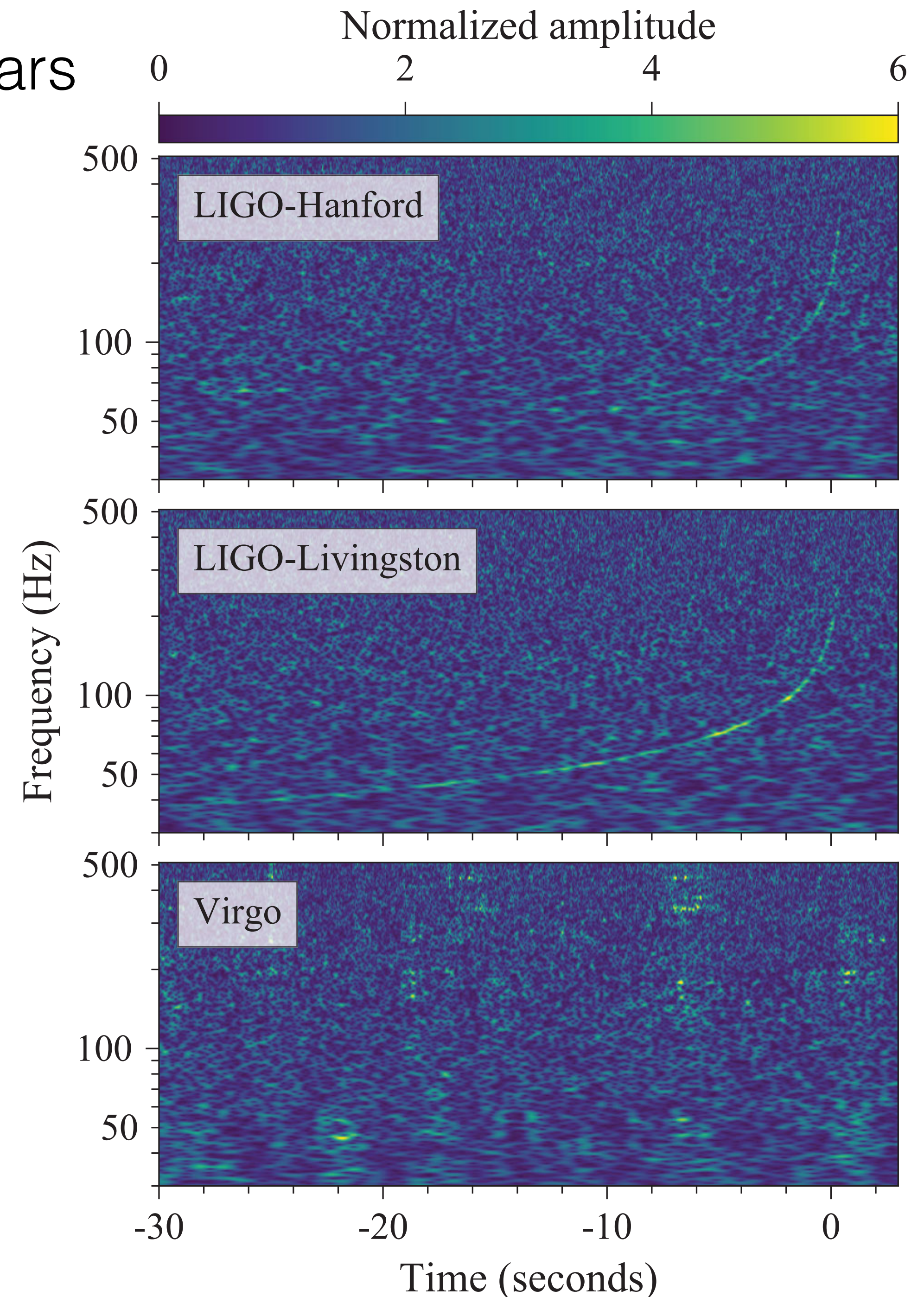
(Received 26 September 2017; revised manuscript received 2 October 2017; published 16 October 2017)

Component masses:

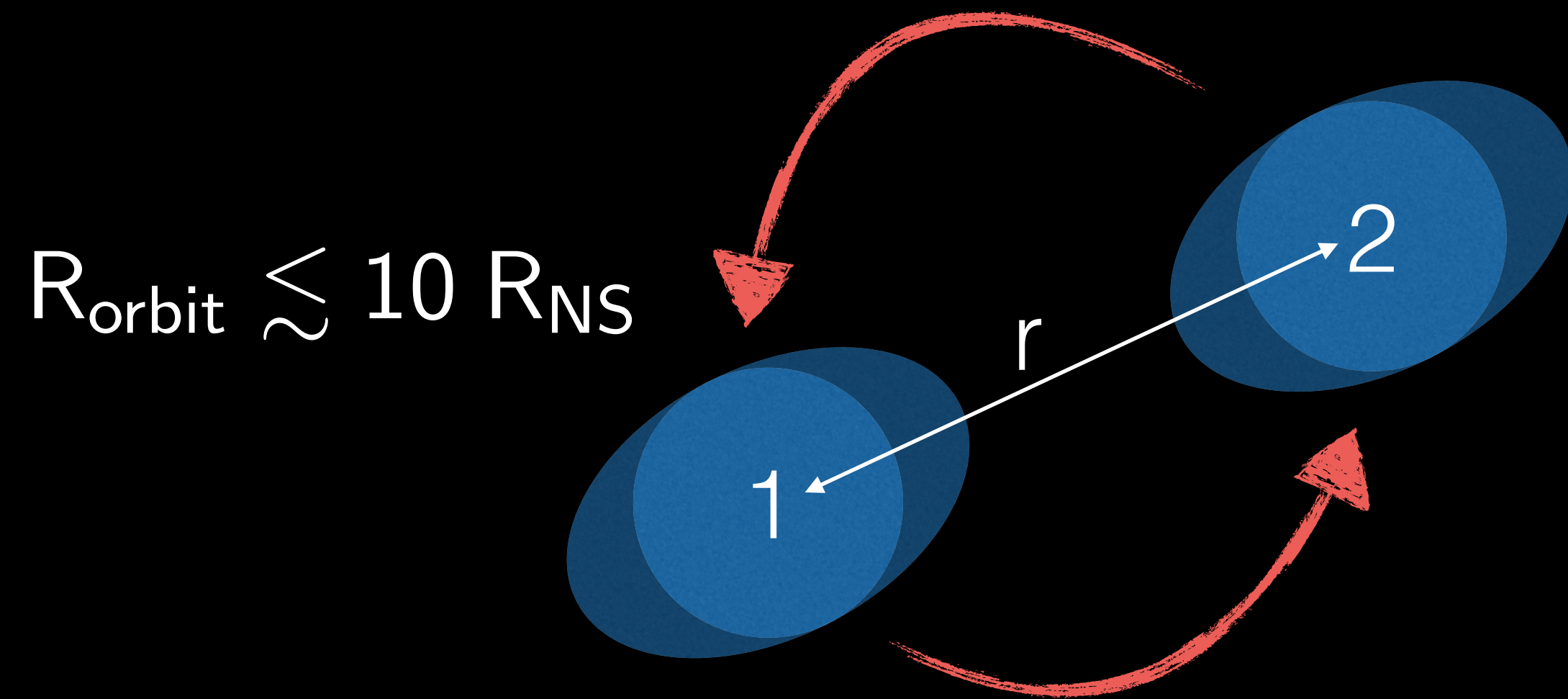
$$m_1 = 1.47 \pm 0.13 M_\odot$$
$$m_2 = 1.17 \pm 0.09 M_\odot$$

Chirp Mass: $\mathcal{M} = \frac{(m_1 m_2)^{3/5}}{(m_1 + m_2)^{1/5}} = 1.188^{+0.004}_{-0.002} M_\odot$

Total Mass: $M = m_1 + m_2 = 2.74^{+0.04}_{-0.01} M_\odot$



Tidal Deformation: Measuring the Radius with GWs



Tidal forces deform neutron stars.
Induces a quadrupole moment.

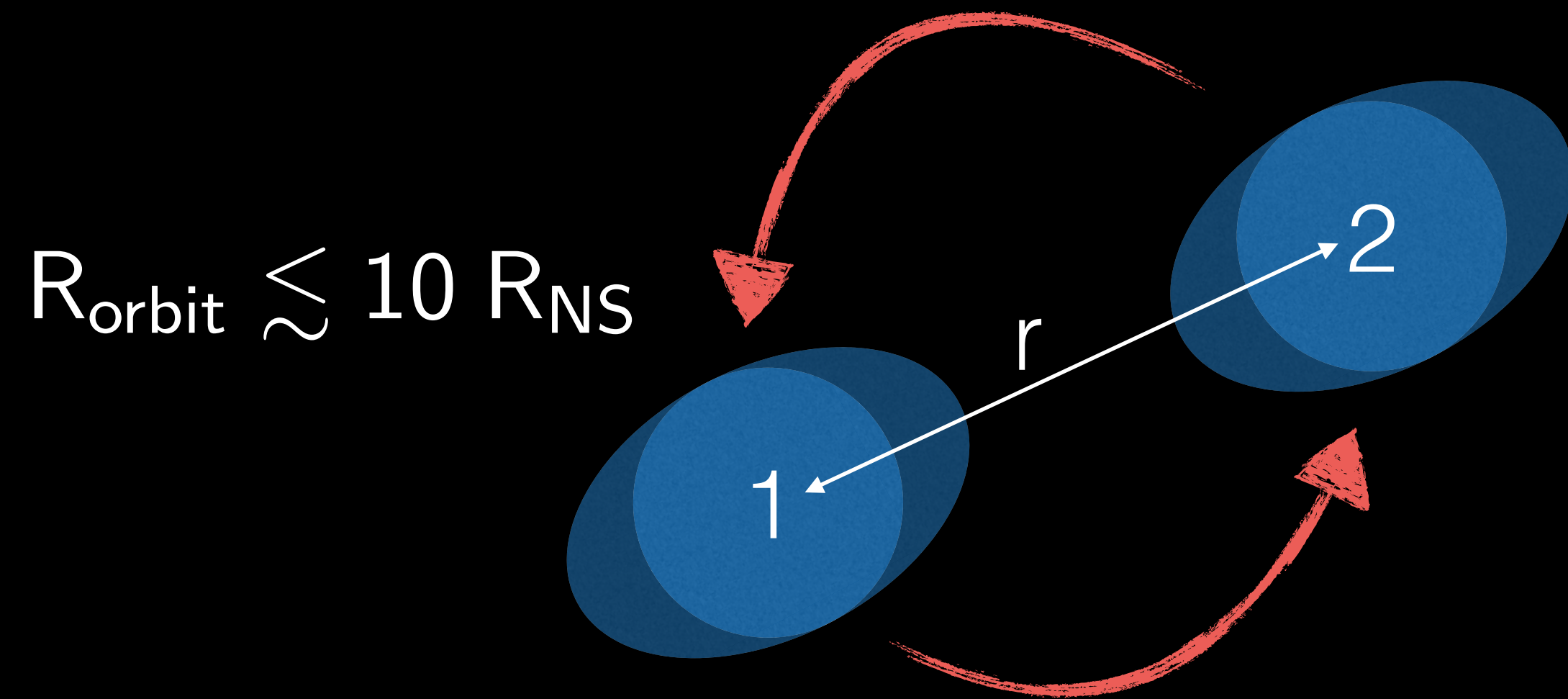
$$Q_{xy} = \lambda E_{xy}$$

↑
tidal deformability

$$E_{xy} = -\frac{\partial^2 V_G}{\partial x \partial y}$$

↑
external field

Tidal Deformation: Measuring the Radius with GWs



Tidal forces deform neutron stars.
Induces a quadrupole moment.

$$Q_{xy} = \lambda E_{xy}$$

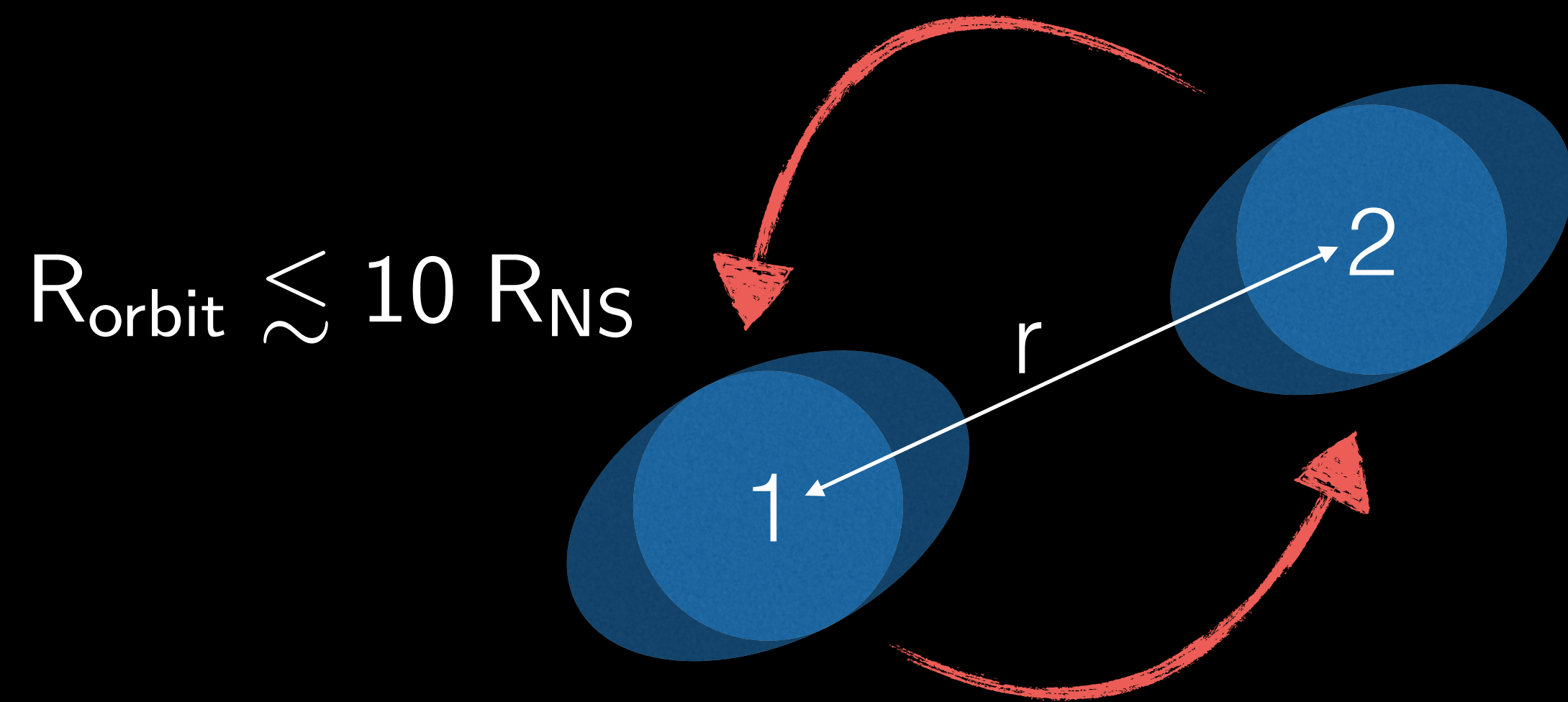
↑
tidal deformability

$$E_{xy} = -\frac{\partial^2 V_G}{\partial x \partial y}$$

↑
external field

Tidal interactions change the rotational phase: $\delta\Phi = -\frac{117}{256} v^5 \frac{M}{\mu} \tilde{\Lambda}$

Tidal Deformation: Measuring the Radius with GWs



Tidal forces deform neutron stars.
Induces a quadrupole moment.

$$Q_{xy} = \lambda E_{xy}$$

↑
tidal deformability

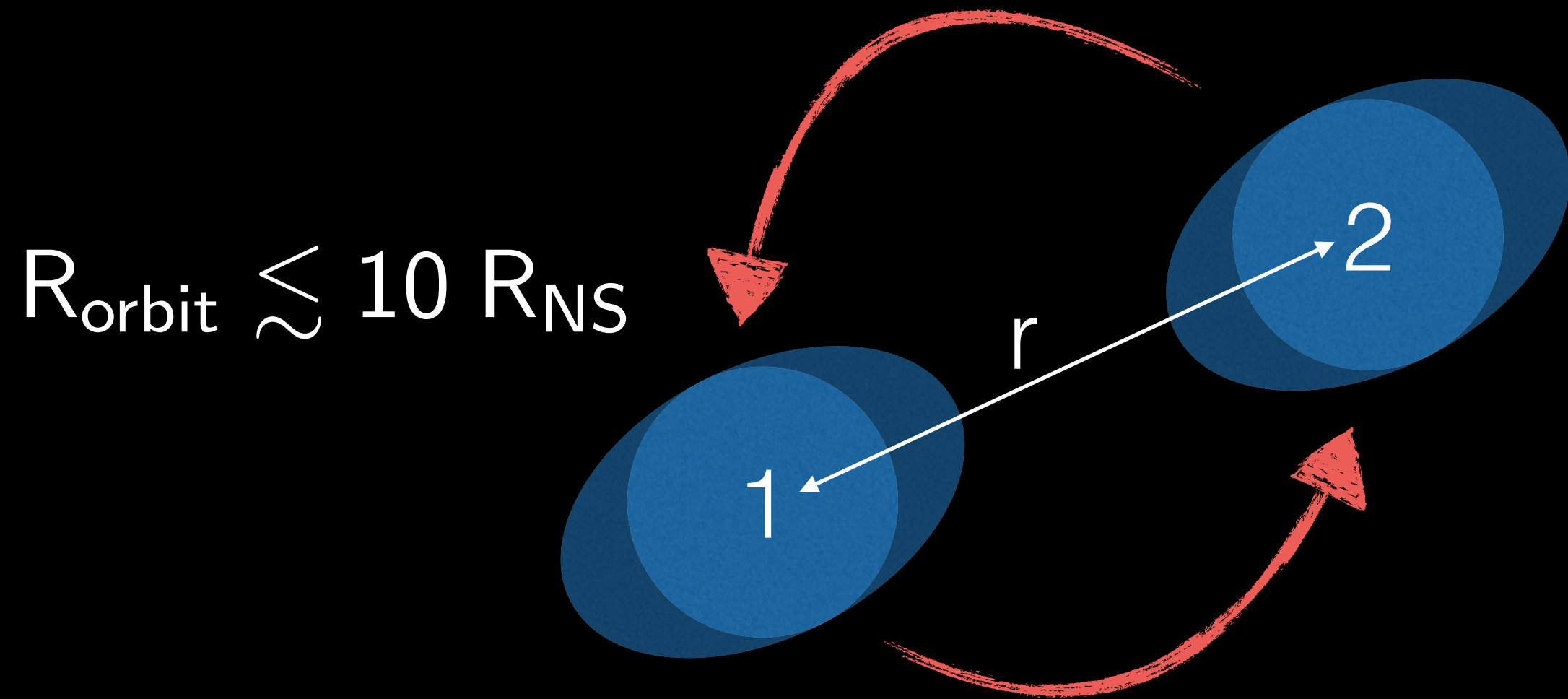
$$E_{xy} = -\frac{\partial^2 V_G}{\partial x \partial y}$$

↑
external field

Tidal interactions change the rotational phase: $\delta\Phi = -\frac{117}{256} v^5 \frac{M}{\mu} \tilde{\Lambda}$

Tidal deformations are large for a large NS: $\Lambda_i = \frac{\lambda_i}{M_i^5} = k_2 \frac{R_i^5}{M_i^5}$

Tidal Deformation: Measuring the Radius with GWs



Tidal forces deform neutron stars.
Induces a quadrupole moment.

$$Q_{xy} = \lambda E_{xy}$$

↑ tidal deformability

$$E_{xy} = -\frac{\partial^2 V_G}{\partial x \partial y}$$

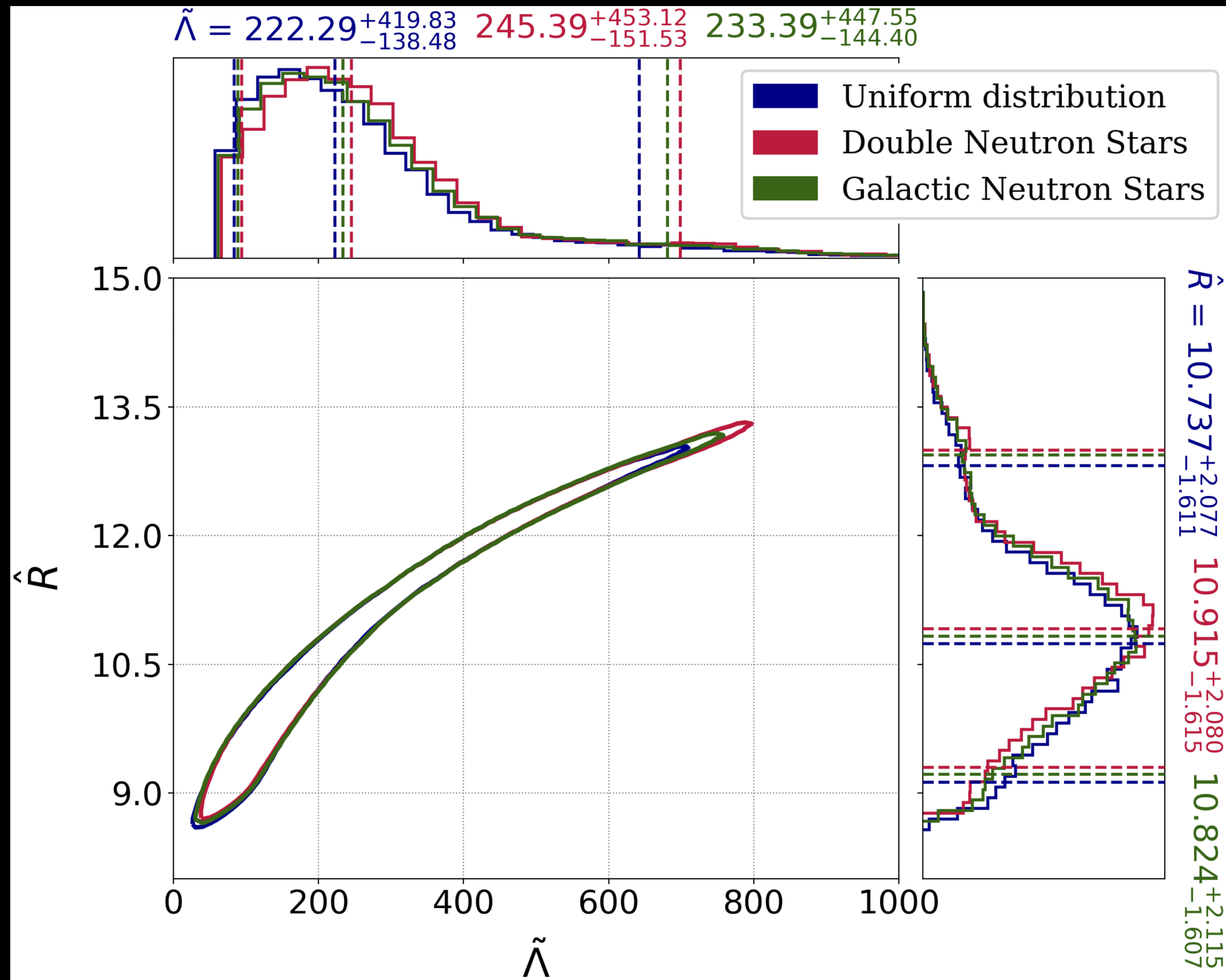
↑ external field

Tidal interactions change the rotational phase: $\delta\Phi = -\frac{117}{256} v^5 \frac{M}{\mu} \tilde{\Lambda}$

Dimensionless binary tidal deformability: $\tilde{\Lambda} = \frac{16}{13} \left(\left(\frac{M_1}{M} \right)^5 \left(1 + \frac{M_2}{M_1} \right) \Lambda_1 + 1 \leftrightarrow 2 \right)$

Tidal deformations are large for a large NS: $\Lambda_i = \frac{\lambda_i}{M_i^5} = k_2 \frac{R_i^5}{M_i^5}$

Bounds on the Neutron Star Radius from Observations



Tidal deformations (not) observed in GW170817 implies a small NS radius:

$$R < 13 \text{ km}$$

Requiring a maximum mass greater than $2 M_{\text{sun}}$ implies:

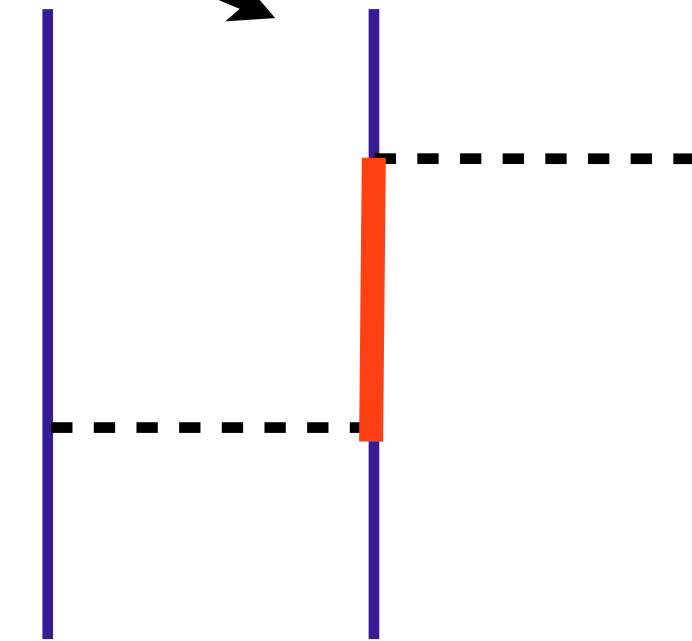
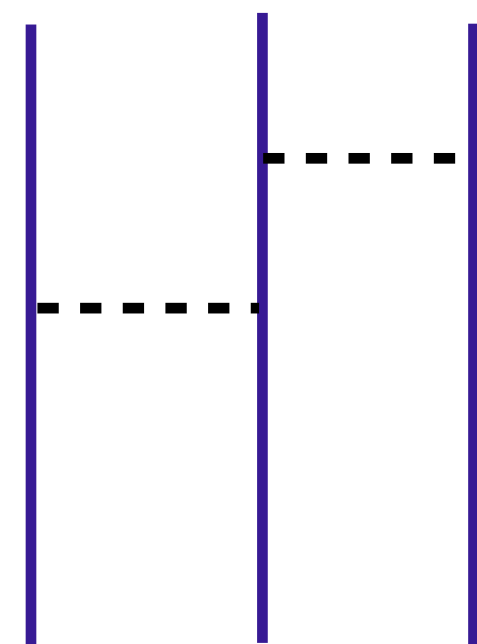
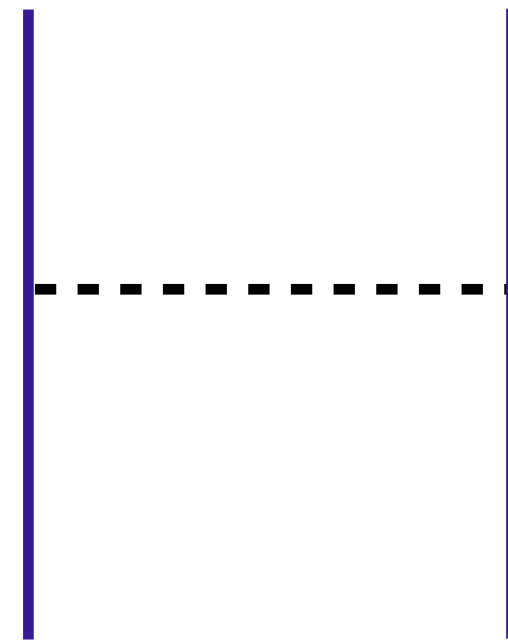
$$R > 9 \text{ km}$$

De et al. PRL (2018)

See also LIGO and Virgo Scientific Collaboration arXiv:1805.11581v1

Nuclear Interactions and Many Body Theory

$$H_{\text{nuclear}} = \frac{\nabla^2}{2M} + V_{\text{NN}} + V_{\text{NNN}} + \dots$$

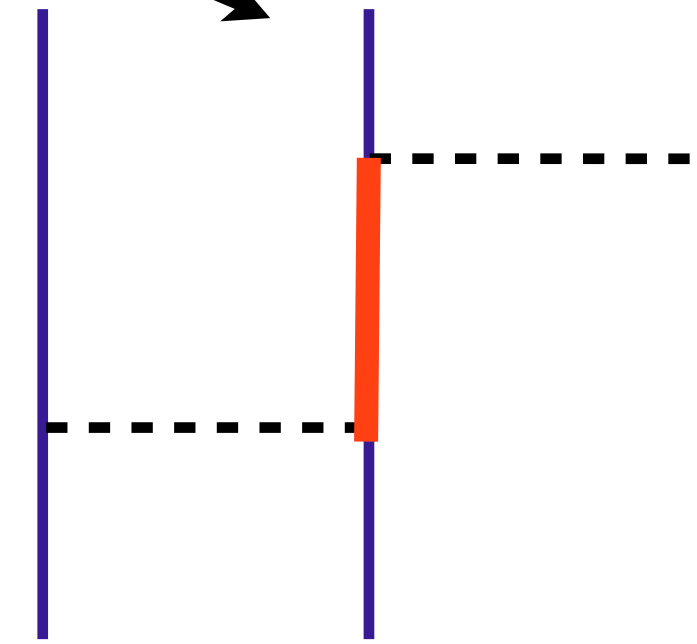
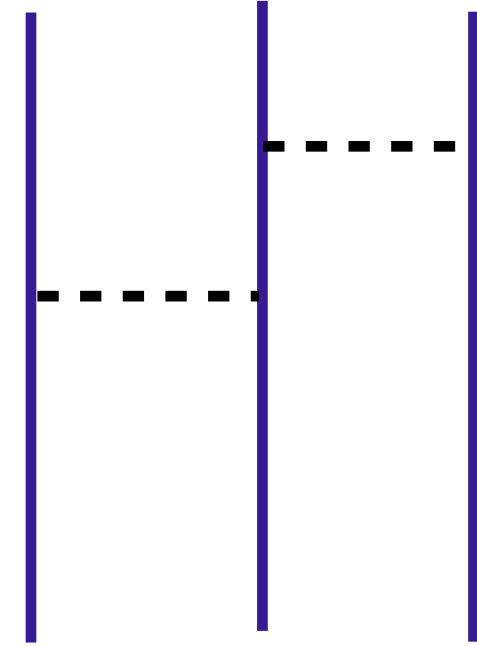
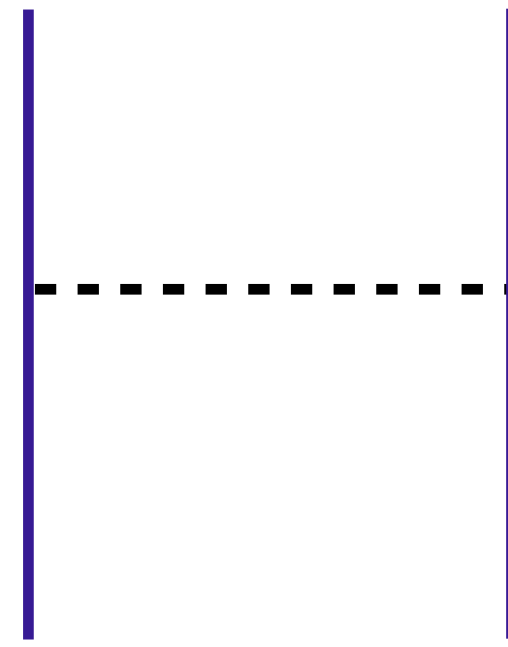


The potential between two neutrons at low energy is well constrained by scattering data but interactions at short distances are model dependent.

Constraints on the three-neutron potential are weaker.

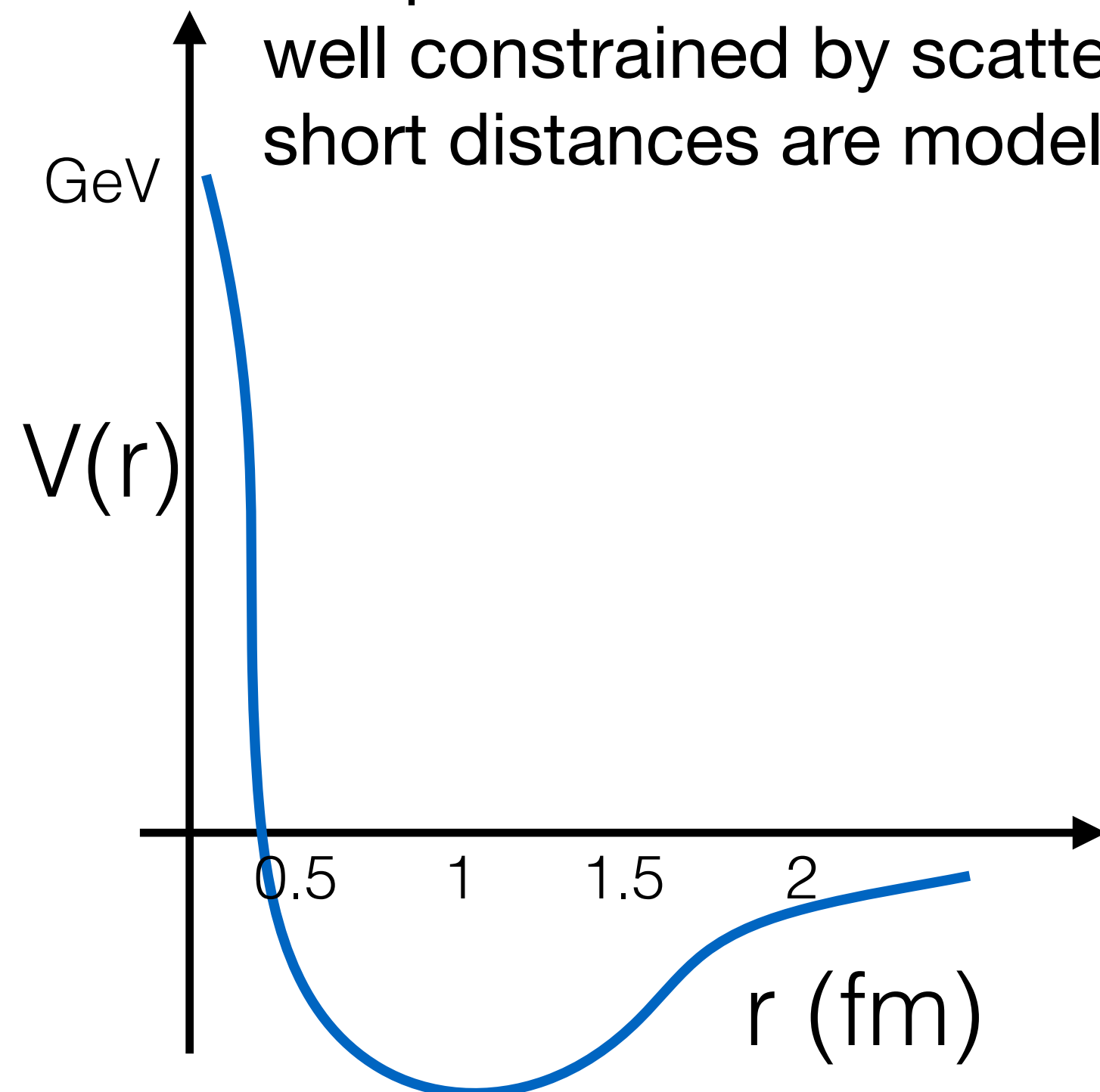
Nuclear Interactions and Many Body Theory

$$H_{\text{nuclear}} = \frac{\nabla^2}{2M} + V_{\text{NN}} + V_{\text{NNN}} + \dots$$



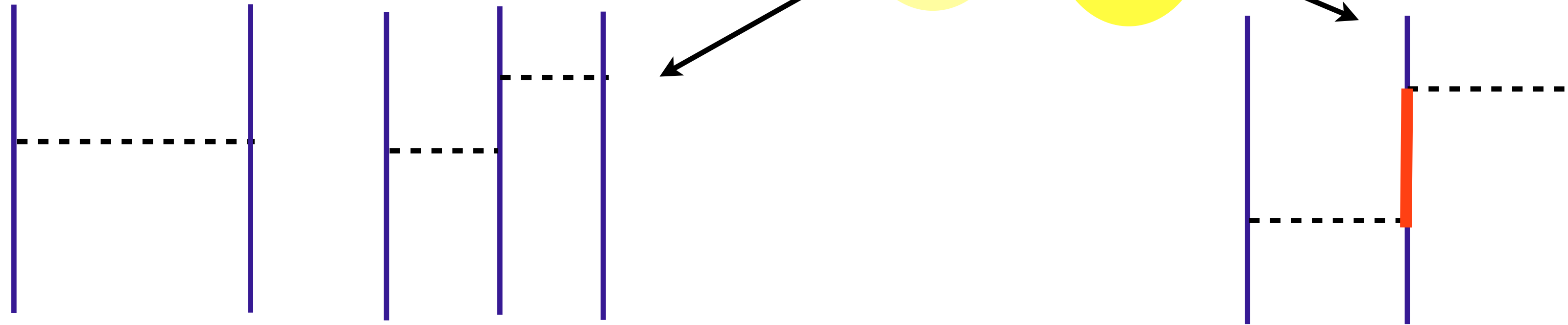
The potential between two neutrons at low energy is well constrained by scattering data but interactions at short distances are model dependent.

Constraints on the three-neutron potential are weaker.



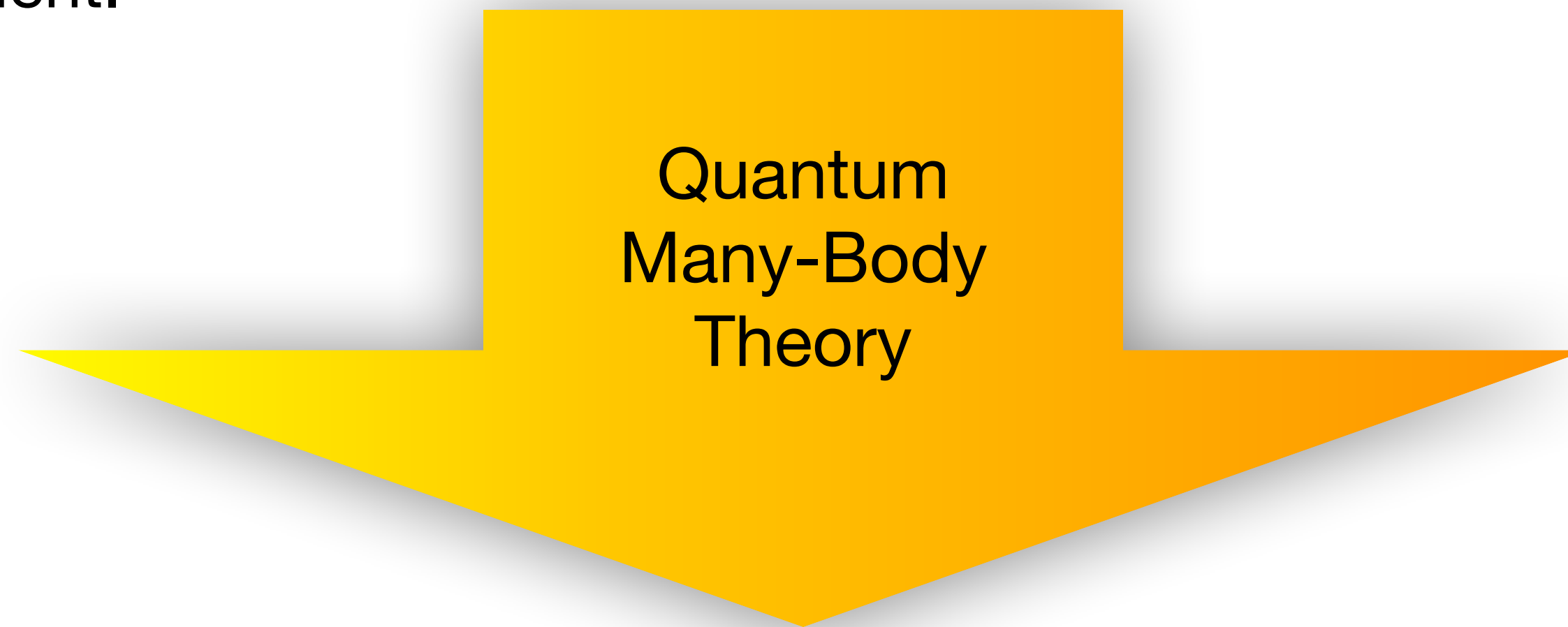
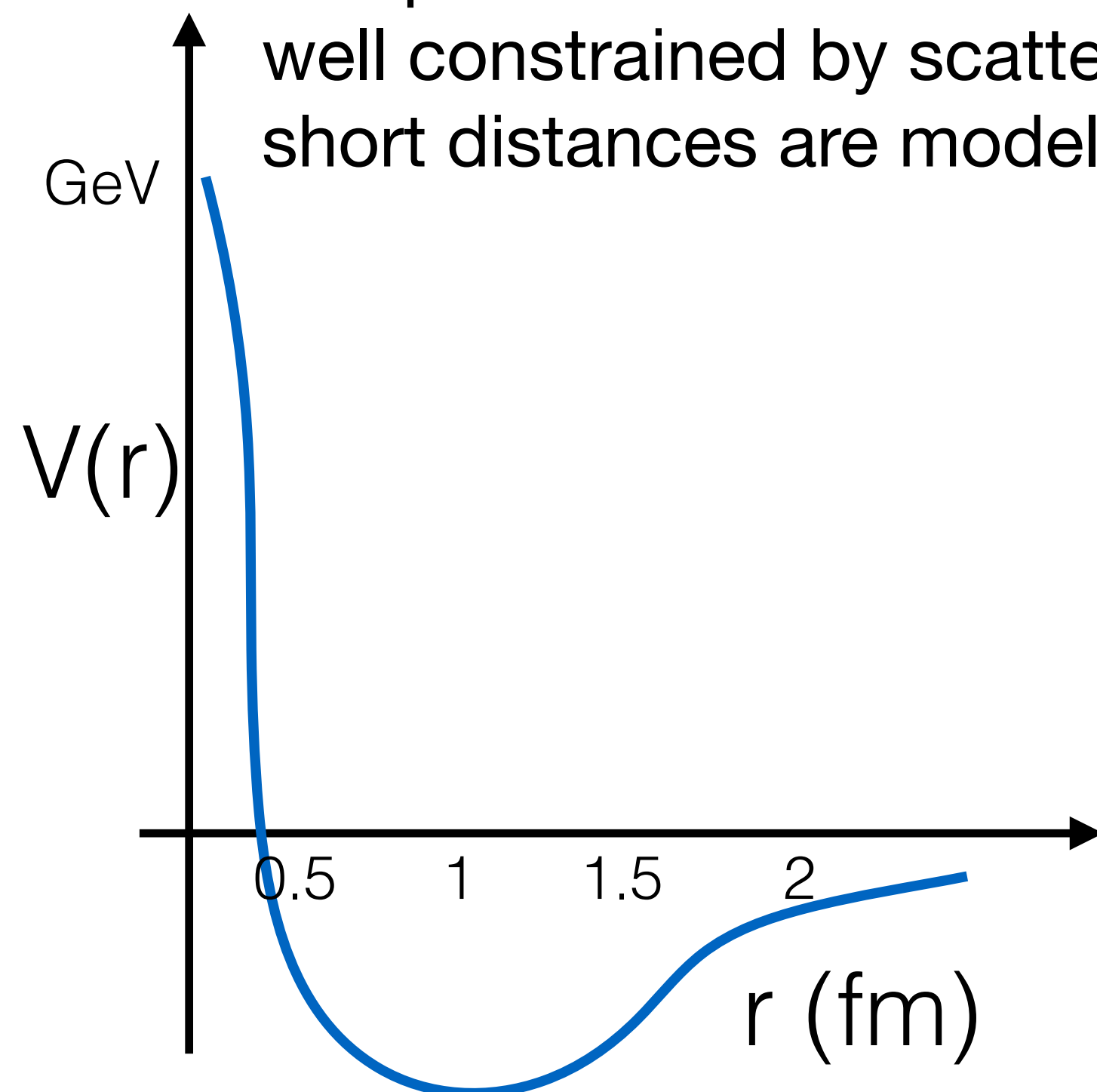
Nuclear Interactions and Many Body Theory

$$H_{\text{nuclear}} = \frac{\nabla^2}{2M} + V_{\text{NN}} + V_{\text{NNN}} + \dots$$



The potential between two neutrons at low energy is well constrained by scattering data but interactions at short distances are model dependent.

Constraints on the three-neutron potential are weaker.



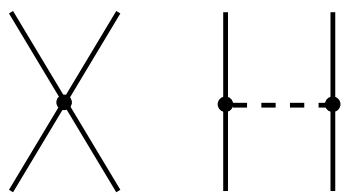
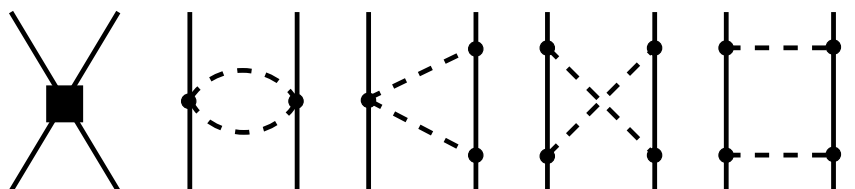
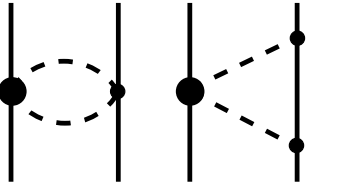
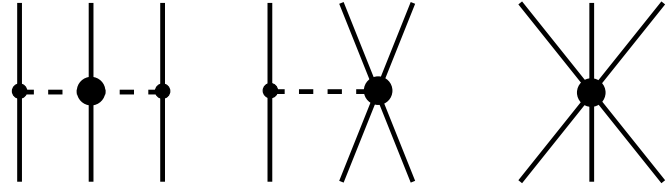
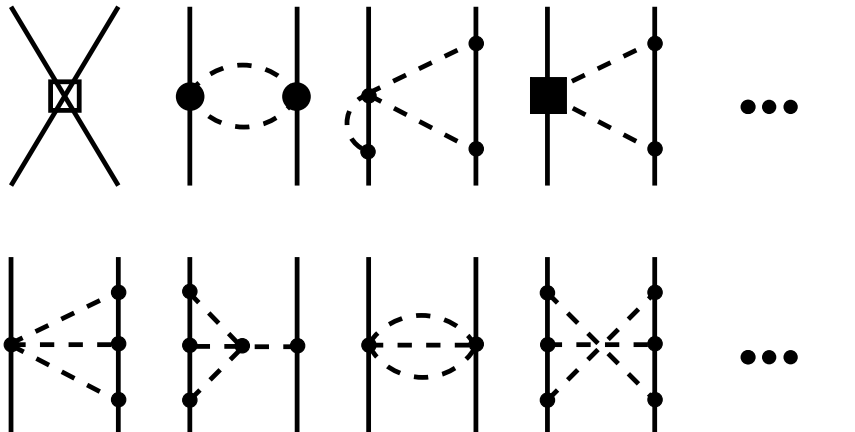
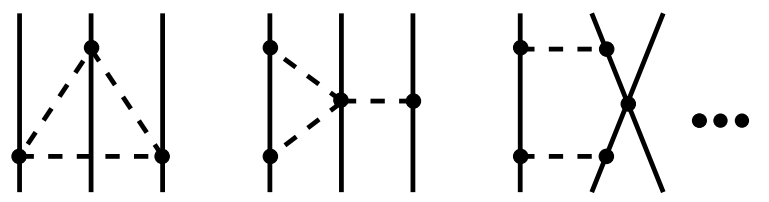
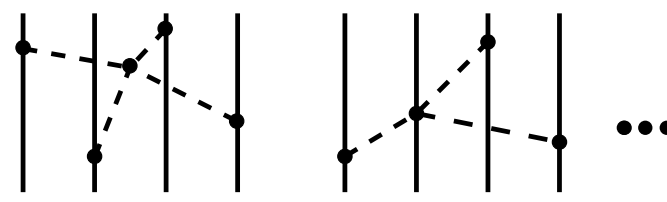
$E(\rho_n, \rho_p)$ & Equation of State

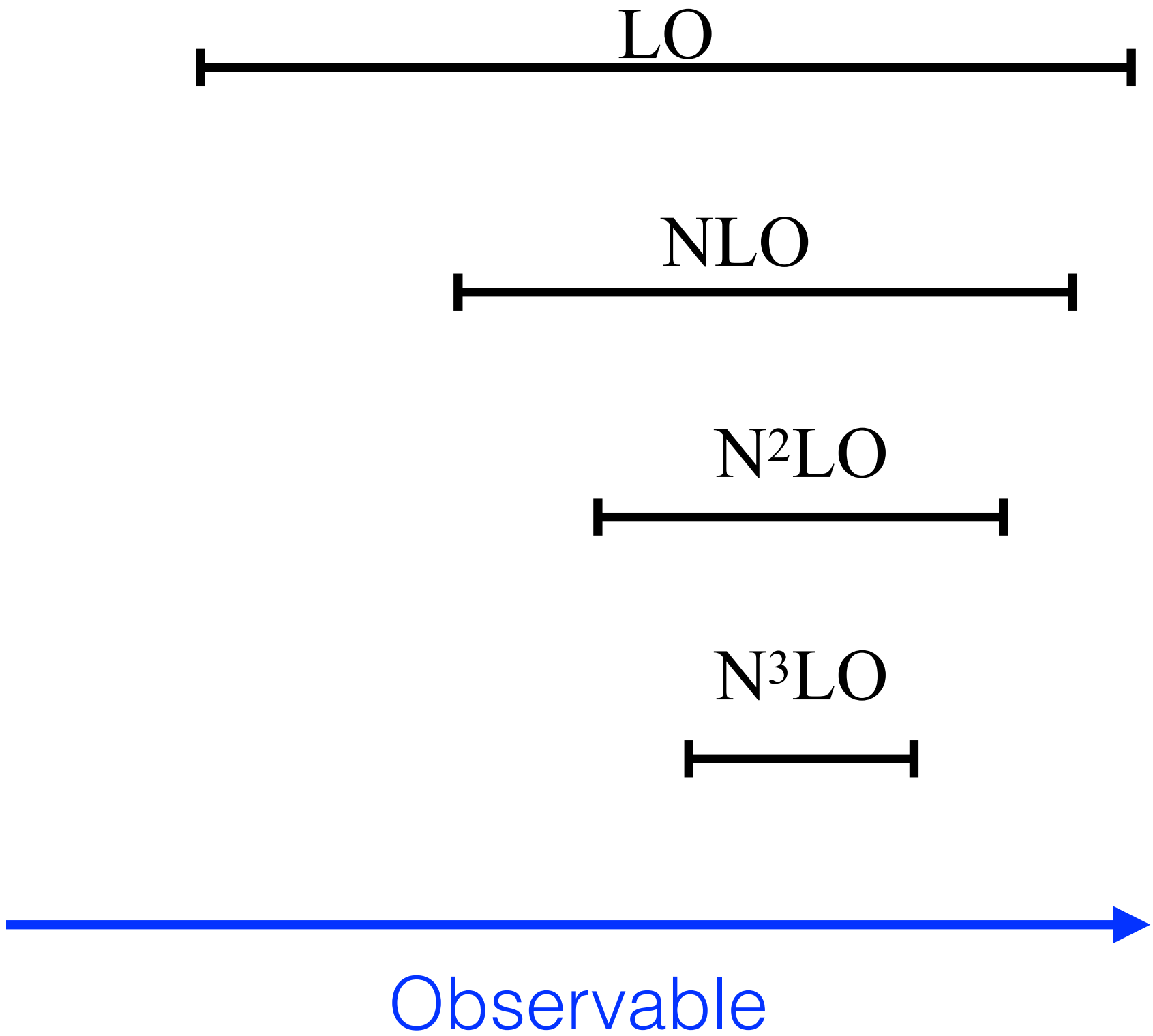
Modern NN & NNN Forces

EFT inspired Hamiltonians organizes operators in powers of the momentum:

$$\frac{Q}{\Lambda_B}$$

$$\Lambda_B \simeq 500 - 600 \text{ MeV}$$

	2N force	3N force	4N force
LO		—	—
NLO		—	—
N ² LO			—
N ³ LO			



Allows for error estimation*. Provides guidance for the structure of three and many-body forces.

Beane, Bedaque, Epelbaum, Kaplan, Machliedt, Meisner, Phillips, Savage, **van Klock**, **Weinberg**, Wise ..

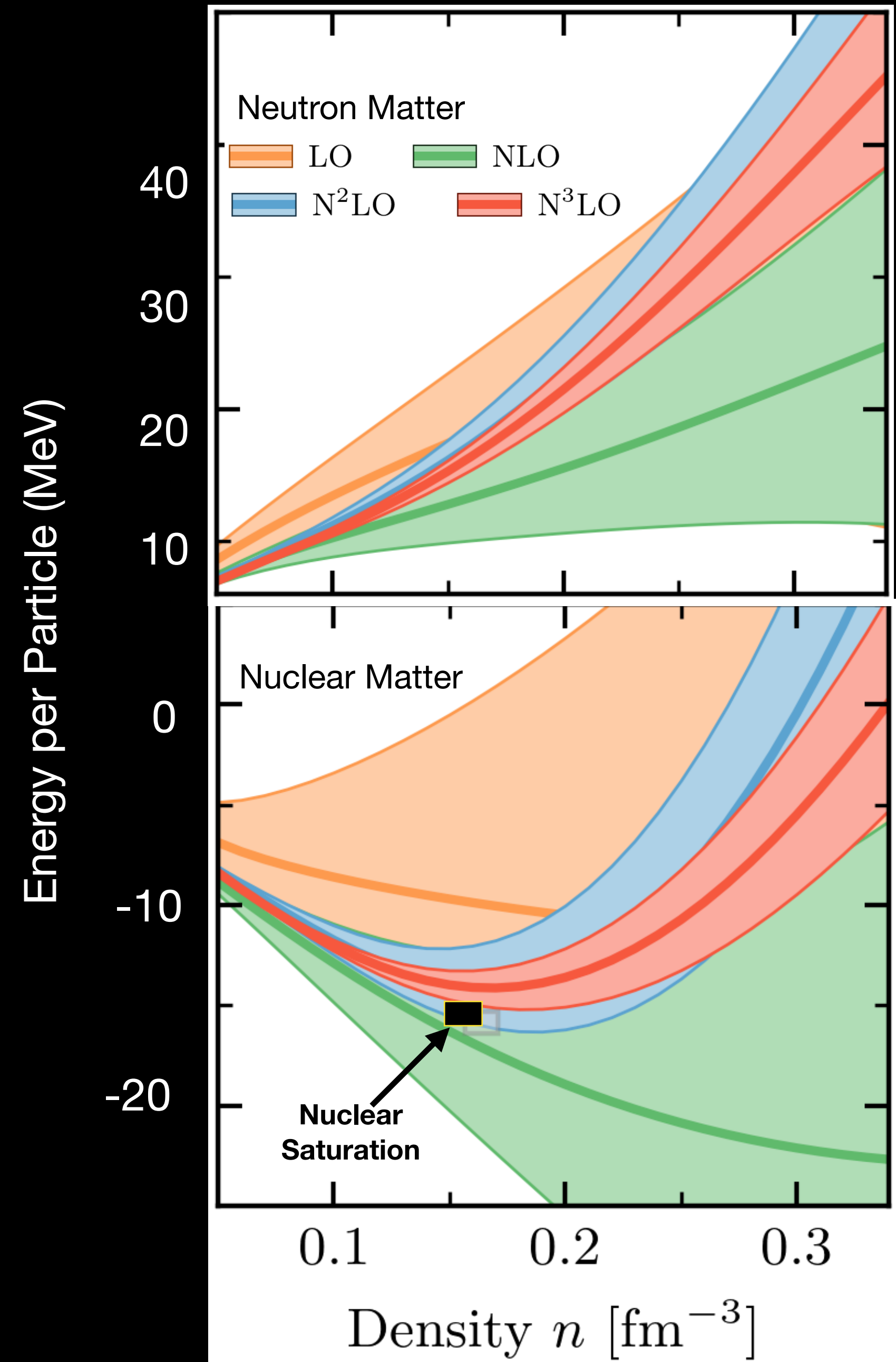
Equation of State of Dense Matter: With Error Estimates.

Many-body calculations provide useful error estimates.

Hebeler and Schwenk (2009),
Gandolfi, Carlson, Reddy (2010), Gezerlis et al. (2013), Tews, Kruger, Hebeler, Schwenk (2013), Holt Kaiser, Weise (2013), Hagen et al. (2013), Roggero, Mukherjee, Pederiva (2014), Wlazlowski, Holt, Moroz, Bulgac, Roche (2014), Lynn et al. (2015), Tews et al. (2018), Drischler et al., (2020).

Calculations suggest that EFT converges up to about twice nuclear saturation density ($\sim 5 \times 10^{14} \text{ g/cm}^3$)

Tews, Carlson, Gandolfi, Reddy (2018)
Drischler, Furnstahl, Melendez, Phillips, (2020).



Drischler et al., (2020).

Chiral-EFT Calculations of Neutron-rich Matter



Finally, a scheme to estimate errors. Several useful insights about 2 and 3 body forces.

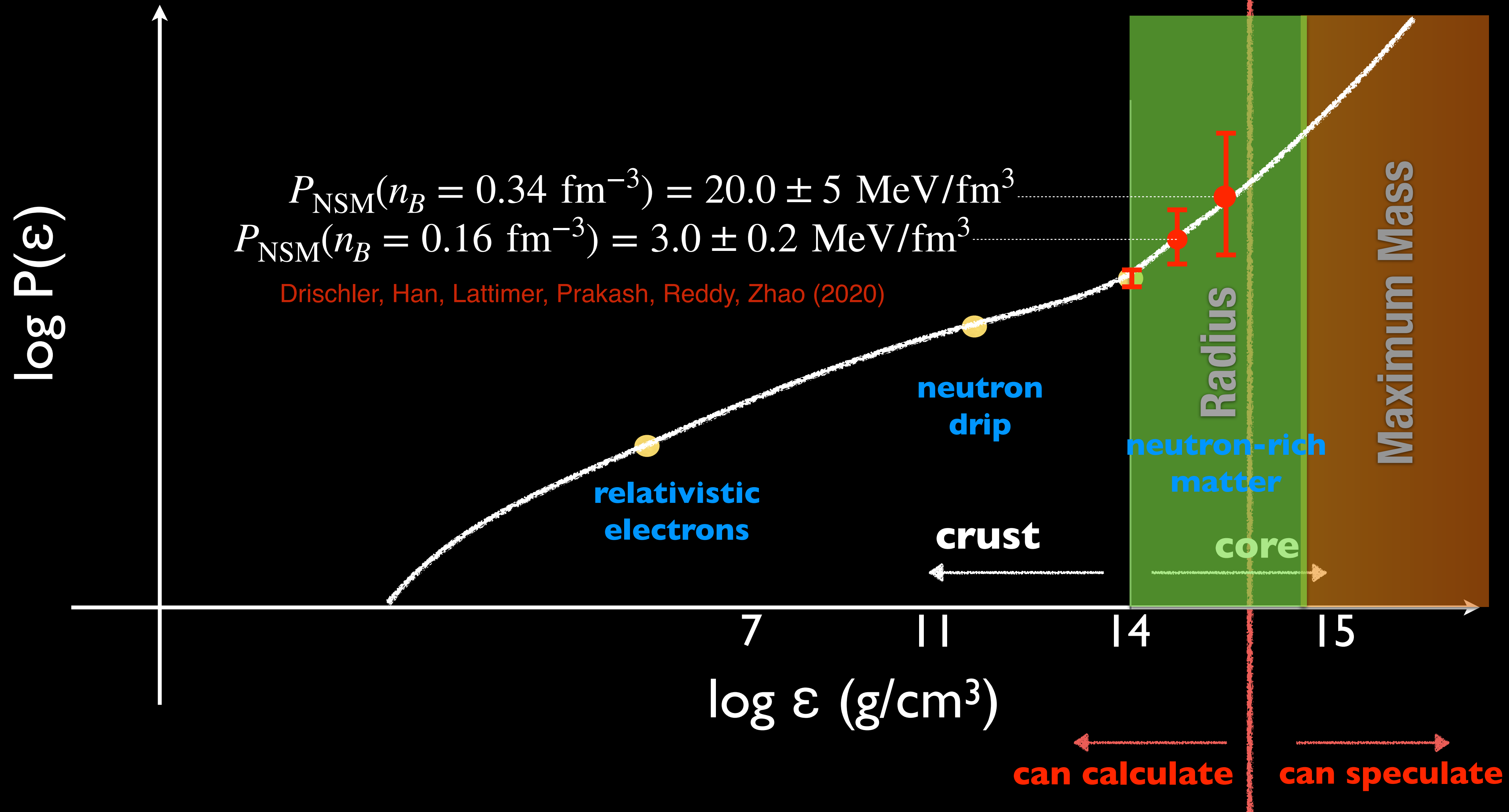


The expansion parameter is not small. Further work is needed to understand convergences and improved error estimates. Does including the Δ lead to improved convergence?

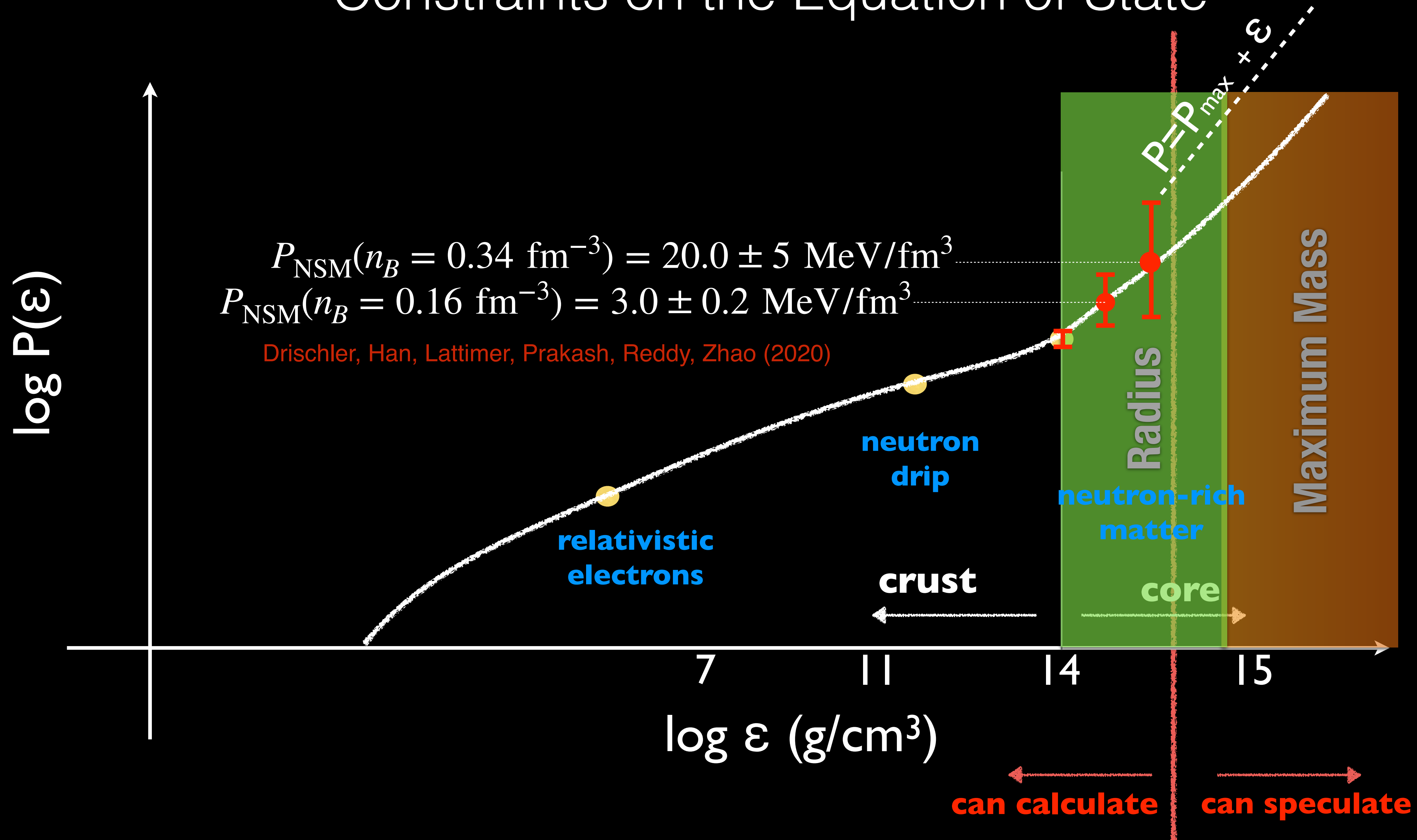


The regulator artifacts are not well understood.

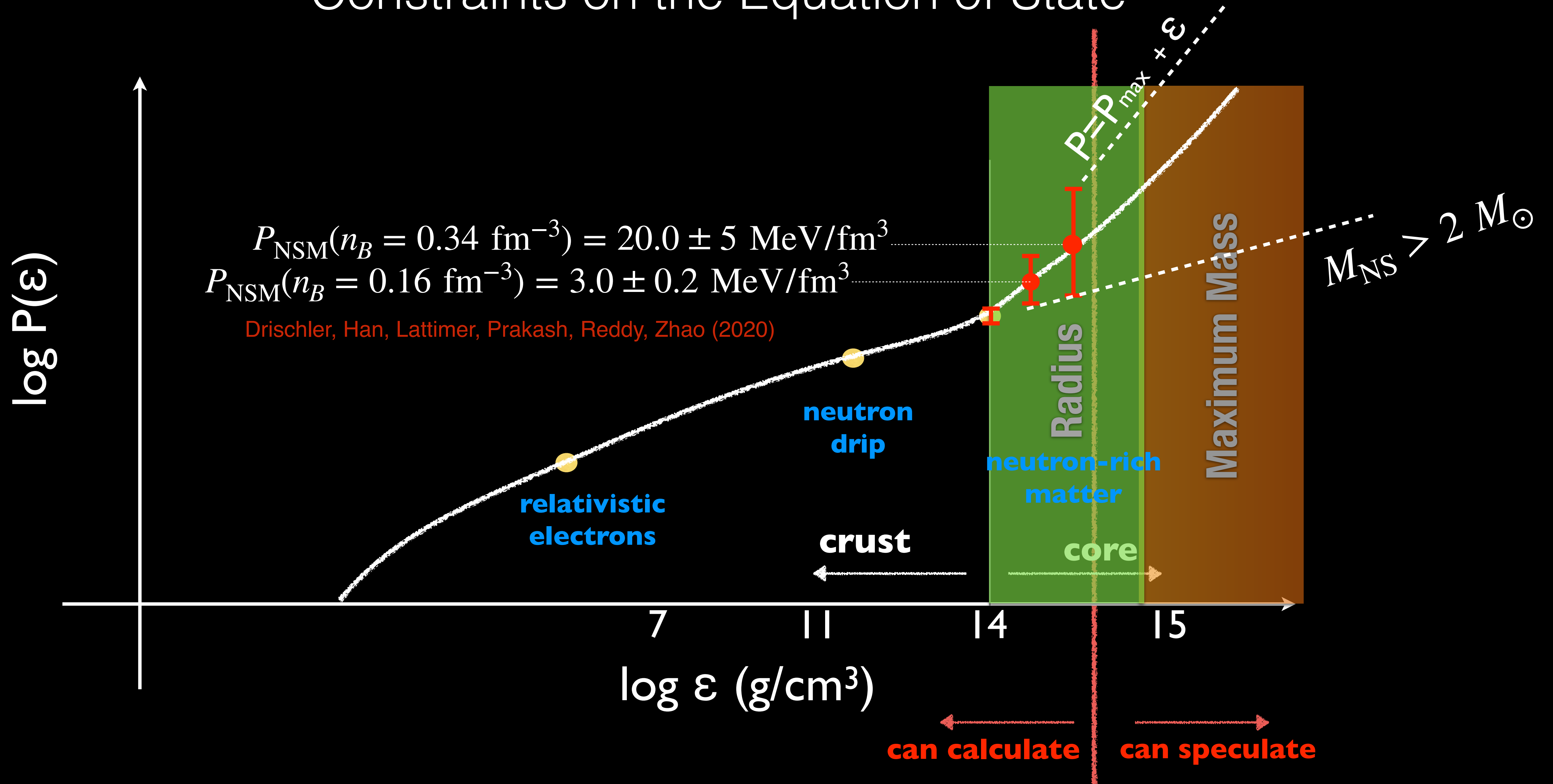
Constraints on the Equation of State



Constraints on the Equation of State



Constraints on the Equation of State



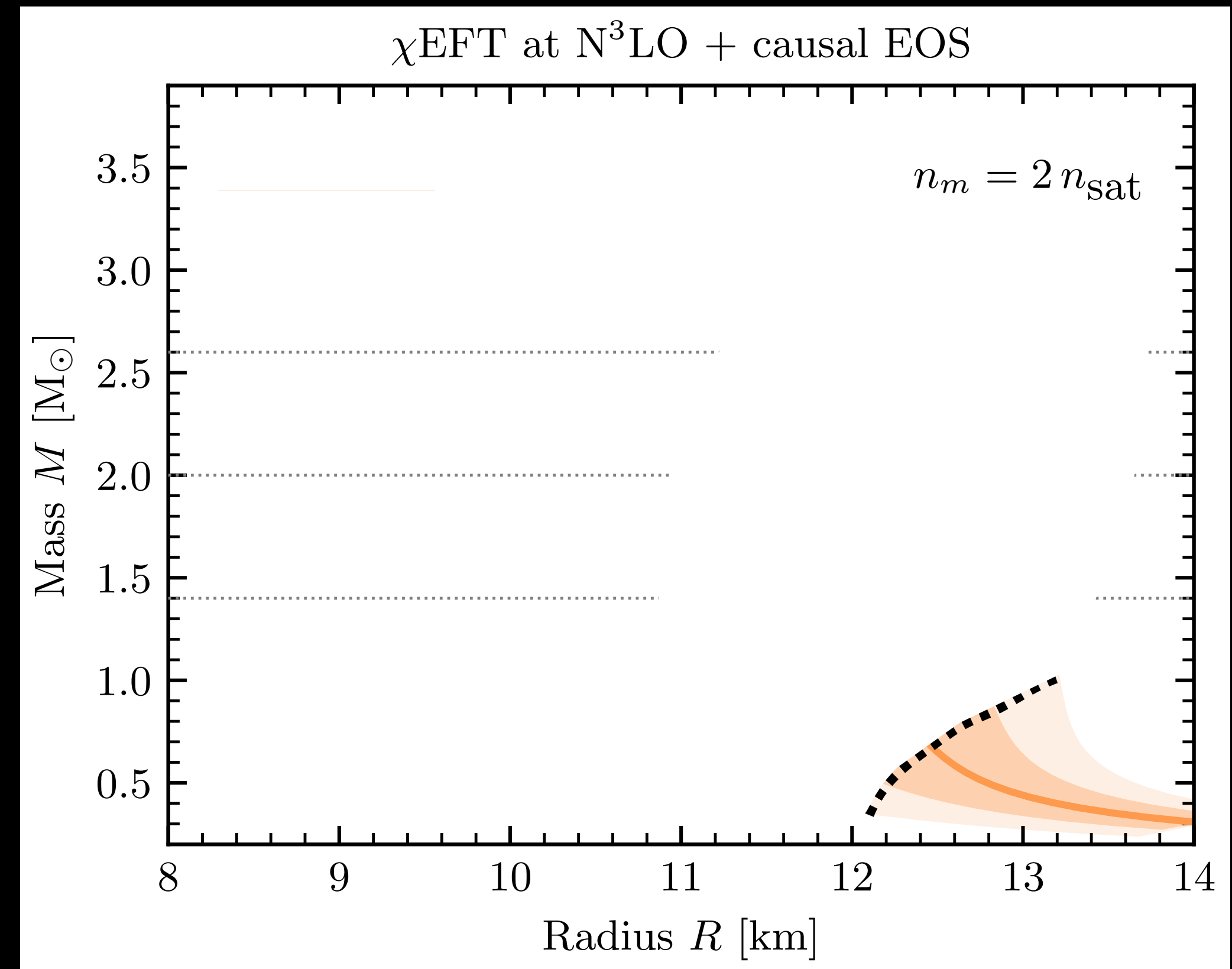
Bounds on Neutron Star Radii

EFT predictions for the EOS can be combined with extremal high-density EOS (with $c_s^2 = 1$) to derive bounds on the radius of NSs of any mass.

The lower limit on the NS maximum mass obtained from observations strengthen these bounds:

- $M_{\max} > 2.0 M_{\odot}$, $9.2 \text{ kms} < R_{1.4} < 13.2 \text{ kms}$
- $M_{\max} > 2.6 M_{\odot}$, $11.2 \text{ kms} < R_{1.4} < 13.2 \text{ kms}$

If $R_{1.4} < 11 \text{ km}$ or if $R_{1.4} > 13 \text{ km}$, it would imply a very large speed of sound in the cores of massive neutron stars.



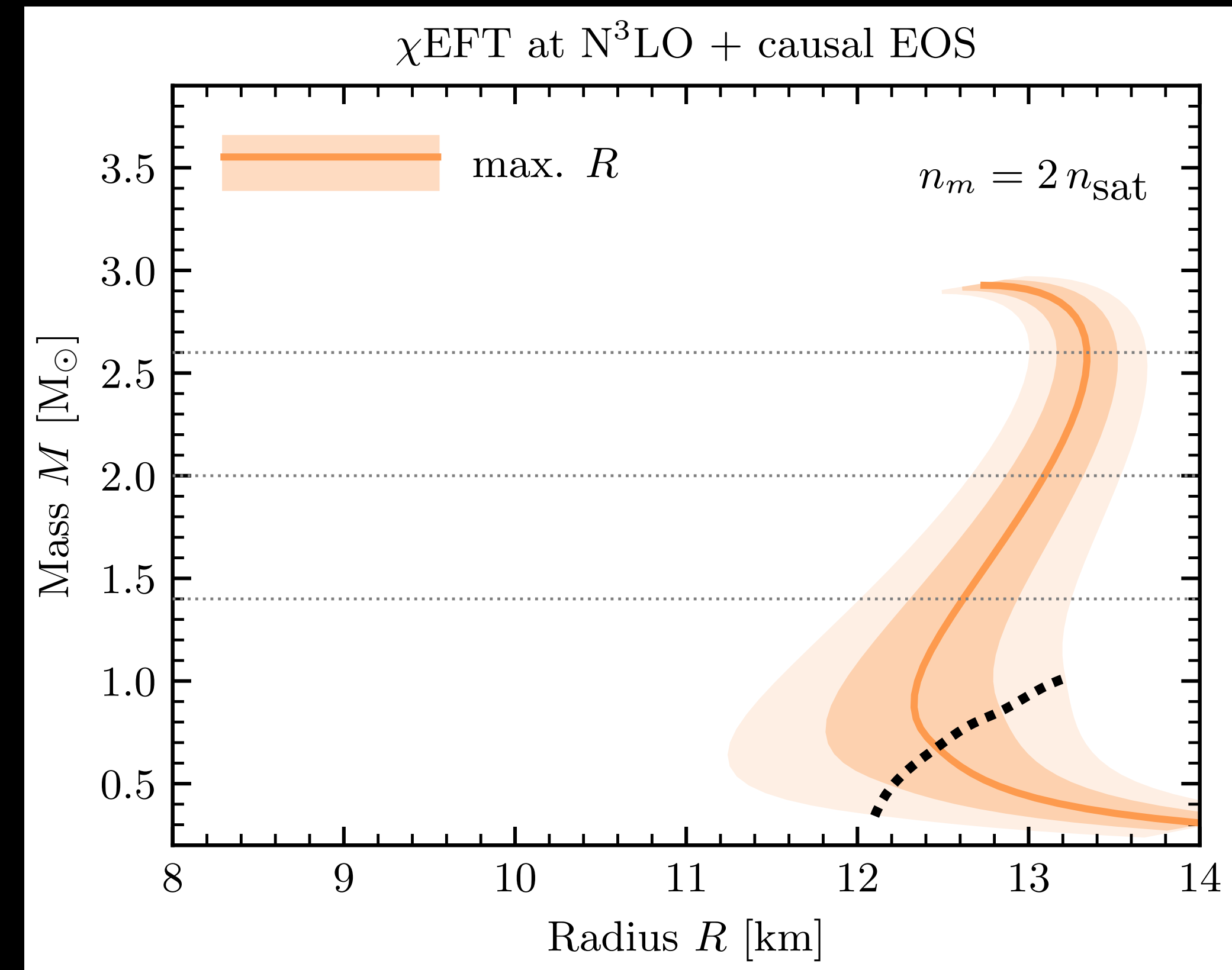
Bounds on Neutron Star Radii

EFT predictions for the EOS can be combined with extremal high-density EOS (with $c_s^2 = 1$) to derive bounds on the radius of NSs of any mass.

The lower limit on the NS maximum mass obtained from observations strengthen these bounds:

- $M_{\text{max}} > 2.0 M_{\odot}$, $9.2 \text{ kms} < R_{1.4} < 13.2 \text{ kms}$
- $M_{\text{max}} > 2.6 M_{\odot}$, $11.2 \text{ kms} < R_{1.4} < 13.2 \text{ kms}$

If $R_{1.4} < 11 \text{ km}$ or if $R_{1.4} > 13 \text{ km}$, it would imply a very large speed of sound in the cores of massive neutron stars.



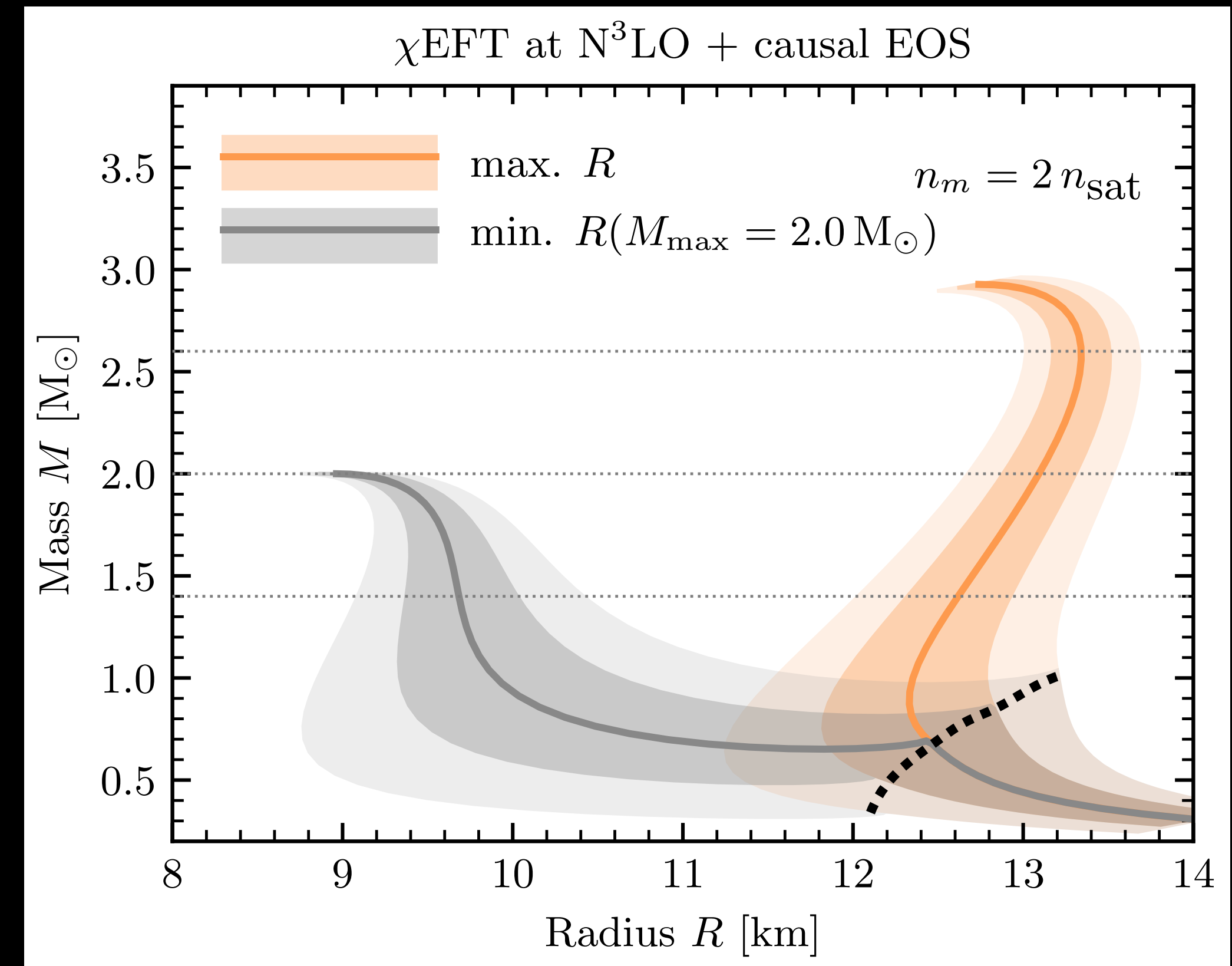
Bounds on Neutron Star Radii

EFT predictions for the EOS can be combined with extremal high-density EOS (with $c_s^2 = 1$) to derive bounds on the radius of NSs of any mass.

The lower limit on the NS maximum mass obtained from observations strengthen these bounds:

- $M_{\max} > 2.0 M_{\odot}$, $9.2 \text{ kms} < R_{1.4} < 13.2 \text{ kms}$
- $M_{\max} > 2.6 M_{\odot}$, $11.2 \text{ kms} < R_{1.4} < 13.2 \text{ kms}$

If $R_{1.4} < 11 \text{ km}$ or if $R_{1.4} > 13 \text{ km}$, it would imply a very large speed of sound in the cores of massive neutron stars.



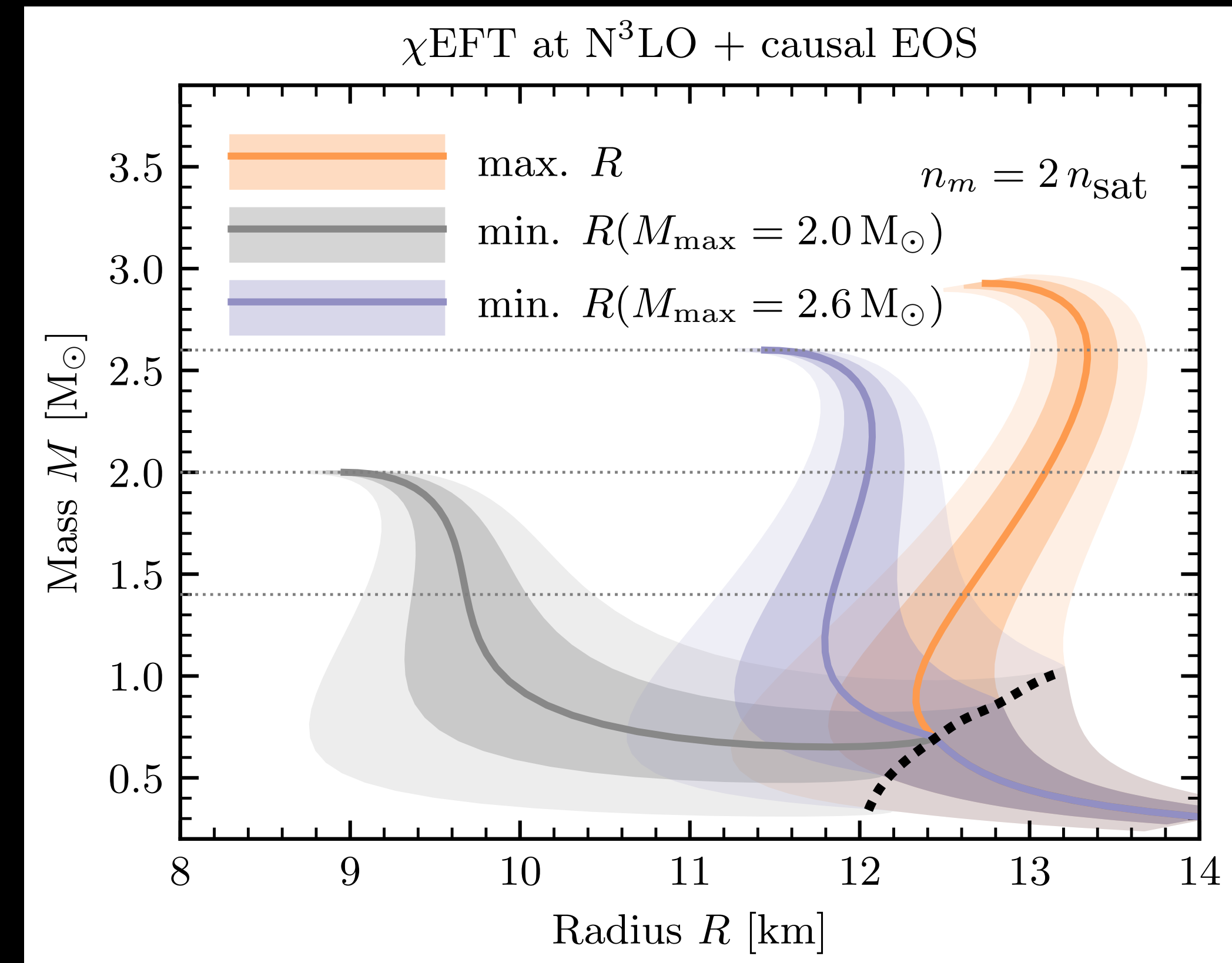
Bounds on Neutron Star Radii

EFT predictions for the EOS can be combined with extremal high-density EOS (with $c_s^2 = 1$) to derive bounds on the radius of NSs of any mass.

The lower limit on the NS maximum mass obtained from observations strengthen these bounds:

- $M_{\max} > 2.0 M_{\odot}$, $9.2 \text{ kms} < R_{1.4} < 13.2 \text{ kms}$
- $M_{\max} > 2.6 M_{\odot}$, $11.2 \text{ kms} < R_{1.4} < 13.2 \text{ kms}$

If $R_{1.4} < 11 \text{ km}$ or if $R_{1.4} > 13 \text{ km}$, it would imply a very large speed of sound in the cores of massive neutron stars.



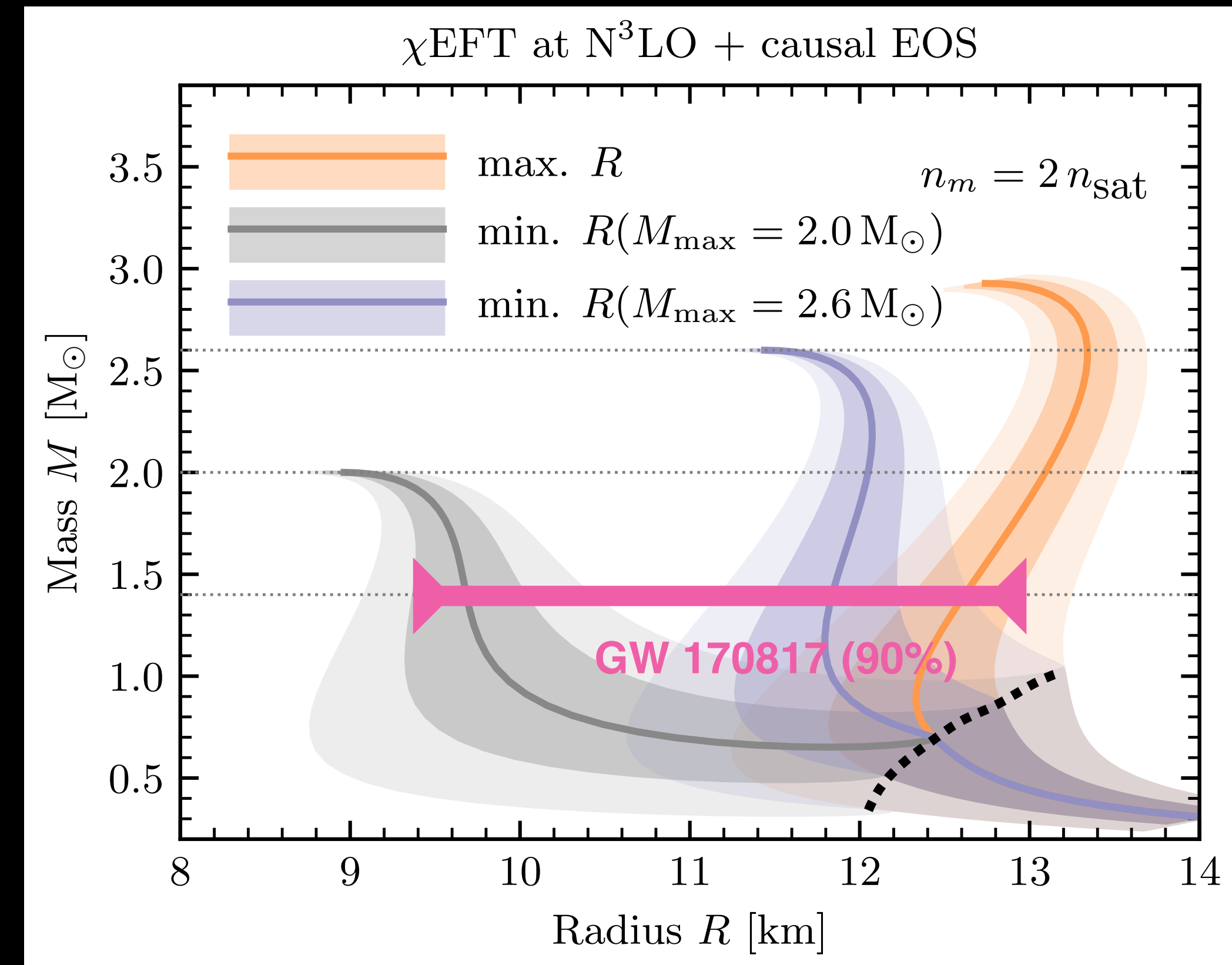
Bounds on Neutron Star Radii

EFT predictions for the EOS can be combined with extremal high-density EOS (with $c_s^2 = 1$) to derive bounds on the radius of NSs of any mass.

The lower limit on the NS maximum mass obtained from observations strengthen these bounds:

- $M_{\max} > 2.0 M_{\odot}$, $9.2 \text{ kms} < R_{1.4} < 13.2 \text{ kms}$
- $M_{\max} > 2.6 M_{\odot}$, $11.2 \text{ kms} < R_{1.4} < 13.2 \text{ kms}$

If $R_{1.4} < 11 \text{ km}$ or if $R_{1.4} > 13 \text{ km}$, it would imply a very large speed of sound in the cores of massive neutron stars.



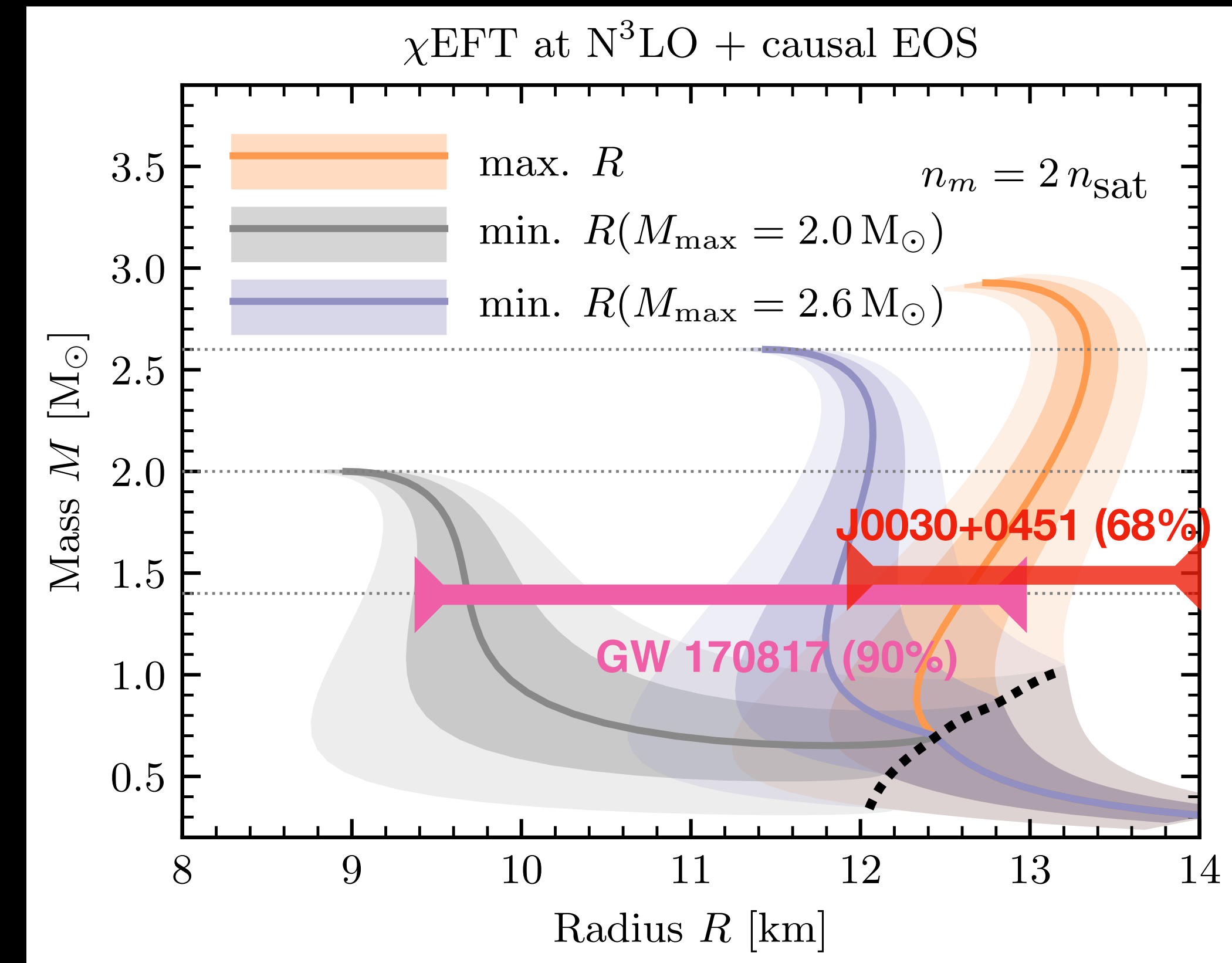
Bounds on Neutron Star Radii

EFT predictions for the EOS can be combined with extremal high-density EOS (with $c_s^2 = 1$) to derive bounds on the radius of NSs of any mass.

The lower limit on the NS maximum mass obtained from observations strengthen these bounds:

- $M_{\max} > 2.0 M_{\odot}$, $9.2 \text{ kms} < R_{1.4} < 13.2 \text{ kms}$
- $M_{\max} > 2.6 M_{\odot}$, $11.2 \text{ kms} < R_{1.4} < 13.2 \text{ kms}$

If $R_{1.4} < 11 \text{ km}$ or if $R_{1.4} > 13 \text{ km}$, it would imply a very large speed of sound in the cores of massive neutron stars.



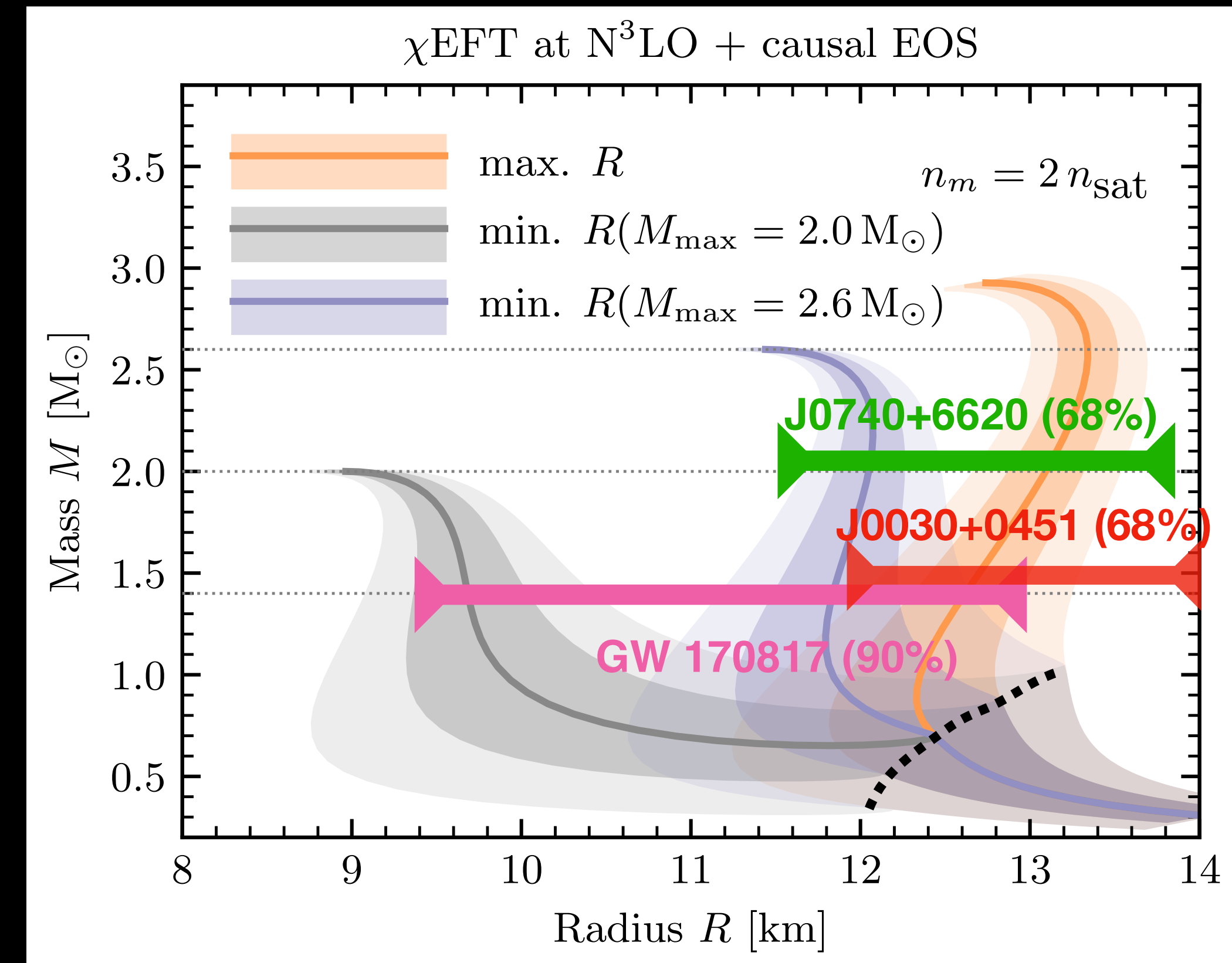
Bounds on Neutron Star Radii

EFT predictions for the EOS can be combined with extremal high-density EOS (with $c_s^2 = 1$) to derive bounds on the radius of NSs of any mass.

The lower limit on the NS maximum mass obtained from observations strengthen these bounds:

- $M_{\max} > 2.0 M_{\odot}$, $9.2 \text{ kms} < R_{1.4} < 13.2 \text{ kms}$
- $M_{\max} > 2.6 M_{\odot}$, $11.2 \text{ kms} < R_{1.4} < 13.2 \text{ kms}$

If $R_{1.4} < 11 \text{ km}$ or if $R_{1.4} > 13 \text{ km}$, it would imply a very large speed of sound in the cores of massive neutron stars.

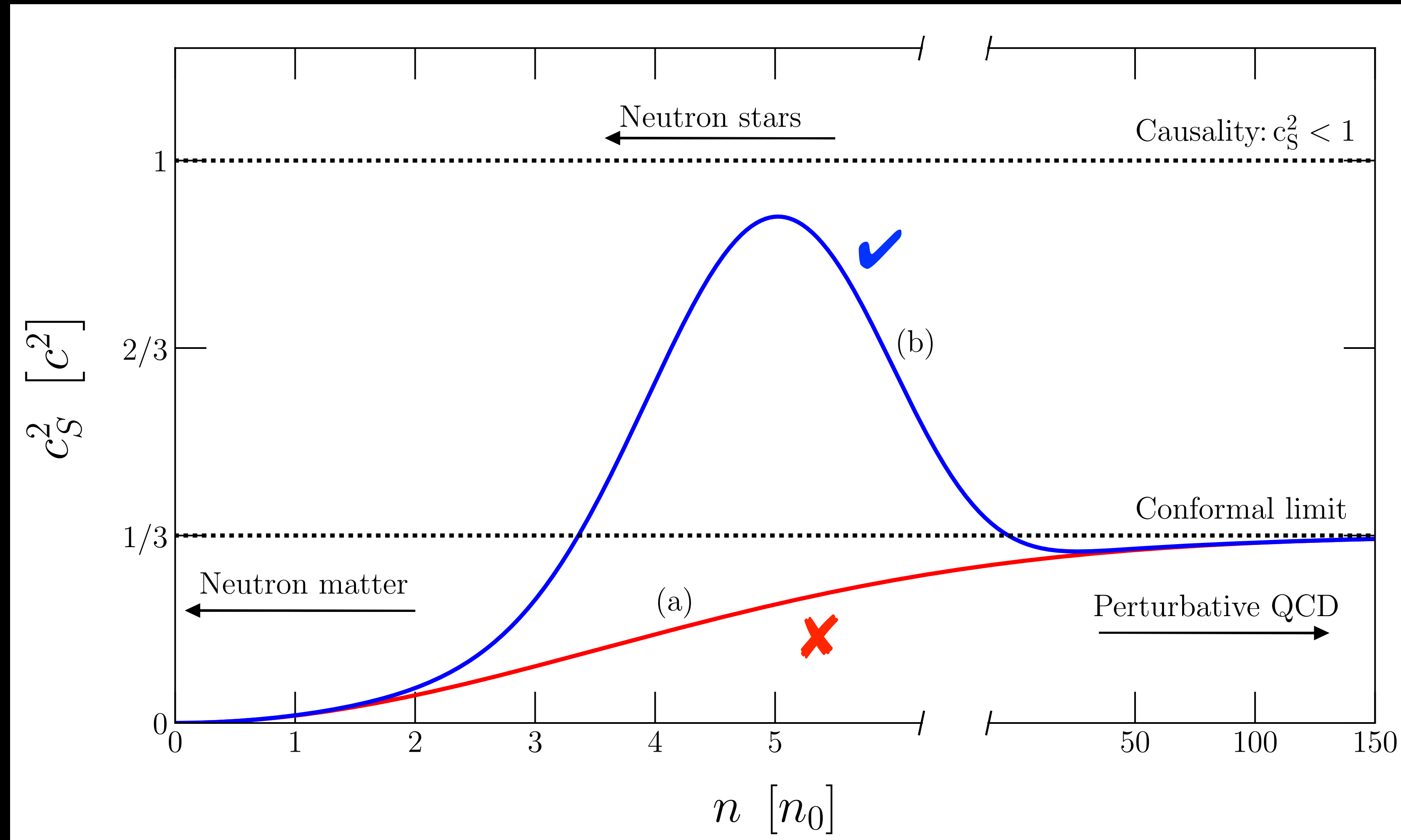


Speed of Sound in Dense Matter

$$c_s^2 = \frac{\partial P}{\partial \epsilon}$$

Large maximum mass combined with small radius and neutron matter calculations suggests a rapid increase in pressure in the neutron star core. This implies a large and non-monotonic sound speed in dense QCD matter.

Suggests the existence of a strongly interacting phase of relativistic matter.

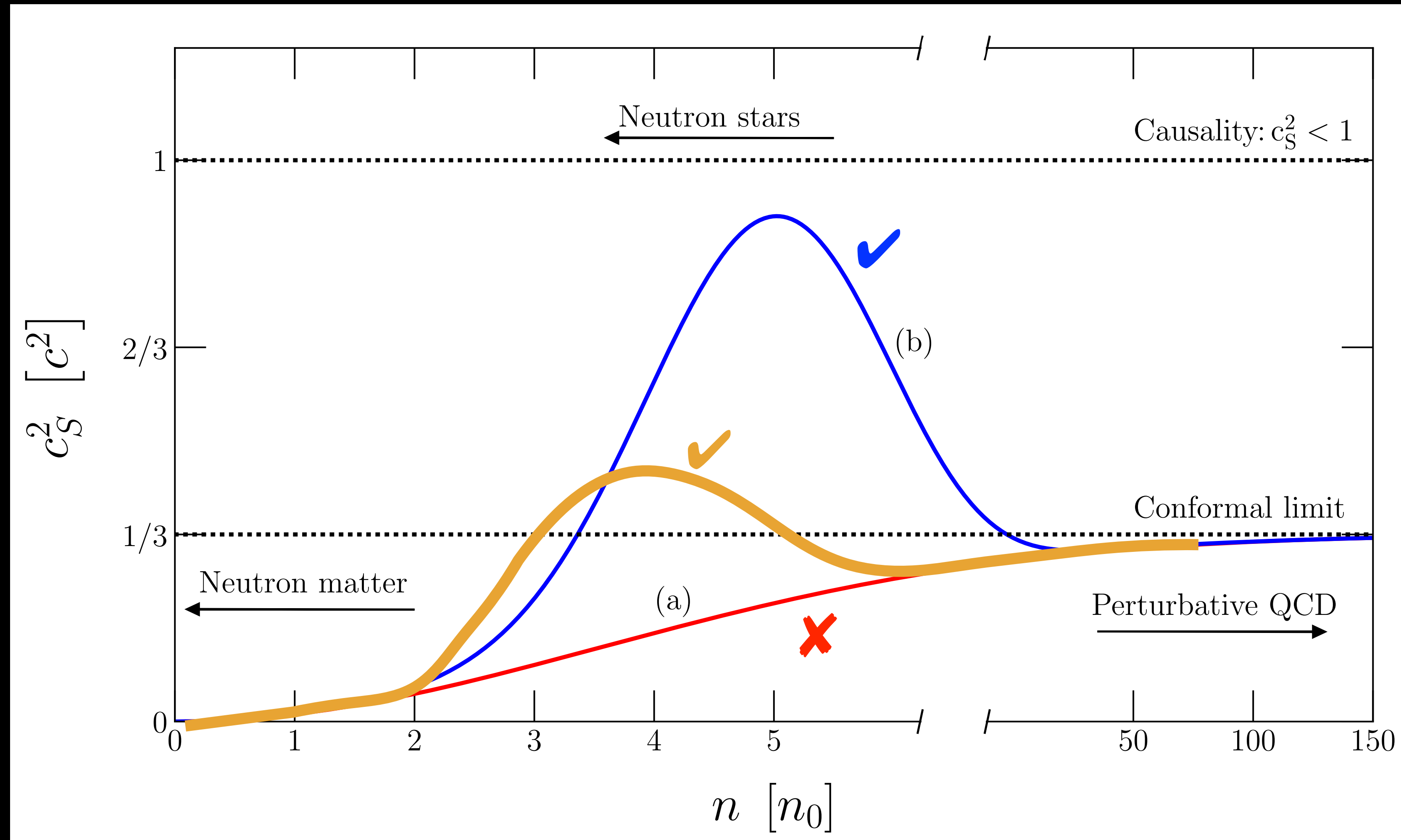


Speed of Sound in Dense Matter

$$c_s^2 = \frac{\partial P}{\partial \epsilon}$$

Large maximum mass combined with small radius and neutron matter calculations suggests a rapid increase in pressure in the neutron star core. This implies a large and non-monotonic sound speed in dense QCD matter.

Suggests the existence of a strongly interacting phase of relativistic matter.

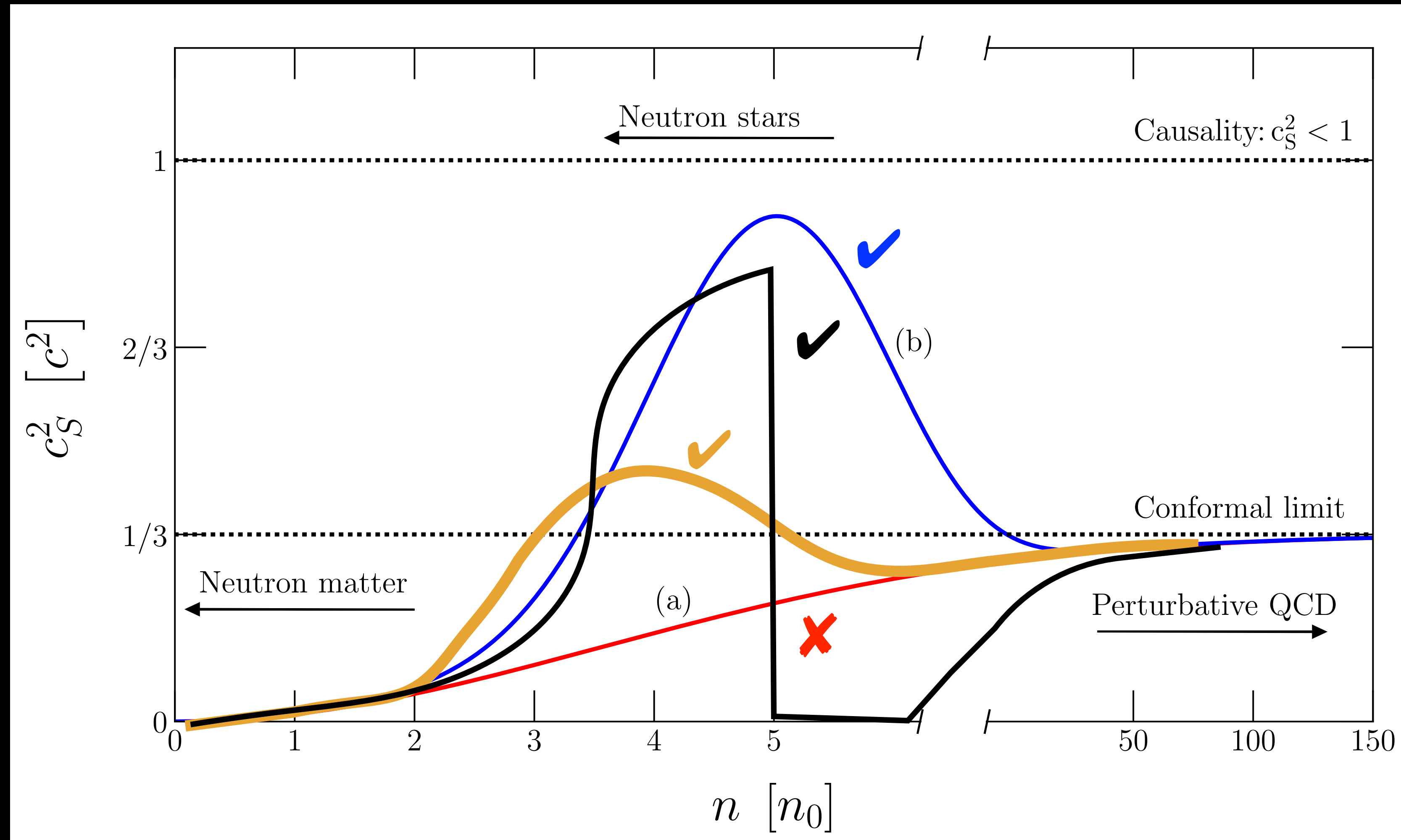


Speed of Sound in Dense Matter

$$c_s^2 = \frac{\partial P}{\partial \epsilon}$$

Large maximum mass combined with small radius and neutron matter calculations suggests a rapid increase in pressure in the neutron star core. This implies a large and non-monotonic sound speed in dense QCD matter.

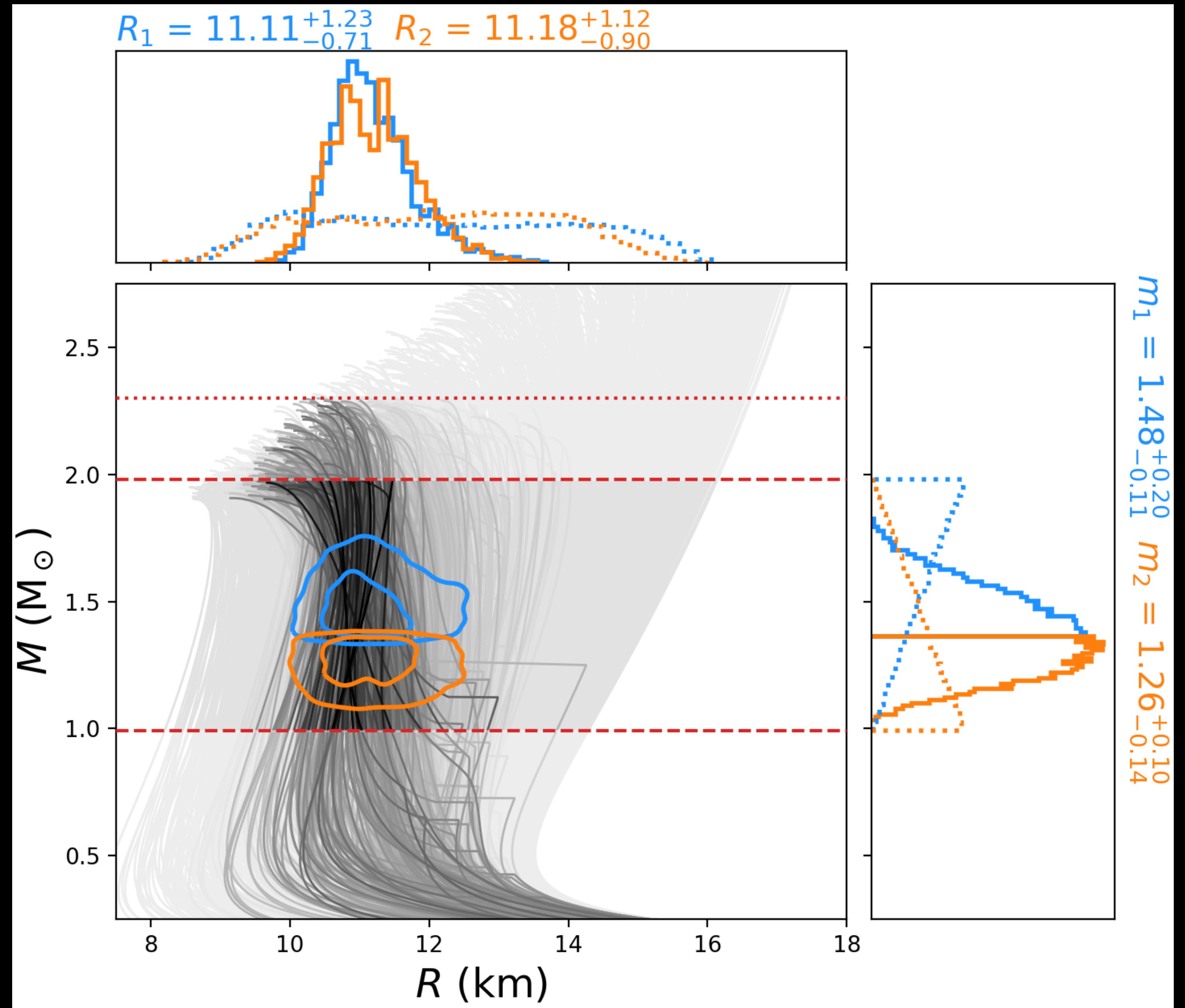
Suggests the existence of a strongly interacting phase of relativistic matter.



Tighter Constraints: Combining Nuclear Physics and GW170817

Nuclear physics input correlates the neutron stars in the binary and provides an informed prior for GW data analysis. Helps extract stringent constraints on the NS radius:

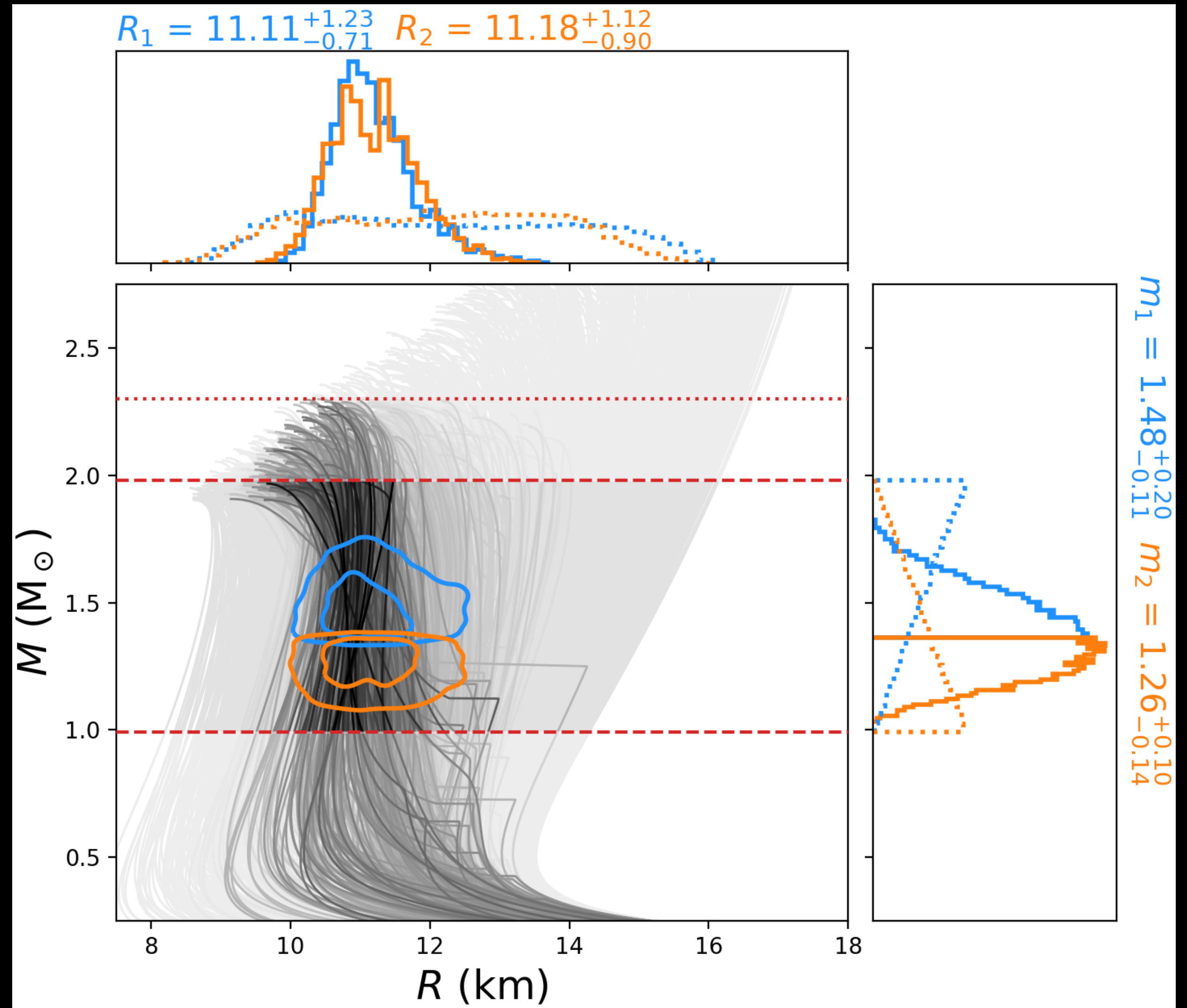
$$R_{1.4} = 11.2^{+1.2}_{-0.8} \text{ km}$$



Tighter Constraints: Combining Nuclear Physics and GW170817

Nuclear physics input correlates the neutron stars in the binary and provides an informed prior for GW data analysis. Helps extract stringent constraints on the NS radius:

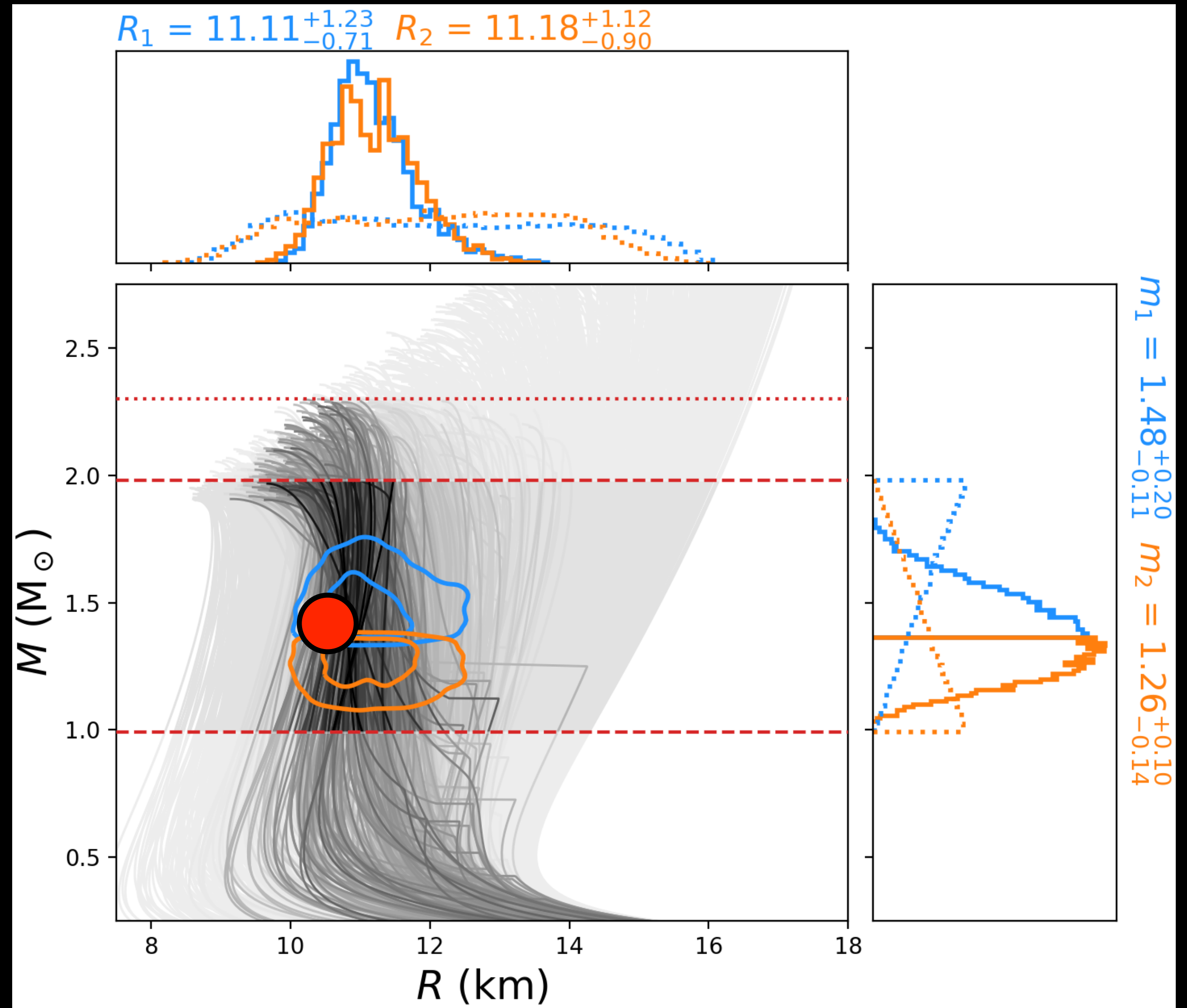
$$R_{1.4} = 11.2^{+1.2}_{-0.8} \text{ km}$$



Tighter Constraints: Combining Nuclear Physics and GW170817

Nuclear physics input correlates the neutron stars in the binary and provides an informed prior for GW data analysis. Helps extract stringent constraints on the NS radius:

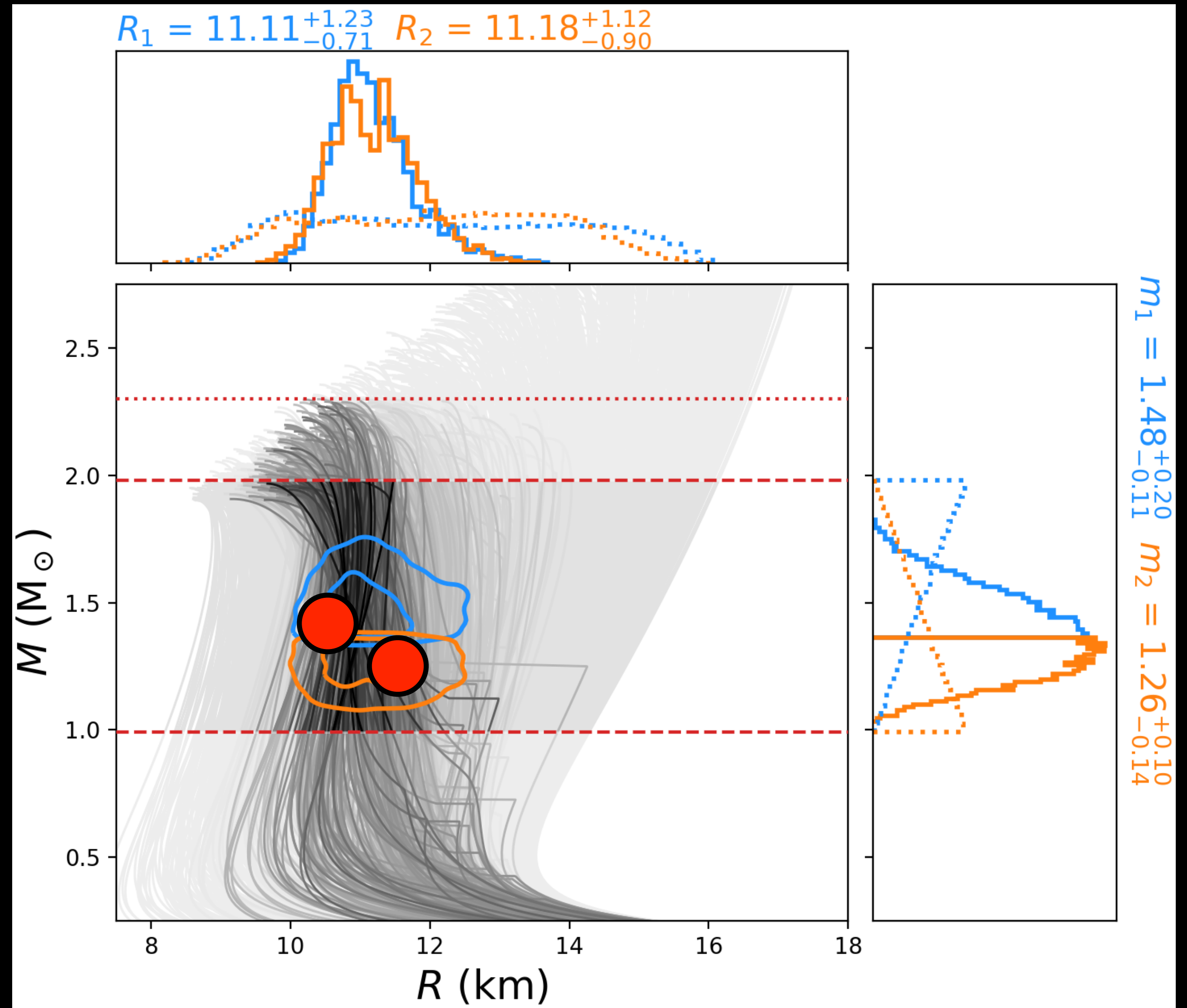
$$R_{1.4} = 11.2^{+1.2}_{-0.8} \text{ km}$$



Tighter Constraints: Combining Nuclear Physics and GW170817

Nuclear physics input correlates the neutron stars in the binary and provides an informed prior for GW data analysis. Helps extract stringent constraints on the NS radius:

$$R_{1.4} = 11.2^{+1.2}_{-0.8} \text{ km}$$

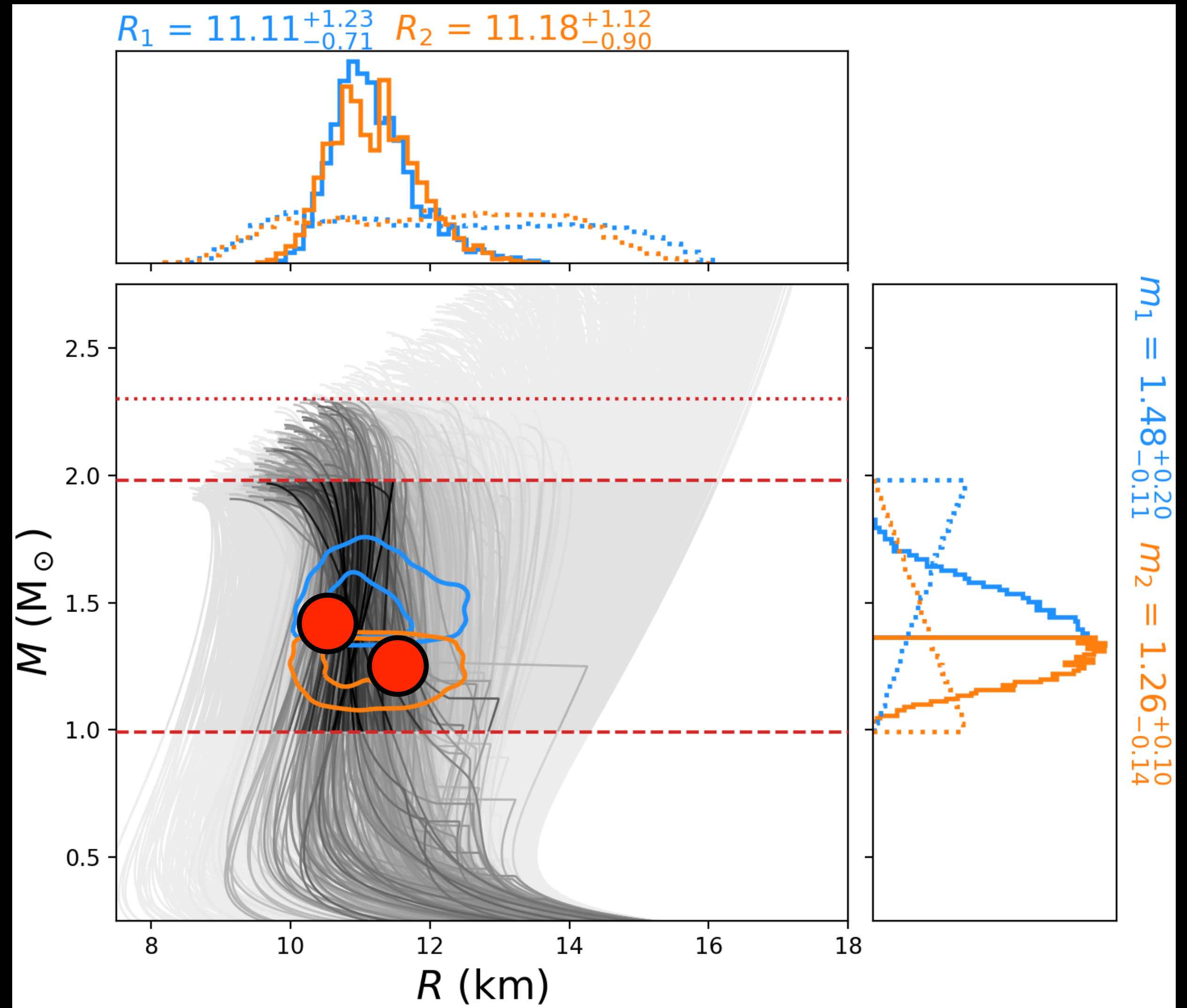


Tighter Constraints: Combining Nuclear Physics and GW170817

Nuclear physics input correlates the neutron stars in the binary and provides an informed prior for GW data analysis. Helps extract stringent constraints on the NS radius:

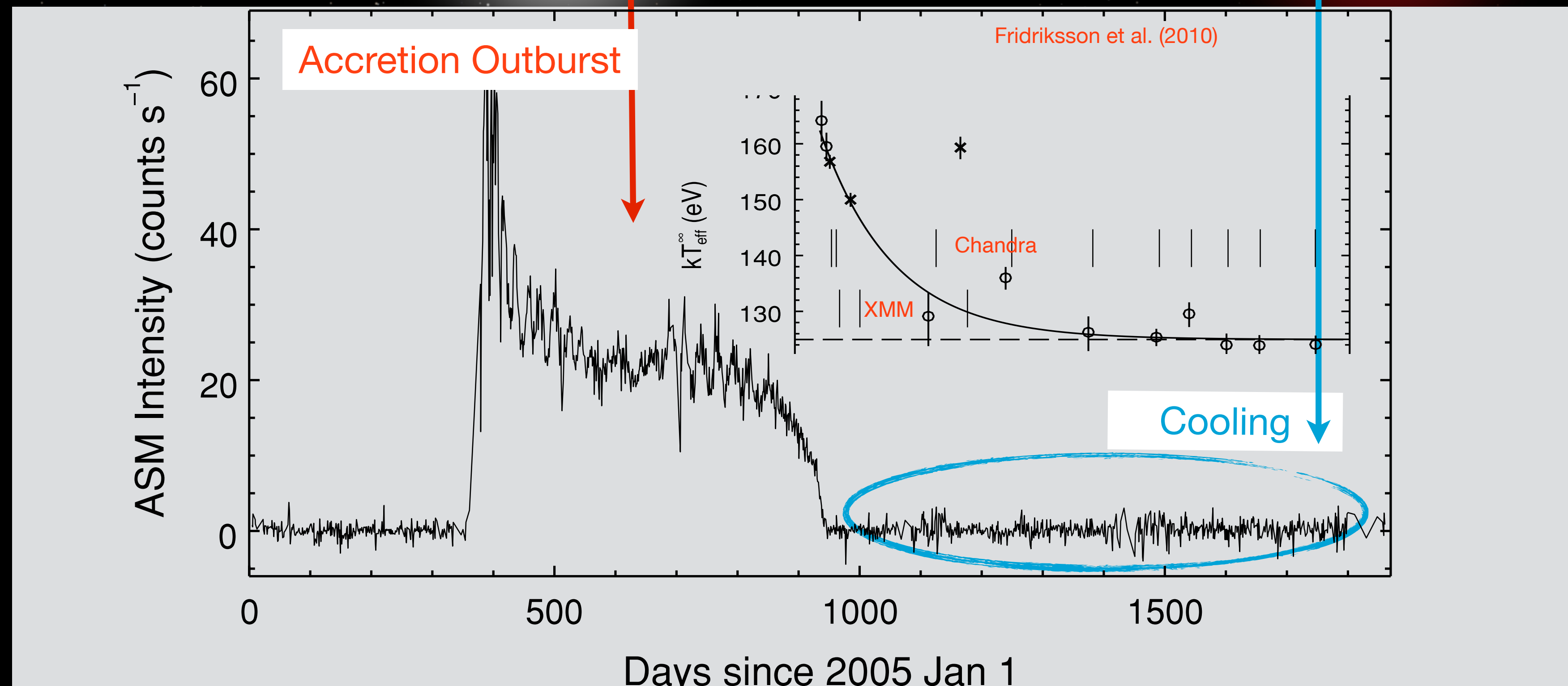
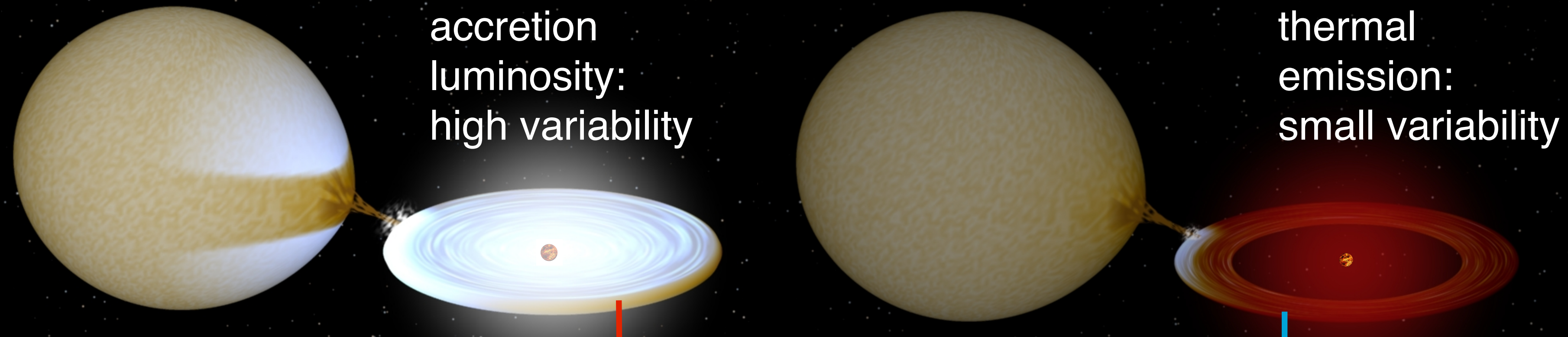
$$R_{1.4} = 11.2^{+1.2}_{-0.8} \text{ km}$$

With tighter future constraints, we could discover phase transitions in the core.



Accreting Neutron Stars: Nature's Low Temperature Laboratory

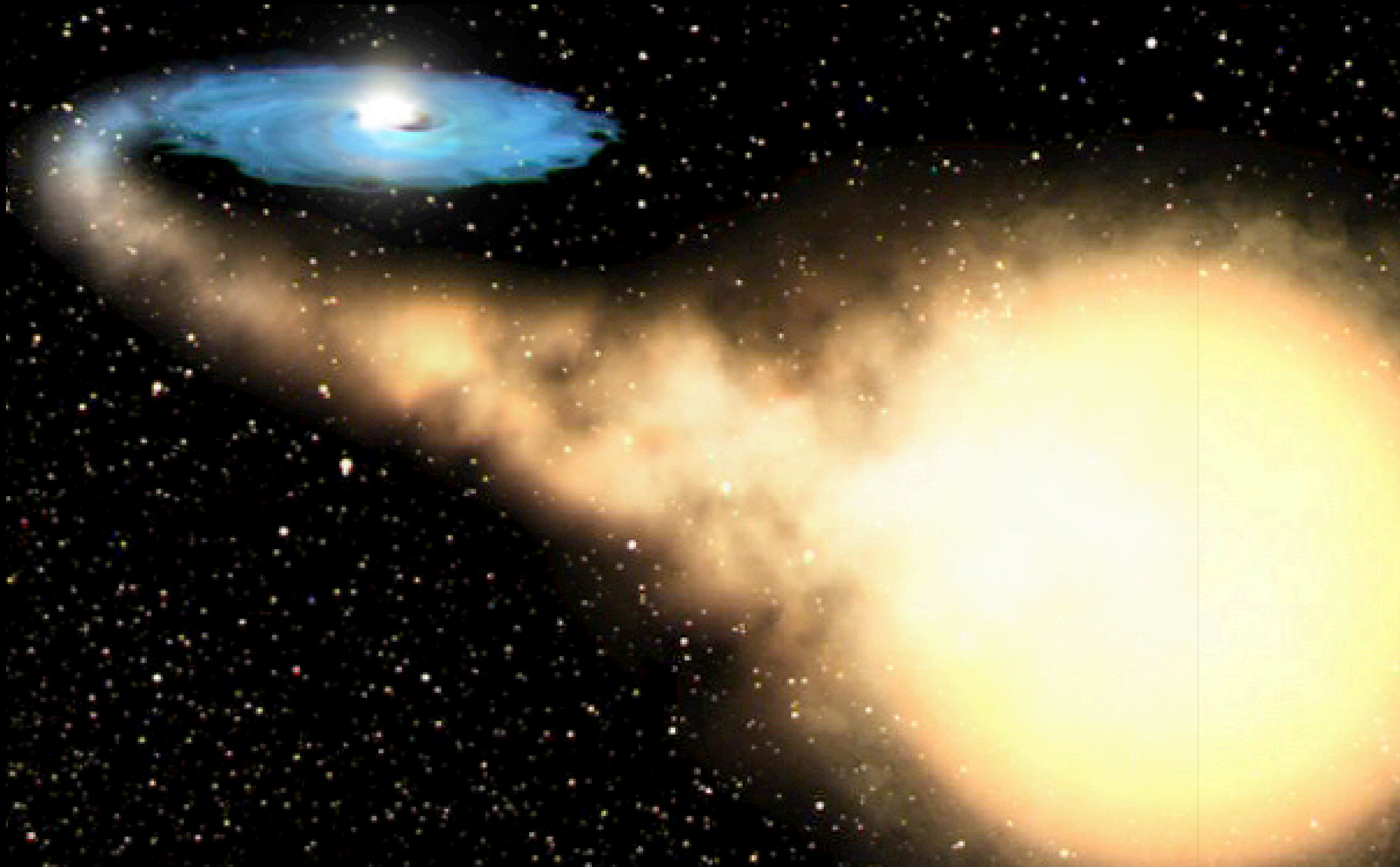
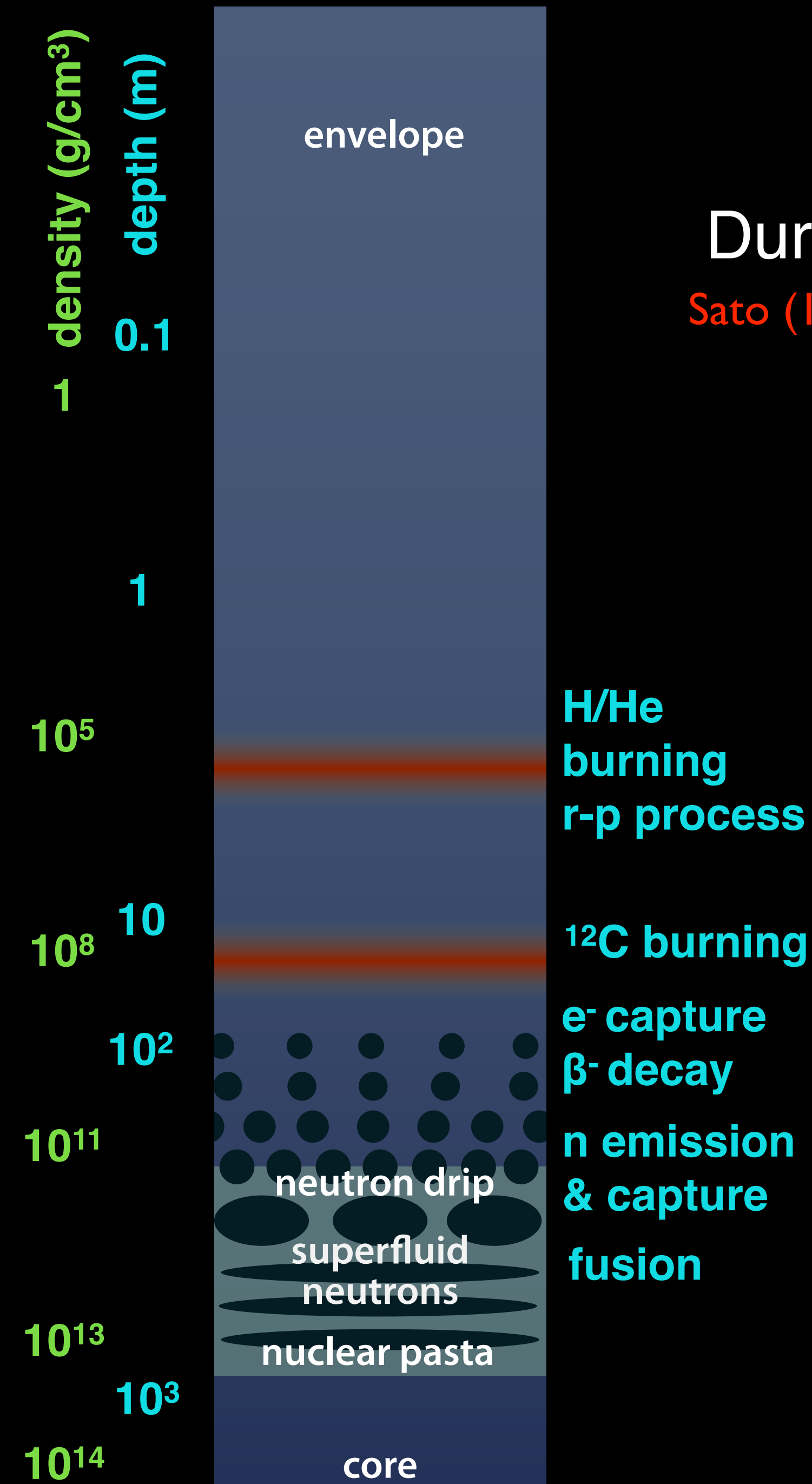
Transiently Accreting Neutron Stars



Deep Crustal Heating

During accretion nuclear reactions release: $\sim 2\text{-}4 \text{ MeV / nucleon}$

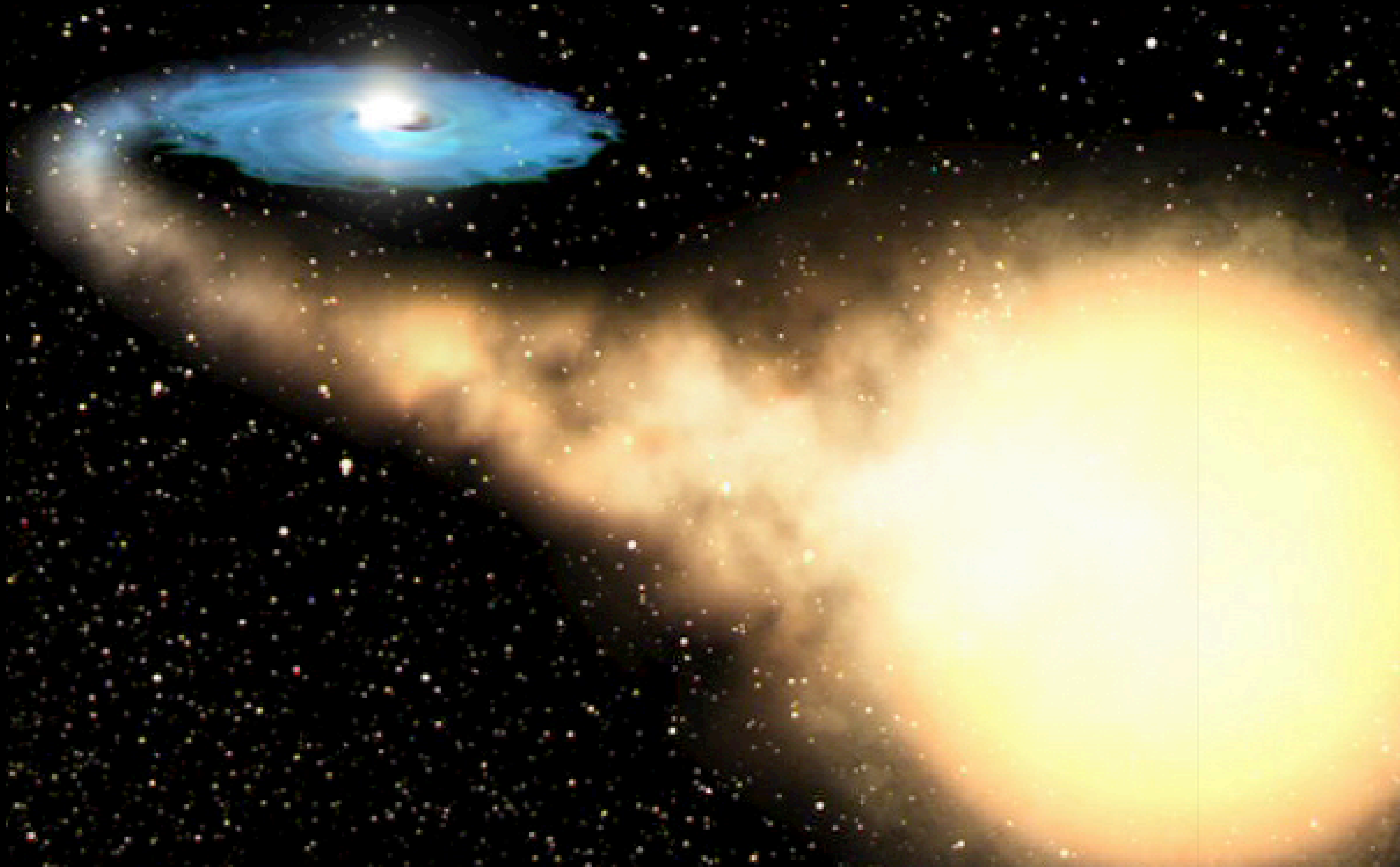
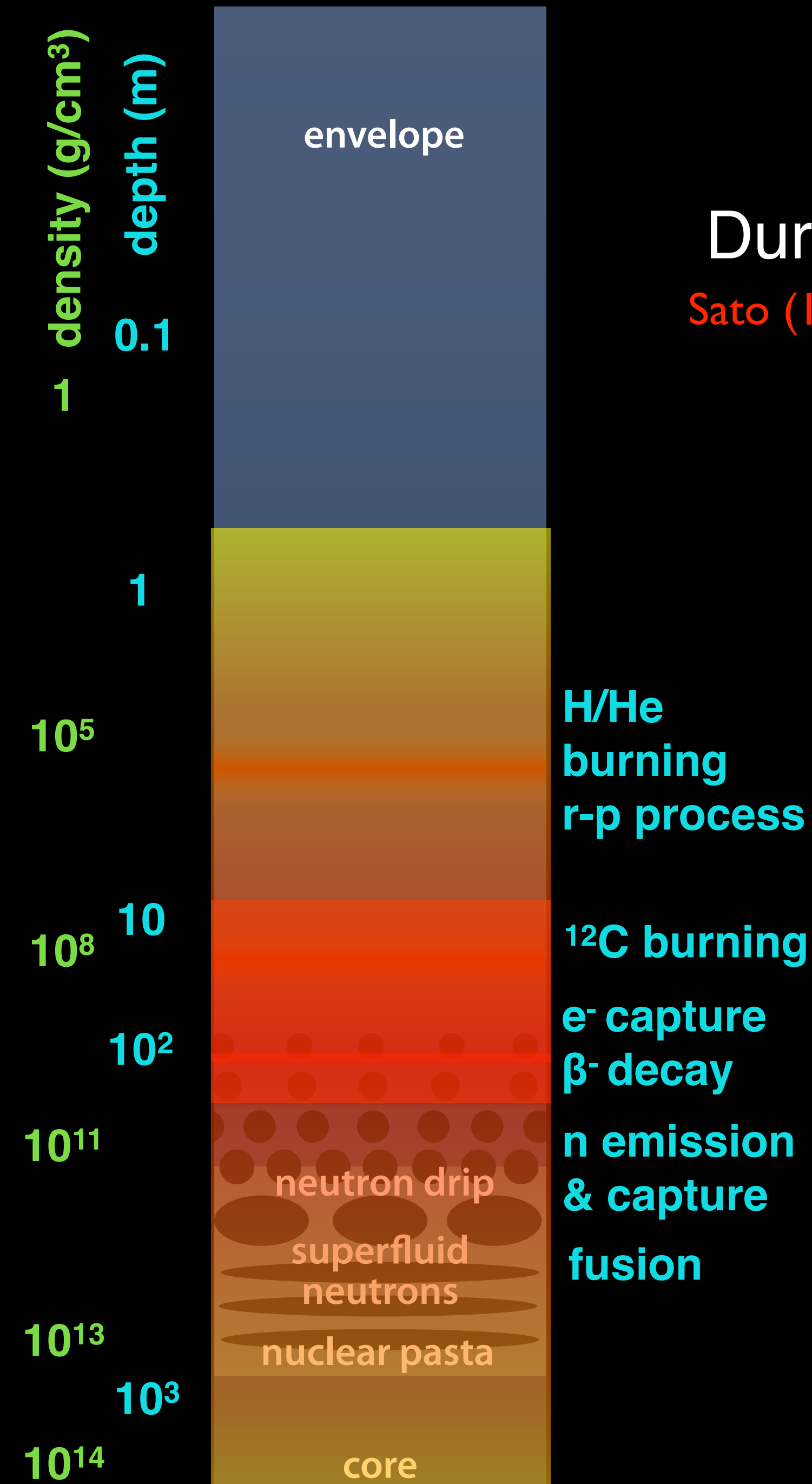
Sato (1974), Haensel & Zdunik (1990), Brown, Bildsten Rutledge (1998) Gupta et al (2007,2011).



Deep Crustal Heating

During accretion nuclear reactions release: $\sim 2\text{-}4 \text{ MeV} / \text{nucleon}$

Sato (1974), Haensel & Zdunik (1990), Brown, Bildsten Rutledge (1998) Gupta et al (2007,2011).



Cooling Post Accretion

- This relaxation was first discovered in 2001 and 7 sources have been studied to date.
- All known Quasi-persistent sources show cooling after accretion
- Cools on a time scale of ~ 1000 days.

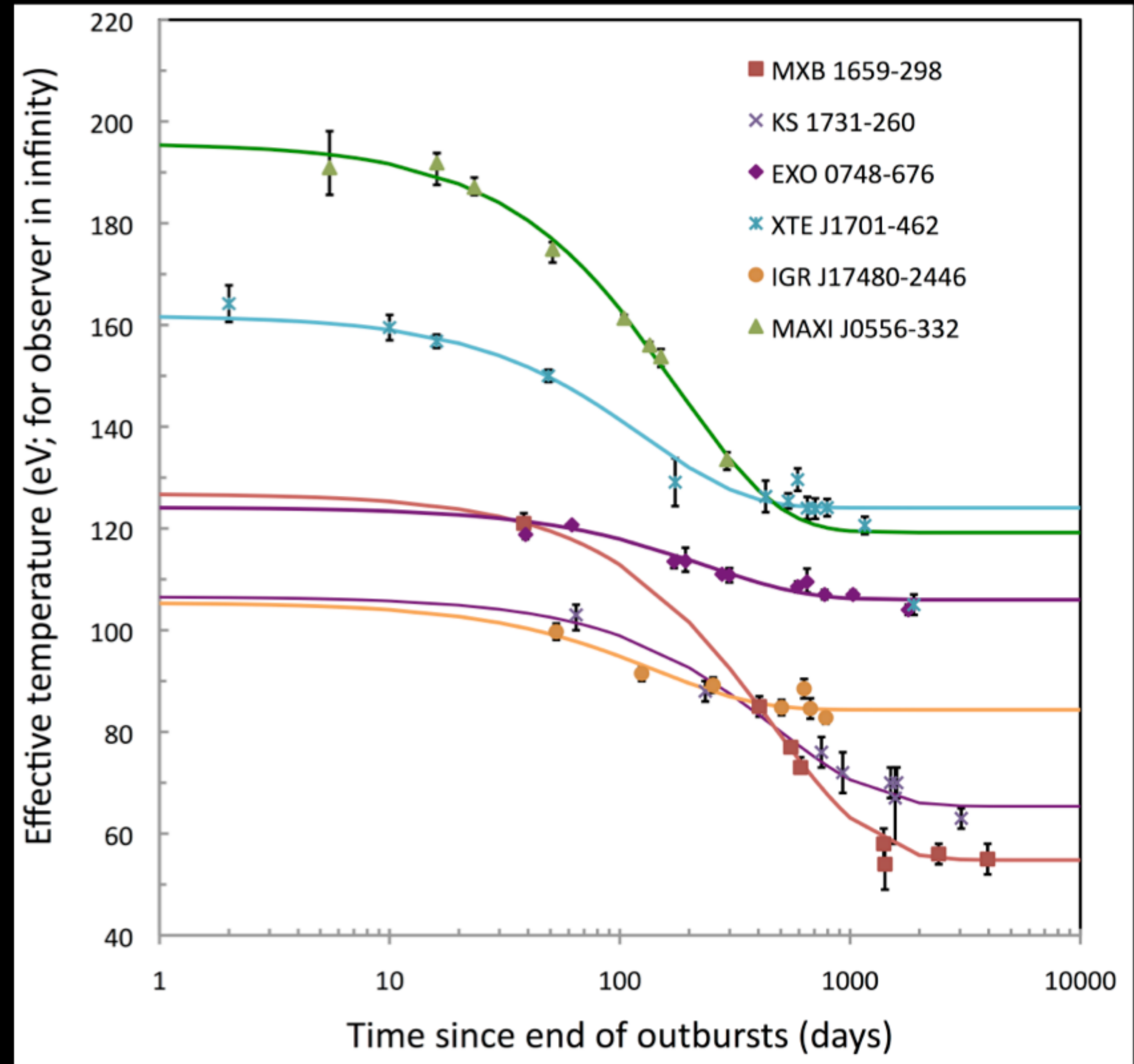


Figure from Rudy Wijnands (2013)

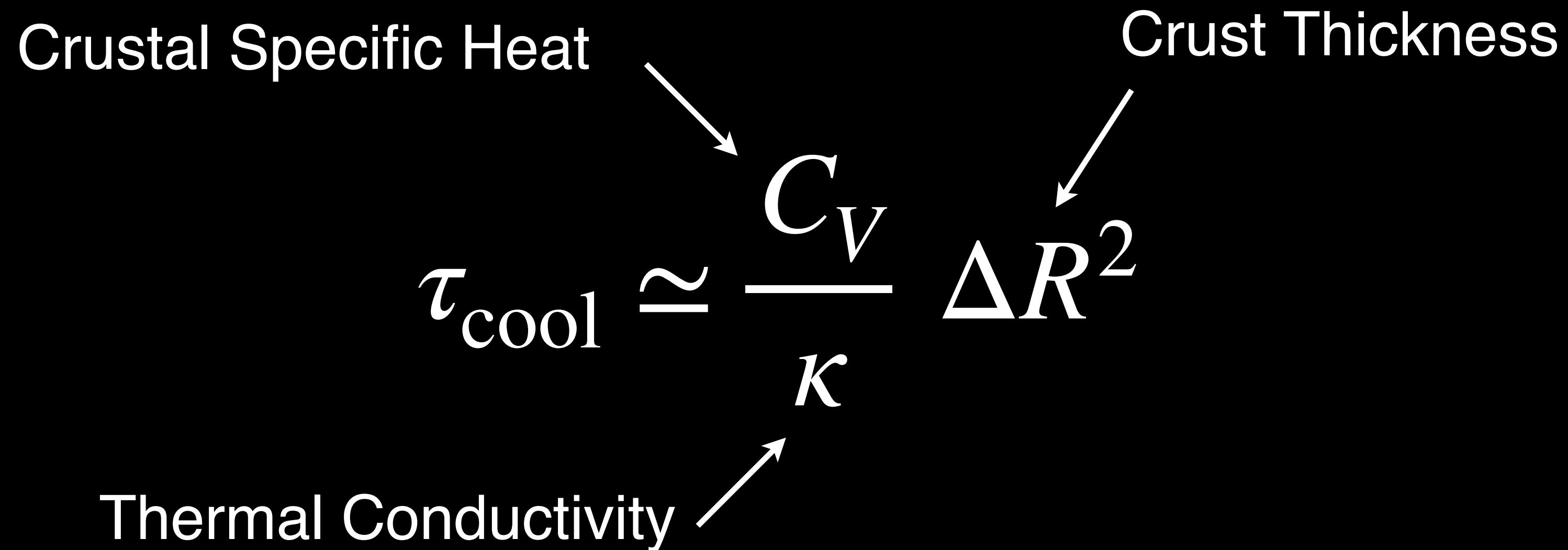
Connecting to Crust Microphysics

Crustal Specific Heat

Crust Thickness

$$\tau_{\text{cool}} \approx \frac{C_V}{\kappa} \Delta R^2$$

Thermal Conductivity



- The observed timescales are short.
- Requires small specific heat and large thermal conductivity.

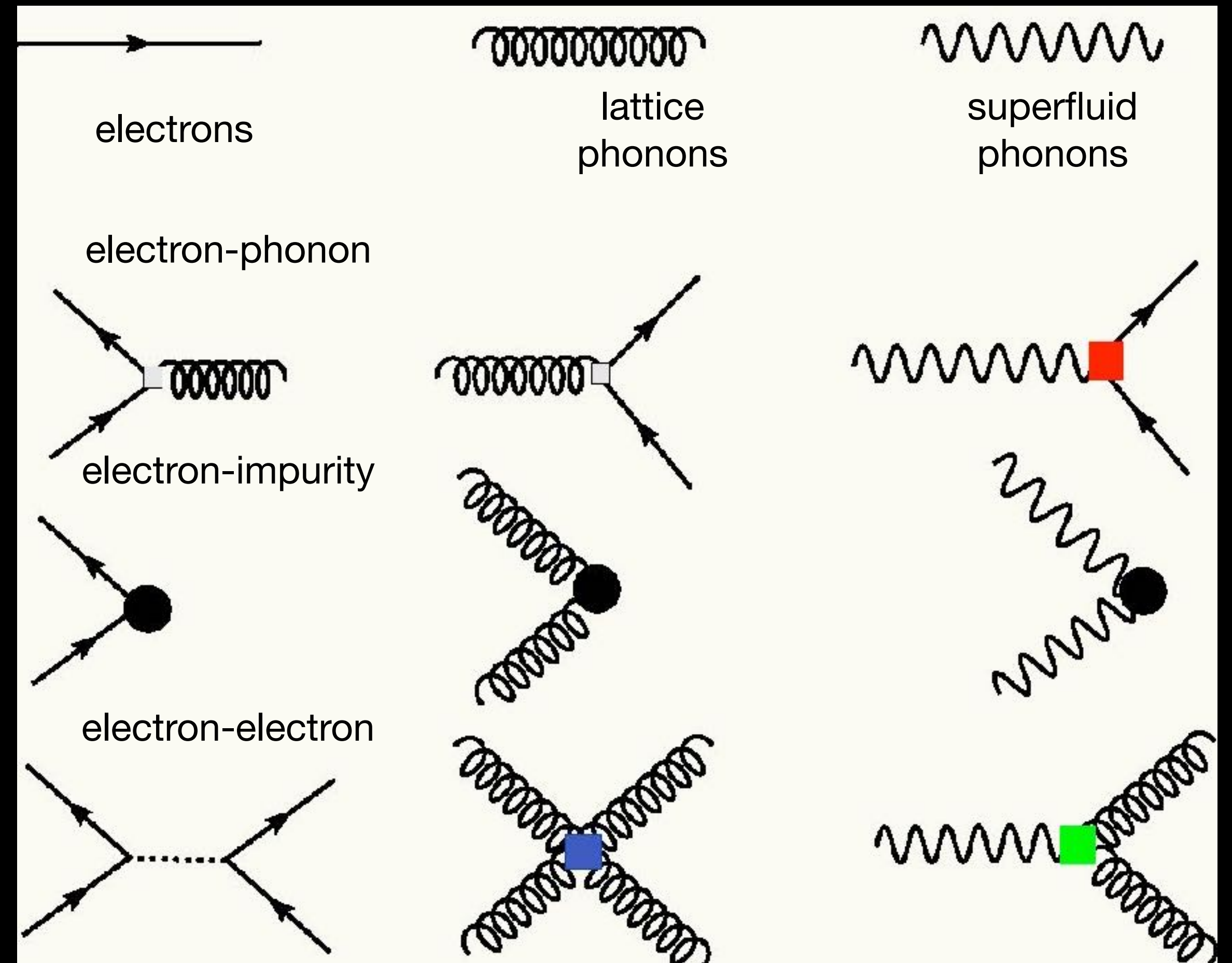
Thermal and transport properties of the inner crust

Electrons, two longitudinal, and two transverse phonons are the relevant excitations.

Thermal and transport properties of the solid and superfluid crust can be calculated using an effective field theory.

Mixing between phonons leads to strong Landau damping. Phonon conduction is highly suppressed.

The short observed cooling timescale favors a solid and superfluid inner crust.



Cirigliano, Reddy & Sharma (2011), Page & Reddy (2012),
Chamel, Page, & Reddy (2013), Roggero & Reddy (2016)

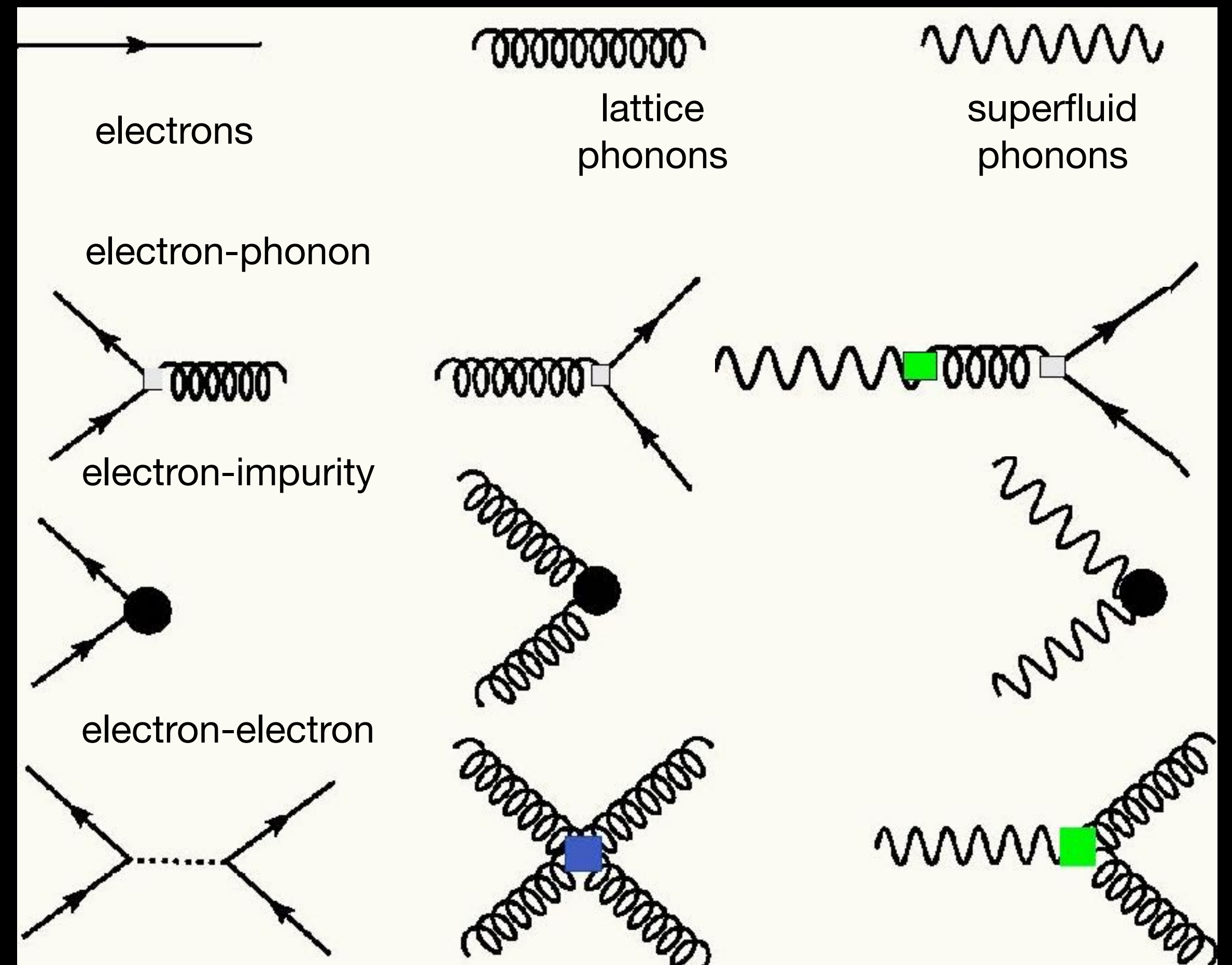
Thermal and transport properties of the inner crust

Electrons, two longitudinal, and two transverse phonons are the relevant excitations.

Thermal and transport properties of the solid and superfluid crust can be calculated using an effective field theory.

Mixing between phonons leads to strong Landau damping. Phonon conduction is highly suppressed.

The short observed cooling timescale favors a solid and superfluid inner crust.



Cirigliano, Reddy & Sharma (2011), Page & Reddy (2012),
Chamel, Page, & Reddy (2013), Roggero & Reddy (2016)

Measuring the Heat Capacity of the Core

Heat the star, allow it to relax, and observe the change in temperature:

$$C_{NS} dT = dQ$$



Measuring the Heat Capacity of the Core

Heat the star, allow it to relax, and observe the change in temperature:

$$C_{NS} dT = dQ$$



Measuring the Heat Capacity of the Core

Heat the star, allow it to relax, and observe the change in temperature:

$$C_{NS} dT = dQ$$

When $C_{NS} = \alpha T$: $\frac{\alpha}{2} (T_f^2 - T_i^2) = \Delta Q$

Lower limit: $C_{NS}(T_f) > 2 \frac{\Delta Q}{T_f}$

$$\Delta Q = \dot{H} \times t_H - L_\nu \times (t_H + t_{obs})$$

heating
rate

duration
of heating

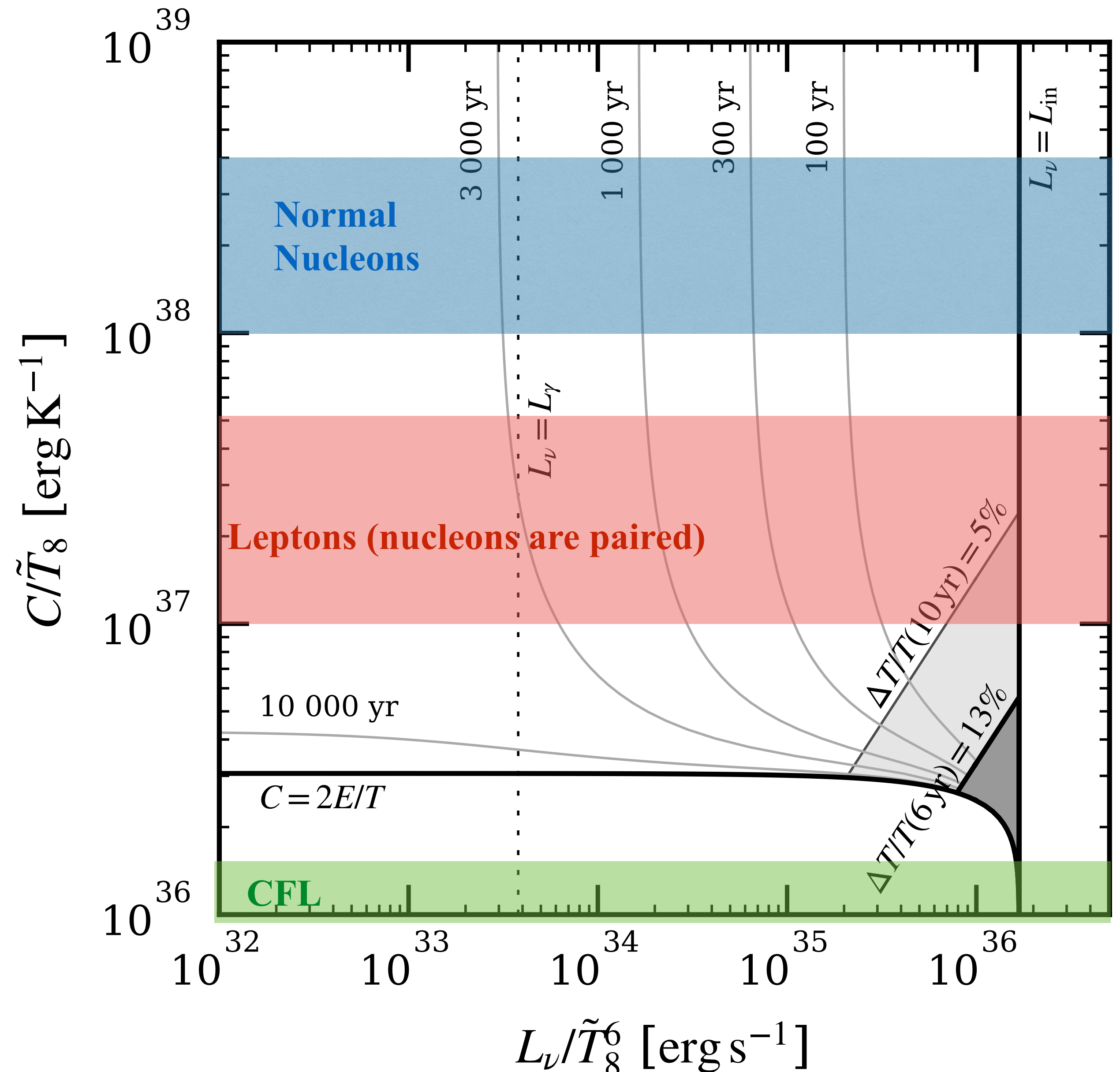
neutrino
cooling rate

time of observation
(after heating ceases)



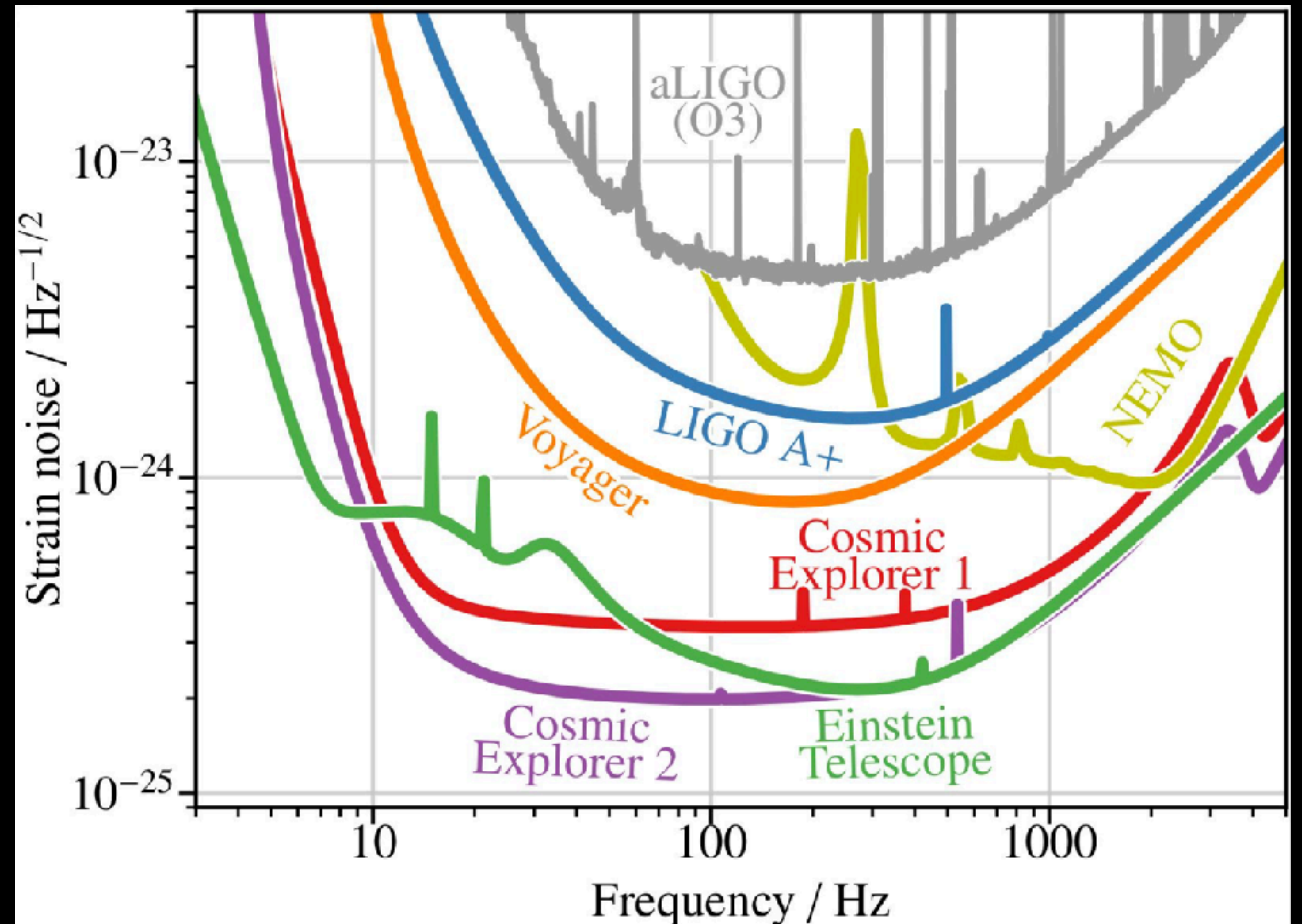
Lower Limit on the Core Specific Heat: Current & Future

- Observations of KS 1731-260 provide a limit.
- The limit is compatible with most models of dense matter.
- One exception is a neutron star core made entirely of CFL quark matter.
- If temperature variation is observed on a 10 year time scale, it would imply some form of exotic matter in which most baryons are frozen!



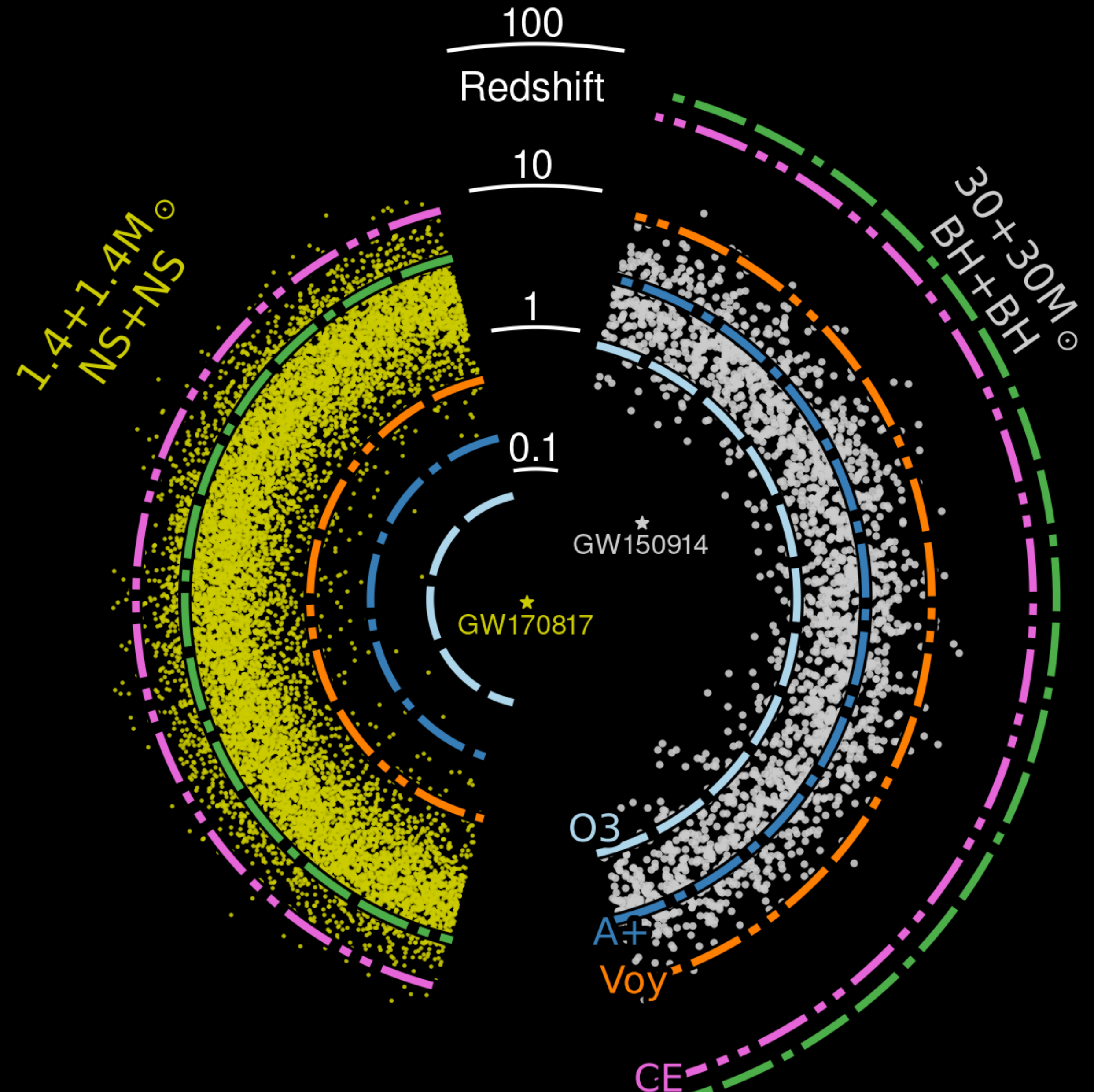
Next Generation GW Detectors

- Cosmic Explorer and Einstein Telescope will observe 300,000 neutron star mergers and 100,000 black hole mergers per year!
- ~ 100 BNS events with $\text{SNR} > 100$ and ~ 5 with > 300 .
- Accurate measurements of tidal deformability of many neutron stars within a few years. $\Delta R \lesssim 0.1$ km!
- High-frequency GWs from the post-merger phase provide a direct probe of neutron star oscillations and dynamics.

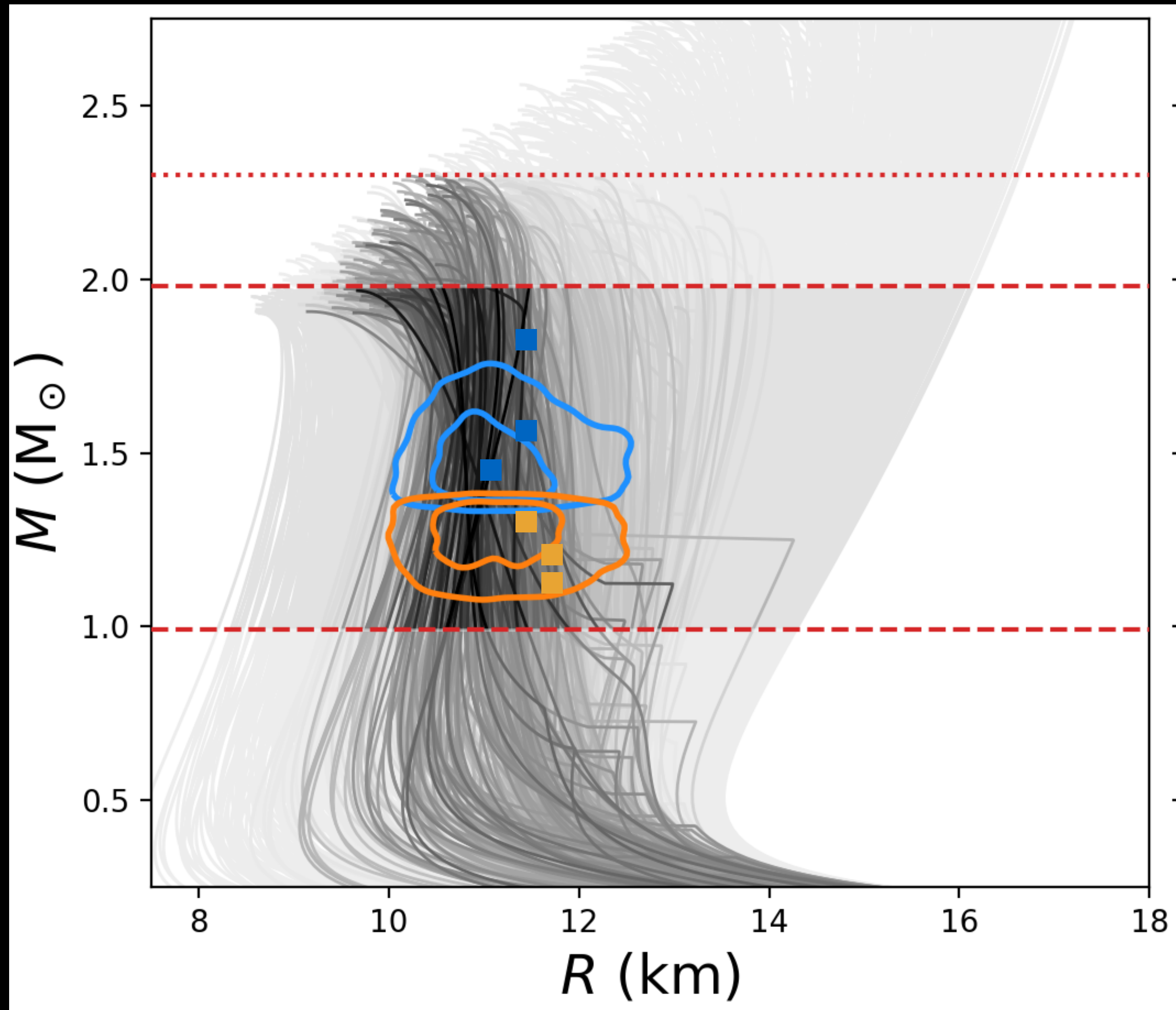


Next Generation GW Detectors

- Cosmic Explorer and Einstein Telescope will observe 300,000 neutron star mergers and 100,000 black hole mergers per year!
- ~100 BNS events with SNR > 100 and ~5 with >300.
- Accurate measurements of tidal deformability of many neutron stars within a few years. $\Delta R \lesssim 0.1$ km!
- High-frequency GWs from the post-merger phase provide a direct probe of neutron star oscillations and dynamics.



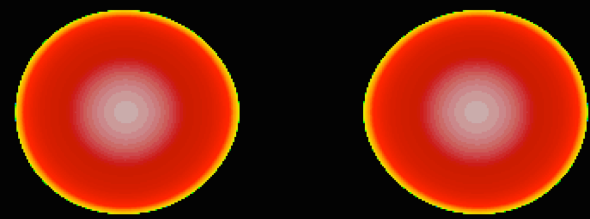
Mass-Radius constraints in 2030? 2040?



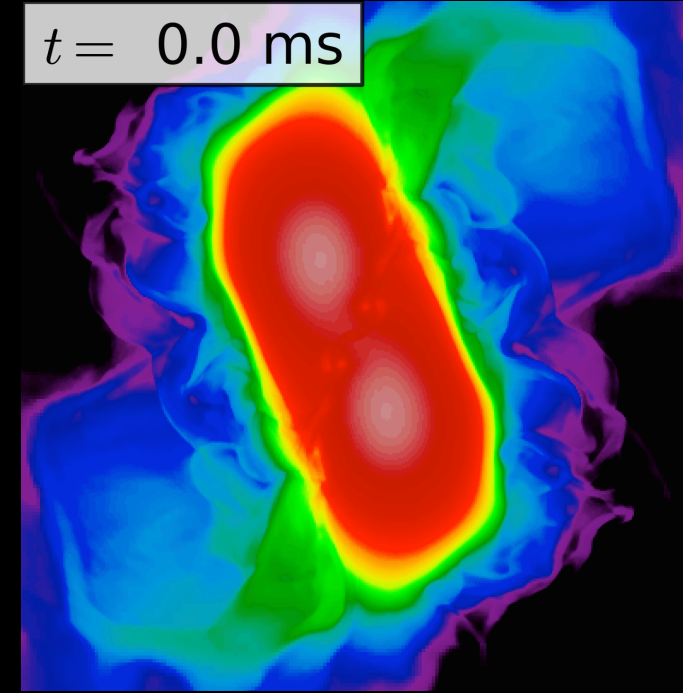
Neutron Star Merger Dynamics

(General) Relativistic (Very) Heavy-Ion Collisions at ~ 100 MeV/nucleon

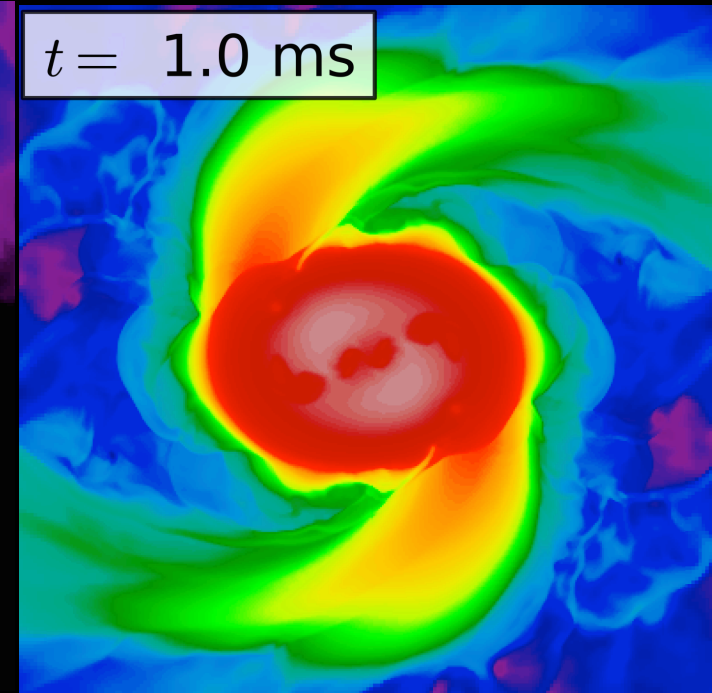
$t = -8.1$ ms



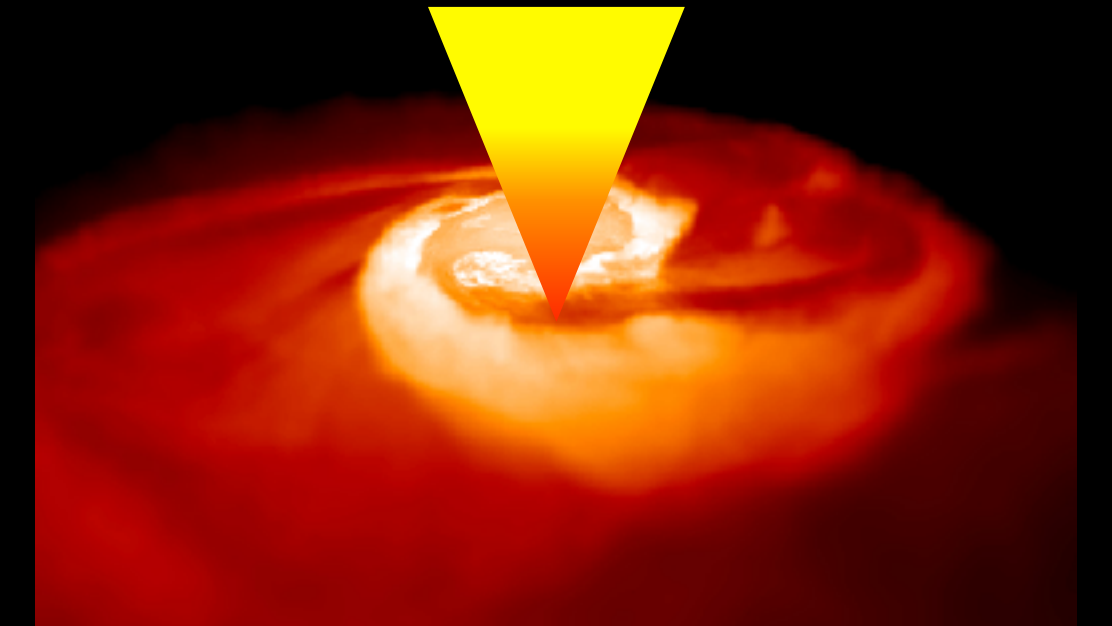
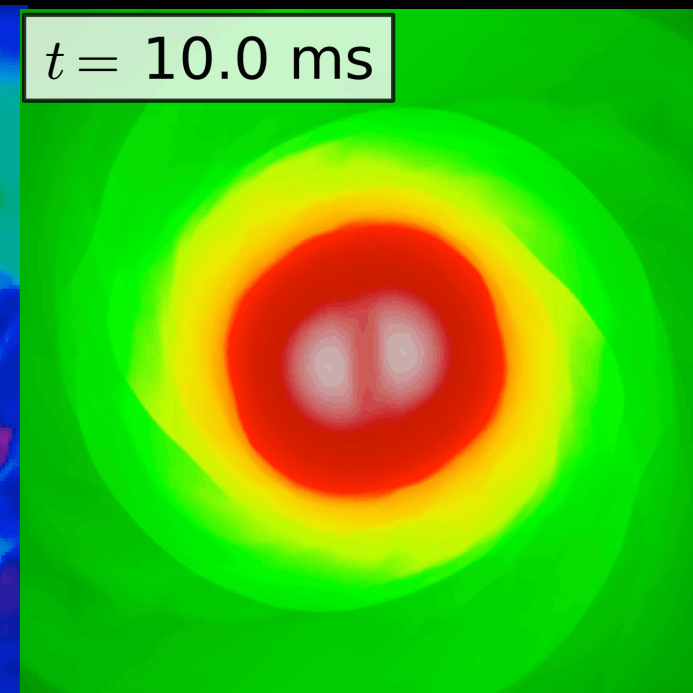
$t = 0.0$ ms



$t = 1.0$ ms



$t = 10.0$ ms



Simulations: Rezzola et al (2013)

Inspiral:

Gravitational waves,
Tidal Effects

Merger:

Disruption, NS oscillations, ejecta
and r-process nucleosynthesis

Post Merger:

GRB, Afterglows, and
Kilonova

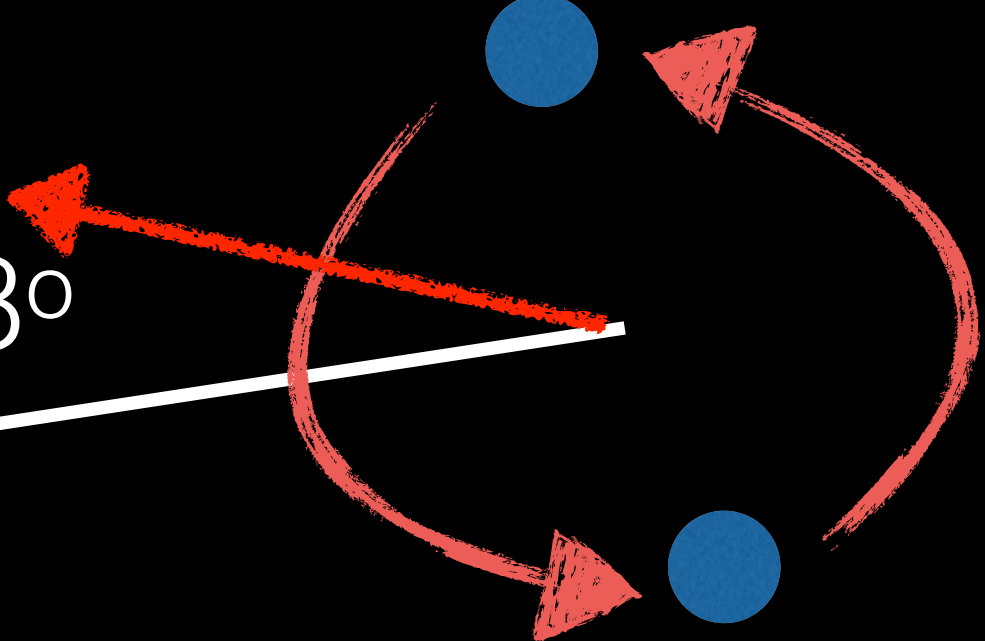
- Post-merger evolution is complex. Relies on multi-physics large-scale numerical relativity simulations.
- Observables are sensitive to the equation of state and response of matter at extreme density and temperature.

GW170817 confirmed expectations!

LIGO

$$D = 40^{+8}_{-14} \text{ Mpc}$$

$$\Theta < 28^\circ$$

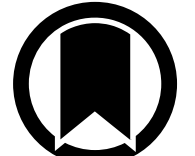


THE ASTROPHYSICAL JOURNAL LETTERS, 848:L12 (59pp), 2017 October 20

© 2017. The American Astronomical Society. All rights reserved.

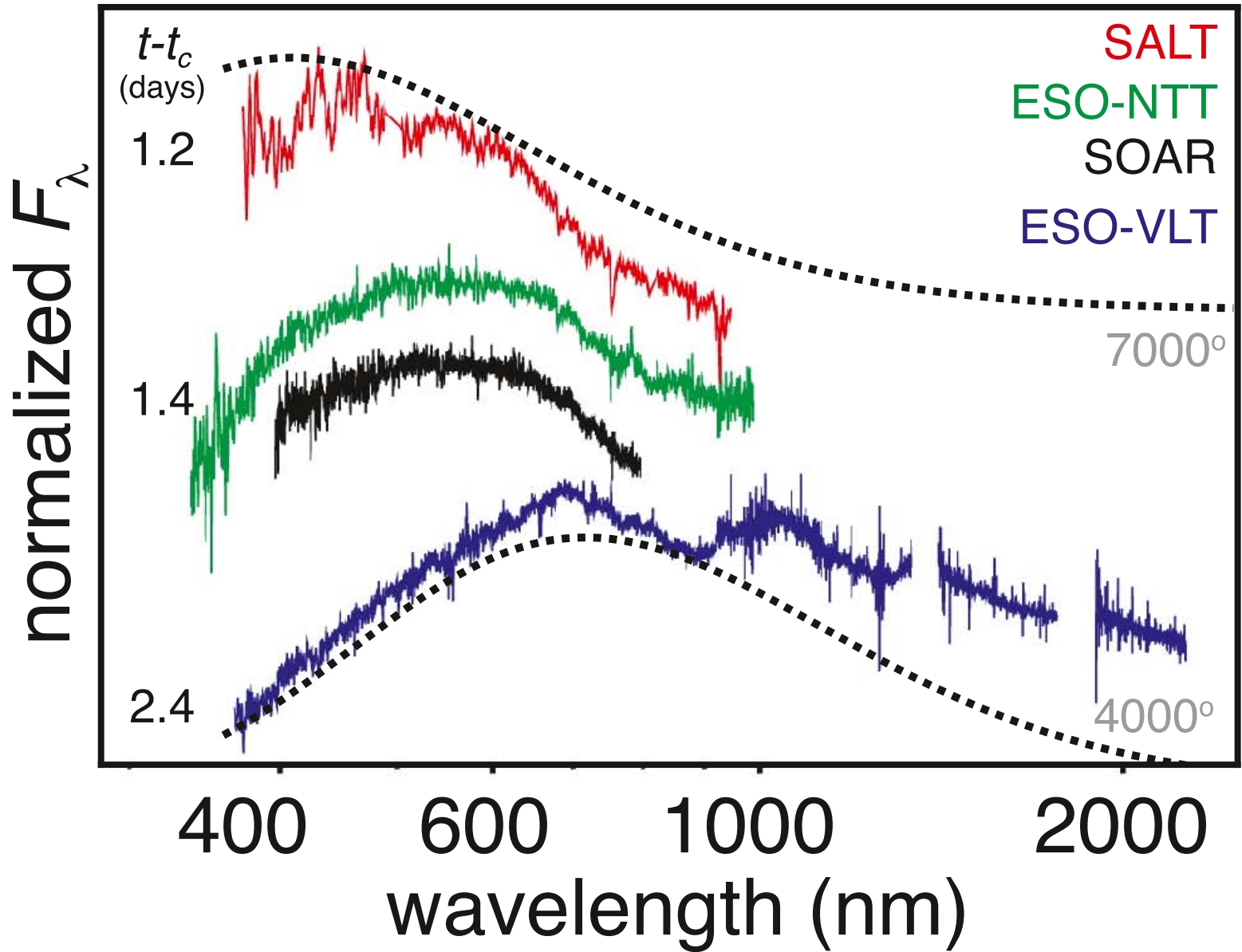
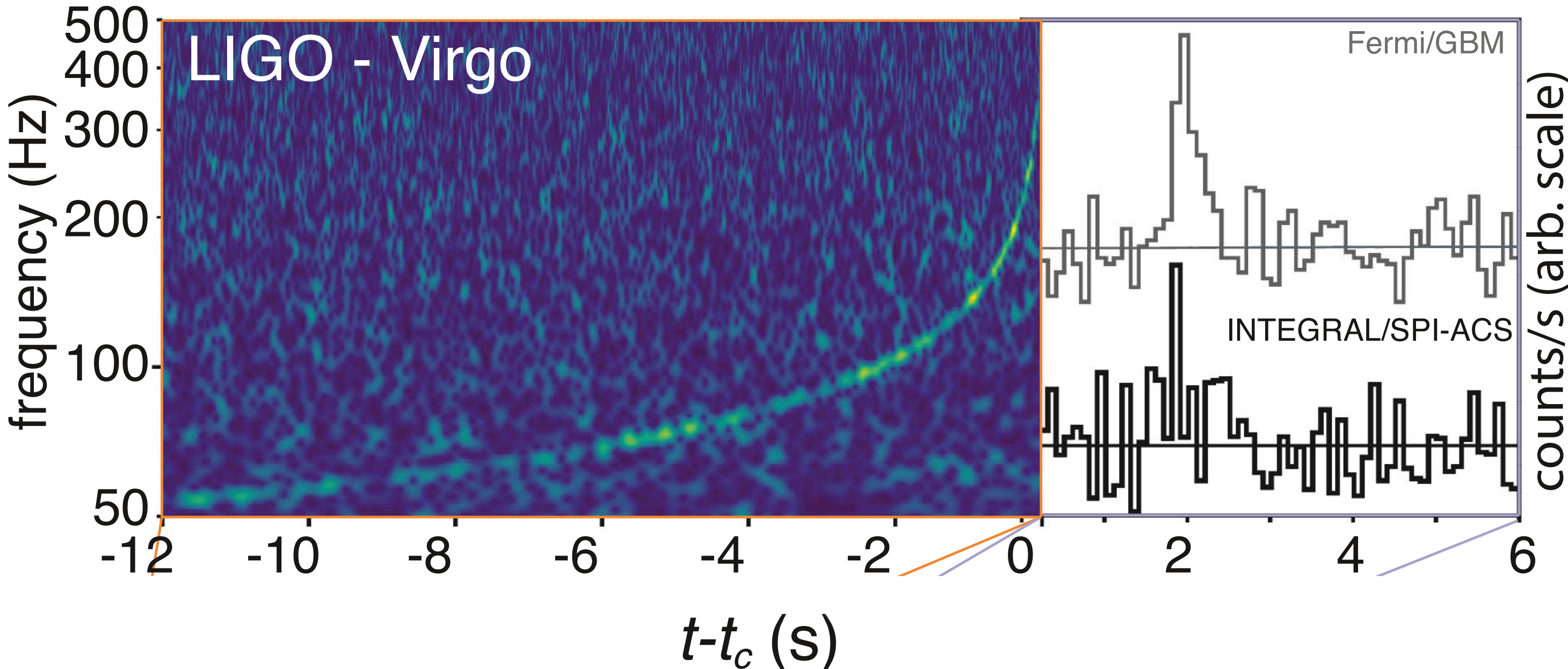
OPEN ACCESS

<https://doi.org/10.3847/2041-8213/aa91c9>



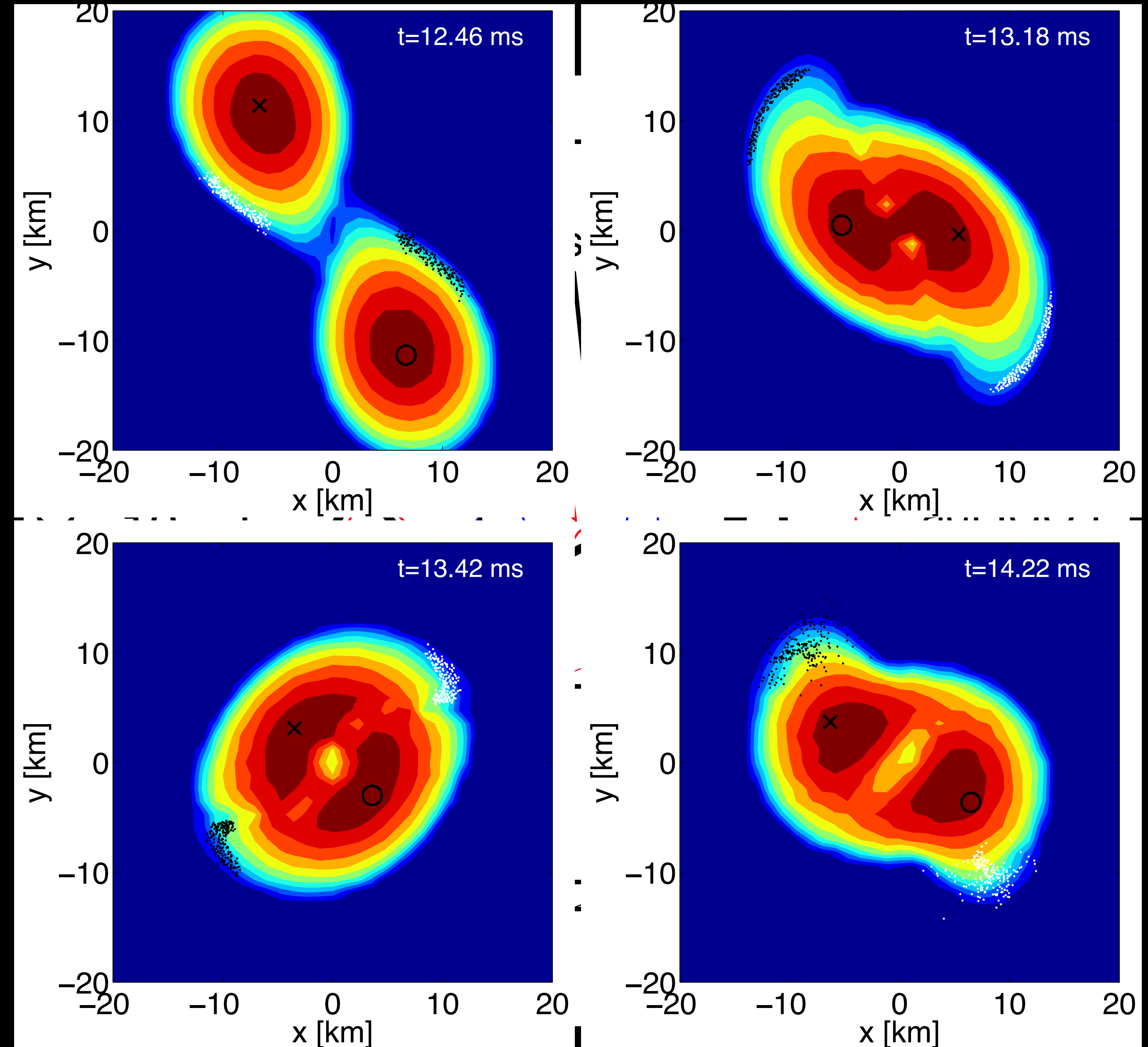
CrossMark

Multi-messenger Observations of a Binary Neutron Star Merger



Asteroseismology with GWs

The spectrum of quasi-normal modes excited is sensitive to the equation of state of hot and dense matter in the hyper massive neutron star.

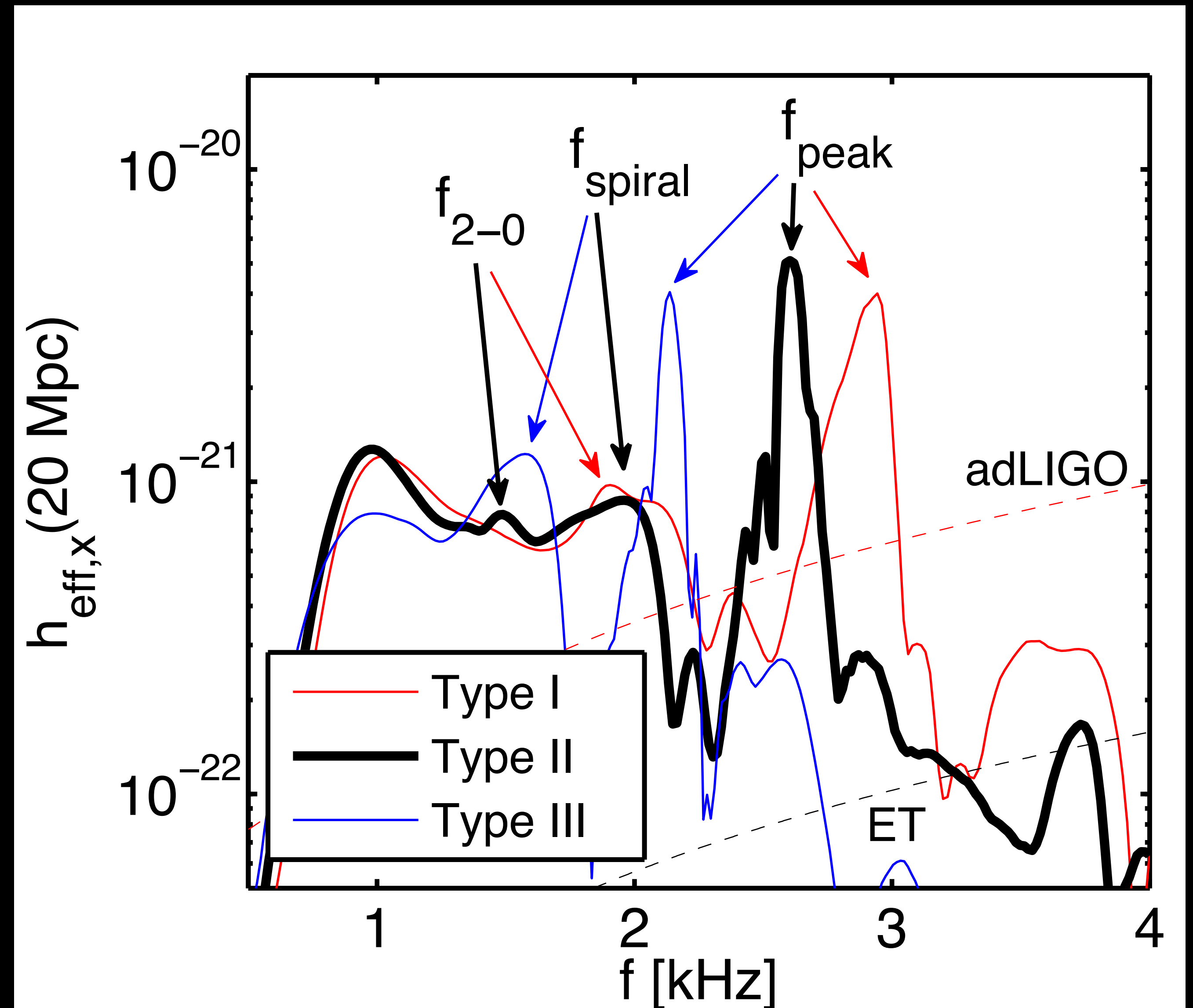


Asteroseismology with GWs

The spectrum of quasi-normal modes excited is sensitive to the equation of state of hot and dense matter in the hyper massive neutron star.

The high-frequency modes are detectable in Cosmic Explorer and Einstein Telescope.

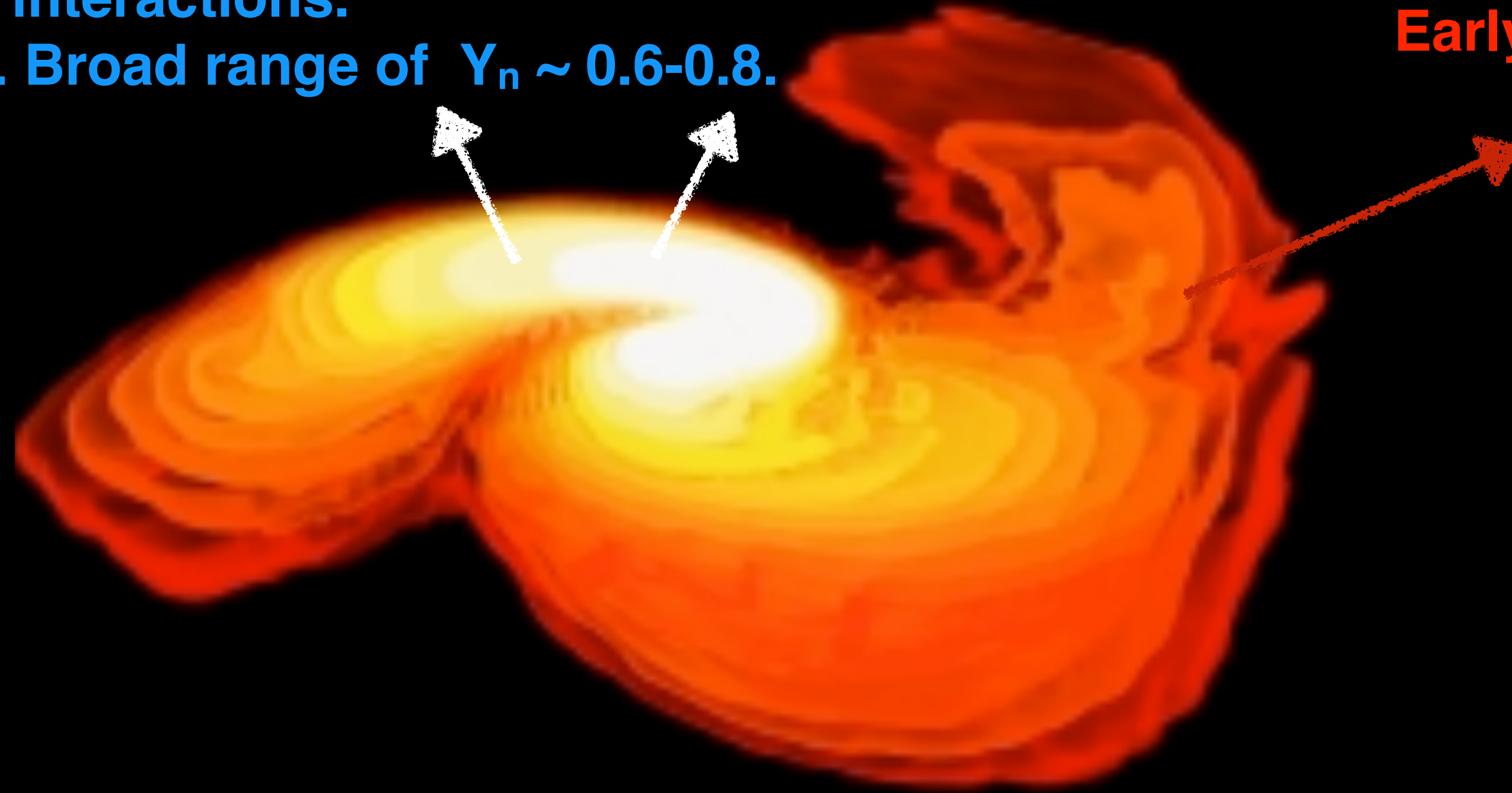
Bauswein & Stergioulas (2015)



Merger Ejecta, Nucleosynthesis, & EM Signals

Shock and neutrino wind driven ejecta:
Processed by weak interactions.
Not as neutron rich. Broad range of $Y_n \sim 0.6-0.8$.

Tidal ejecta:
Early, and very neutron-rich. $Y_n > 0.8$



The properties of the ejecta depend on the lifetime, internal dynamics, and neutrino emission from the hyper massive rapidly rotating neutron star.

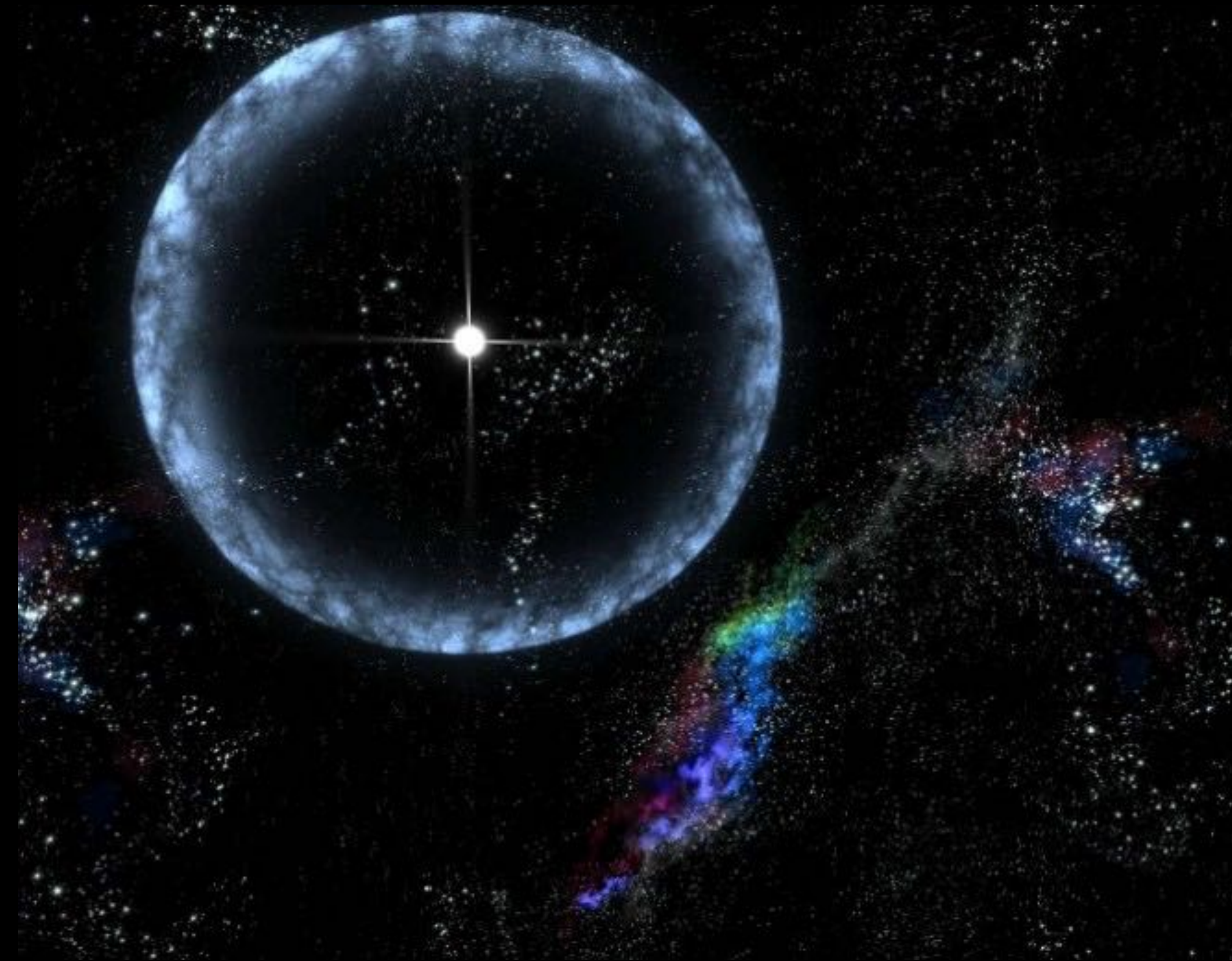
The amount, composition, and velocities of the ejecta determine the associated electromagnetic signals.

The Dark Side of Neutron stars

Using Neutron Stars to Discover or Constrain Particle Dark Matter

Neutron stars are great places to look for dark matter:

- They accrete and trap dark matter.
- Produce dark matter due to their high density.
- Produce dark matter due to high temperatures at birth or during mergers.



Constraining Dark Baryons

Particles in the MeV-GeV mass range that couple to baryons or mix with baryons are natural dark matter candidates.

There was speculation that a dark baryon with mass m_χ between 937.76 - 938.78 MeV might explain the discrepancy between neutron lifetime measurements. [Fornal & Grinstein \(2018\)](#)

$$n \rightarrow \chi + \dots$$

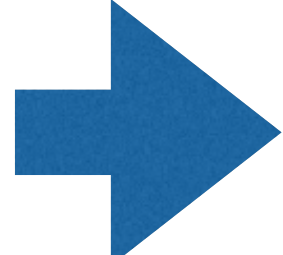
$$\tau_n^{\text{bottle}} = 879.6 \pm 0.6 \text{ s} \quad \text{--- counts neutrons}$$

$$\text{Br}_{n \rightarrow \chi} = 1 - \frac{\tau_n^{\text{bottle}}}{\tau_n^{\text{beam}}} = (0.9 \pm 0.2) \times 10^{-2}$$

$$\tau_n^{\text{beam}} = 888.0 \pm 2.0 \text{ s} \quad \text{--- counts protons}$$

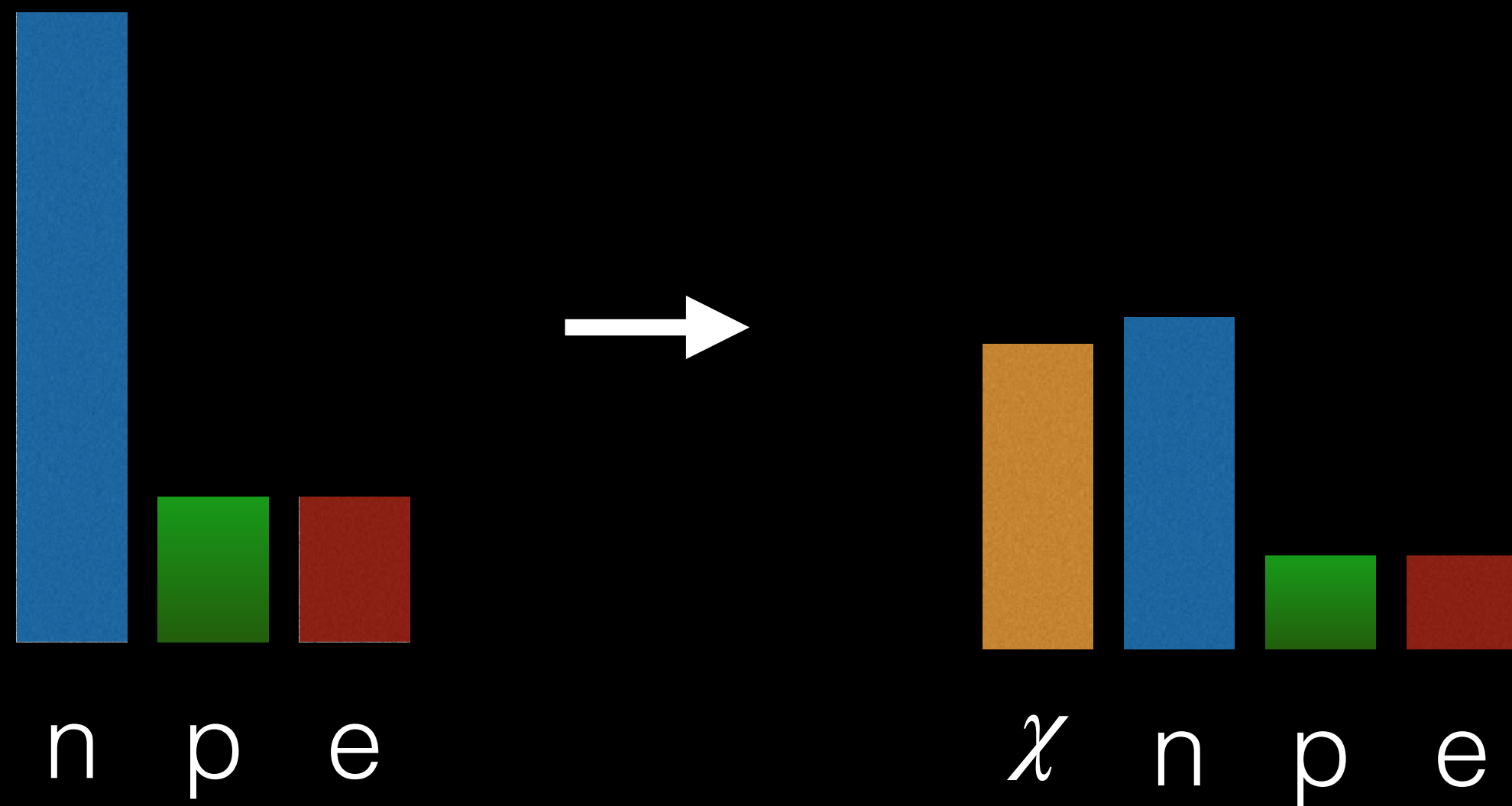
A model for hidden baryons which mix with the neutron:

$$\mathcal{L}_{\text{eff}} = \bar{n} (i\not{\partial} - m_n) n + \bar{\chi} (i\not{\partial} - m_\chi) \chi - \delta (\bar{\chi} n + \bar{n} \chi)$$

Mixing angle: $\theta = \frac{\delta}{\Delta M}$  An explanation of the anomaly requires $\theta \simeq 10^{-9}$

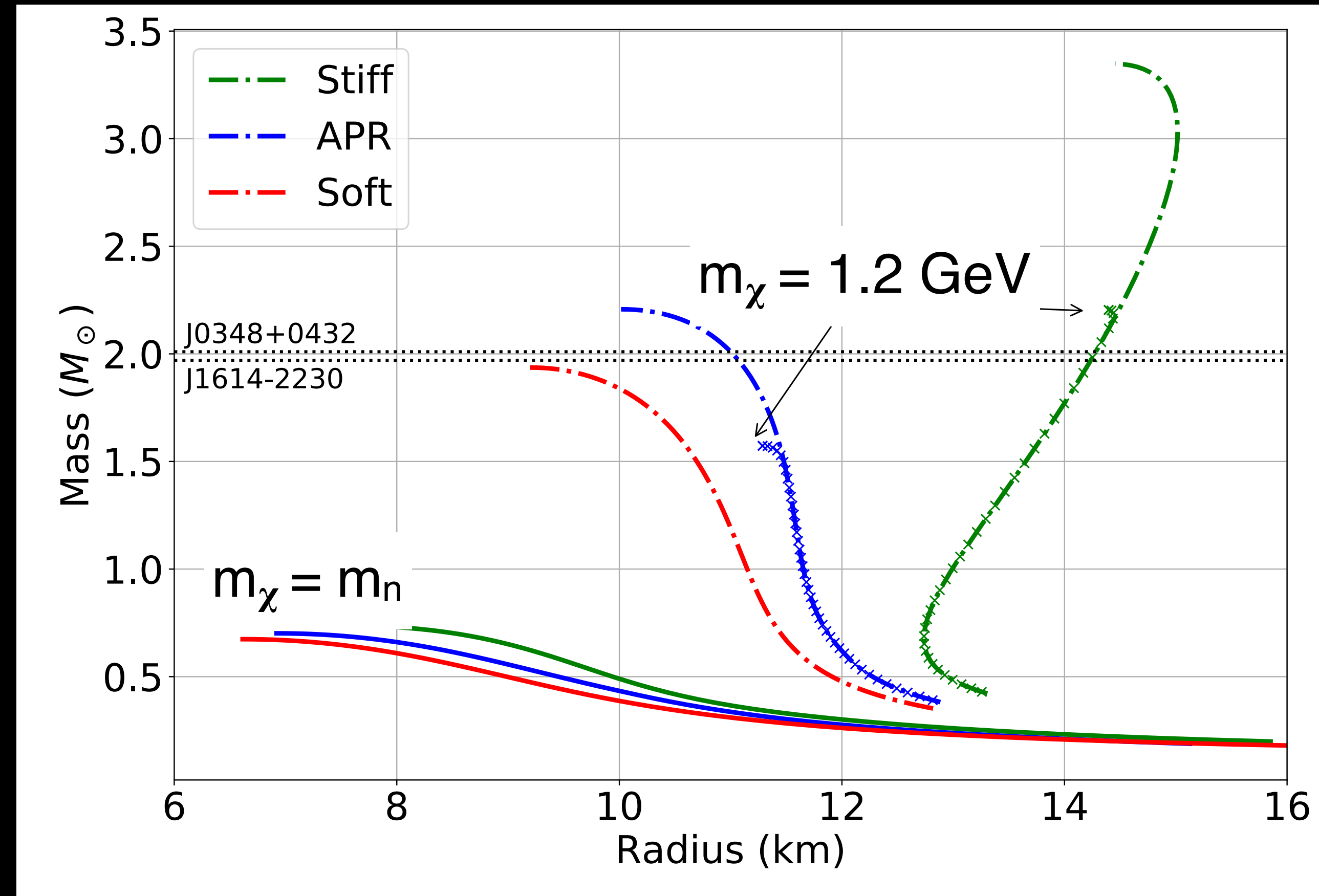
Neutron stars can probe much smaller mixing angles: $\theta \simeq 10^{-18}$

Weakly Interacting Dark Baryons Destabilize Neutron Stars



Neutron decay lowers the nucleon density at a given energy density.

When dark baryons are weakly interacting the equation of state is soft ~ similar to that of a free fermi gas.



This lowers the maximum mass of neutron stars.

Self-interacting Dark Matter

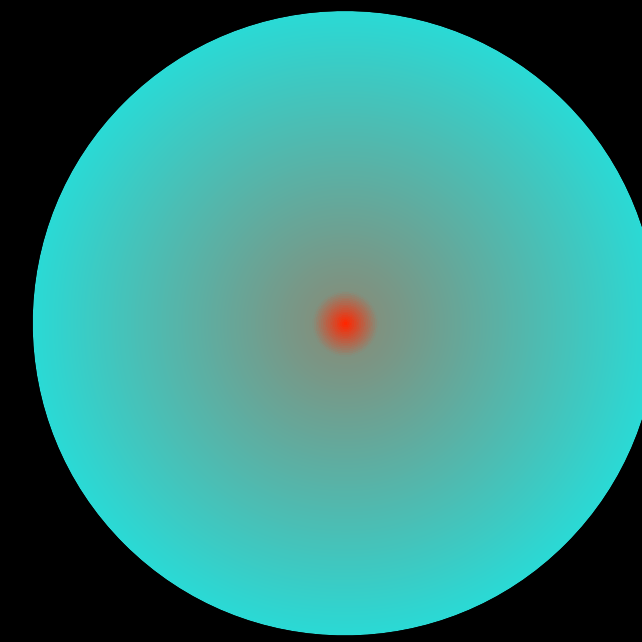
Using Gravitational Waves to Discover Hidden Sectors

Self-interacting dark matter can be stable and bound to neutron stars - a new class of compact dark objects.

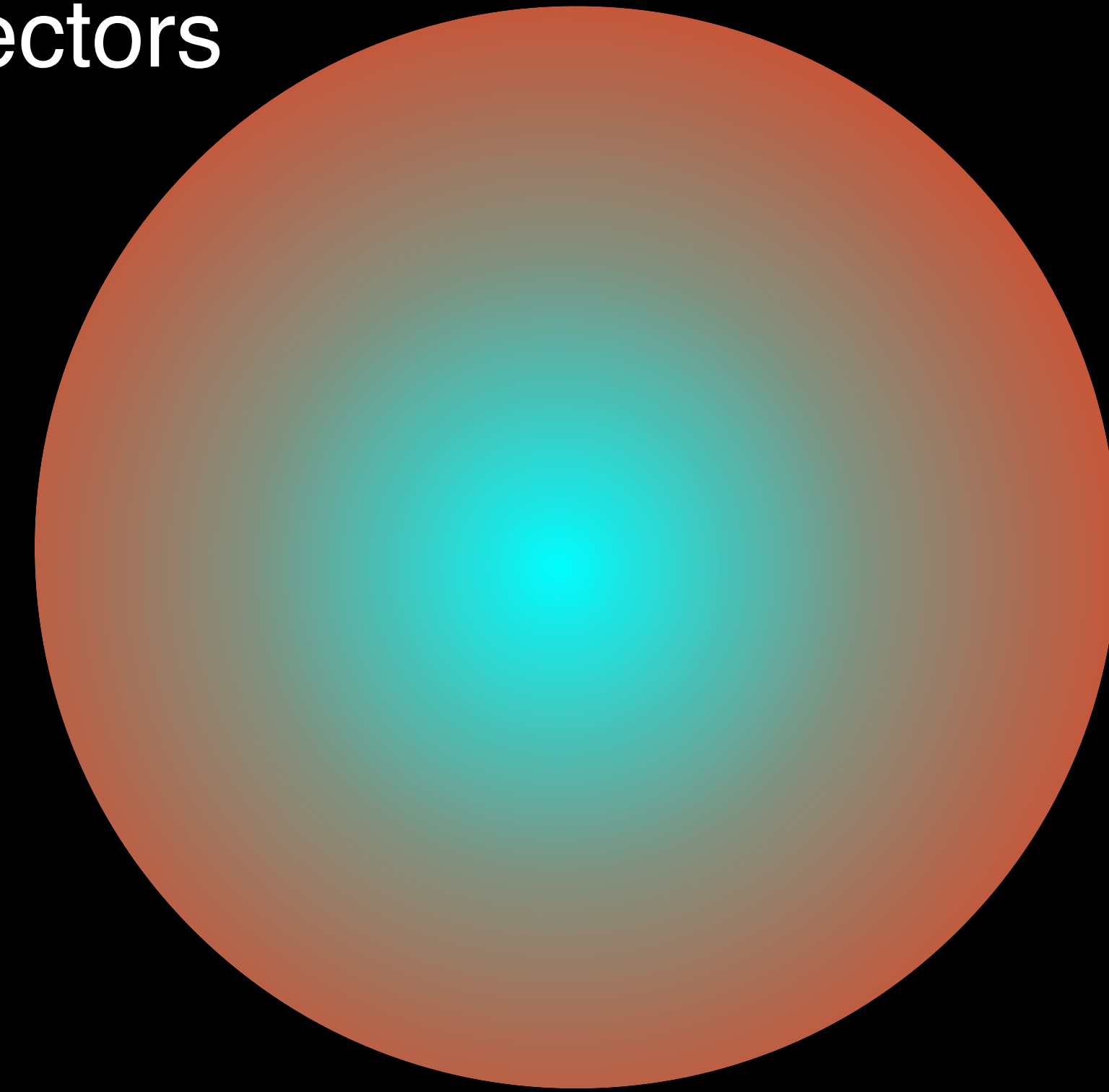
Gravitational wave observations of binary compact objects whose masses and tidal deformability's differ from those expected from neutron stars and stellar black holes would provide conclusive evidence for a strongly self-interacting dark sector:

Mass $< 0.1 M_{\text{solar}}$

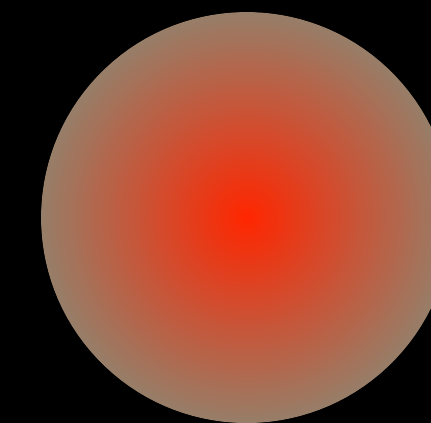
Tidal Deformability > 600



NS + dark-core



NS + dark-halo



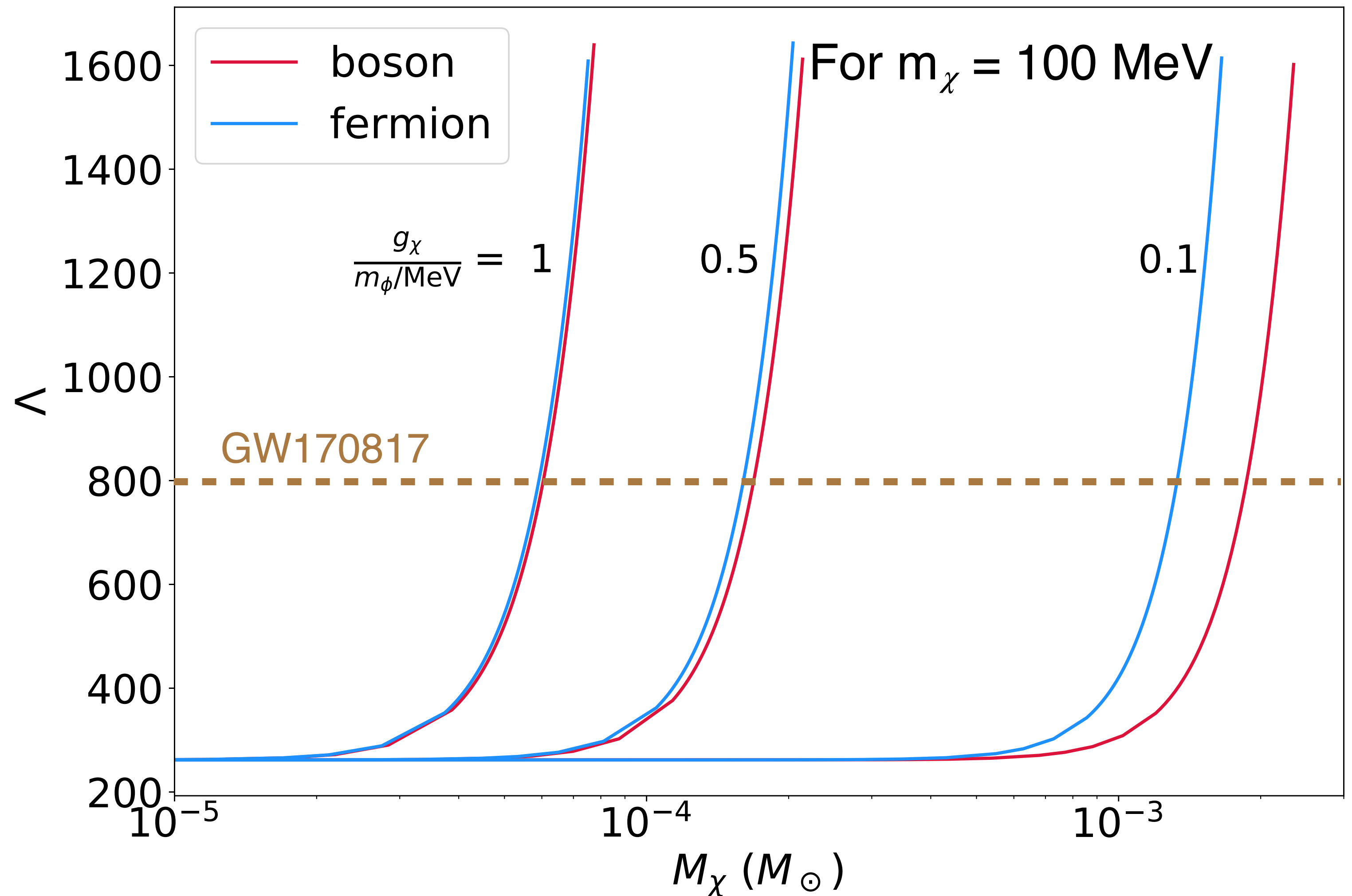
Compact Dark Objects

Dark Halos Alter Tidal Interactions

Trace amount of light dark matter $\sim 10^{-4}$ - $10^{-2} M_{\text{solar}}$ is adequate to enhance the tidal deformability $\Lambda > 800$!

Self-Interactions of “natural” can provide adequate repulsion.

$$g_{\chi}/m_{\phi} = (0.1/\text{MeV}) \text{ or } (10^{-6}/\text{eV})$$



Conclusions

- New insights about neutron stars: A rapid increase in the sound speed and observational support for a solid and superfluid inner crust.
- The first observation of a neutron star merger event exceeded our expectations. Next-generation GW detectors will revolutionize the field.
- Interpreting multi-messenger observations of mergers will rely on a coordinated effort that combines computational astrophysics and nuclear and particle physics. Has excellent potential for discovery.
- Provide unique opportunities to either constrain or discover dark sectors.

Acknowledgements

Neutron star structure and EOS: Joe Carlson (LANL), Christian Drischler (MSU), Stefano Gandolfi (LANL), Sophia Han (T. D. Lee Inst.), Jim Lattimer (Stony Brook), Jerome Margueron (IPN), Madappa Prakash (OU), Ingo Tews (LANL), Tianqi Zhao (OU).

Accreting Neutron Stars: Ed Brown (MSU), Andrew Cumming (McGill), Alex Deibel (IU), Farrukh Fattoyev (Manhattan Coll.), Chuck Horowitz (IU), Dany Page (UNAM).

Gravitational Waves: Duncan Brown (Syracuse), Collin Capano (Umass, Dartmouth), Reed Essick (Perimeter), Badri Krishnan (Max Planck, Hannover), Jocelyn Read (Fullerton), Bangalore Sathyaprakash (Penn. State),

Dark Matter in Neutron Stars: David Mckeen (TRIUMF), Ann Nelson (UW), Ermal Rrapaj (UC Berkeley), Dake Zhou (UC Berkeley),